MEASUREMENT OF ORGANIC SUBSTANCES IN THE GAS PHASE USING ON-LINE ELECTROCHEMICAL TECHNIQUES

by

MALCOLM GRAHAM TAYLOR, C.CHEM., M.R.S.C.

A Doctoral Thesis
submitted in partial fulfilment of the
requirements for the award of

DOCTOR OF PHILOSOPHY
of
Loughborough University of Technology

1988

Supervisor: Dr T.E. Edmonds
B.Sc., M.Sc., Ph.D., D.I.C., C.Chem., M.R.S.C.
Lecturer in Analytical Chemistry
Department of Chemistry
Loughborough University of Technology

To my parents for all their help and support

ACKNOWLEDGEMENTS

I am extremely grateful to Dr Tony E. Edmonds for his help and constant encouragement throughout the period of this research.

I would also like to thank Dr Adrian Clarke for his help and interest as liason officer for this project. I would like to express my thanks to Dr Arnold G. Fogg for the loan of equipment and for some interesting discussions.

I am grateful to the technical staff of the chemistry department for their cooperation and advice, especially John Swithenbank and Allan Stevens.

The encouragement and helpful advice of my friends and fellow colleagues during the research was invaluable and I would like to acknowledge some of them: Hilbert Henriques, Steve Bysouth, David Stone, Peter Murray-Jones, Andrew Marsden, Rajani Shrestha, Martin Forrest and Peter Wong.

I am indebted to the Ministry of Defence for the provision of the grant.

Finally I would like to acknowledge the encouragement and support of my parents.

ABSTRACT

Aniline was chosen as an atmospheric pollutant which might be monitored using an electrochemical sensor. The effect of pH and of different organic solvents on electrode poisoning was investigated for the analysis of aniline by voltammetry and it was concluded that it was not possible to prevent poisoning of the electrode by the reaction products. The analysis of aniline by flow injection analysis (fia) with DC (constant potential) and pulsed (double pulse) amperometric detection also suffered from electrode poisoning and the latter had a relatively high detection limit.

Secondary and tertiary substituted anilines with similar volatilities to aniline at room temperature were examined as suitable alternatives to aniline using voltammetry. Dimethyl–p–toluidine poisoned the electrode to a small extent when analysed by voltammetry. Detection of this compound by fia with pulsed amperometric detection showed improved electrode stability but was not judged suitable for long term monitoring of atmospheric samples of the amine.

A satisfactory method for monitoring aniline on line was developed using fia with triple pulse amperometric detection (PAD). The PAD waveform was optimised with respect to a low detection limit and a degree of selectivity towards possible atmospheric interferents for the detection of aniline in dilute aqueous acid at a platinum electrode.

A wall jet cell was designed for the analysis of aniline vapour in air which was continuously trapped in dilute acid and periodically injected into a fia system. The cell was not affected by small gas bubbles and was reasonably portable.

A computer program to fit a curve to the PAD calibration data was developed from a basic program for fitting polynomial functions by least squares analysis. Rational functions derived from the Langmuir isotherm were linearised into a polynomial form and these equations were fitted to the data by the program. The goodness of fit was acceptable for most concentration ranges.

Apparatus for the generation and collection of known concentrations of aniline vapour were constructed. A fia system with UV detection was developed to sample from the collection vessel periodically in order to check the trapping efficiency and the constancy of the vapour generation rate. The apparatus was used to investigate the detection of low levels of aniline in air using fia / PAD system sampling from the collector periodically. The detection limit for aniline in air was higher than 5 mg m^{-3}.

An assessment was made of the relative performance of valves and flow through detector cells used during the research for fia with amperometric detection. The influence of the electrode and its condition was investigated for the following systems.
a) A commercial glassy carbon electrode was compared with a composite electrode constructed from reticulated vitreous carbon for fia / amperometric detection.
b) The selectivity of a glassy carbon electrode coated with a polymer film was investigated.

CONTENTS

CHAPTER 1
INTRODUCTION

1.1 Introduction to Voltammetry

1.1.1 Definitions

A revised set of recommendations for the classification and nomenclature of electroanalytical techniques was made by Meites, Nurnburg and Zuman[1] in 1975, for the commission on electroanalytical chemistry (IUPAC). It is recommended that the term "voltammetry" is used to denote the study of relationships between electric current and applied e.m.f. or potential with stationary and solid indicator electrodes, such as hanging drops and pools, regardless of the material from which they are made. By "polarography", we understand the special case of voltammetry in which the measurements are carried out at the dropping mercury electrode. It is recommended that this term also covers the use of other metals or liquid conductors, either as dropping or streaming electrodes. The term "amperometry" is recommended for the measurement of current as a function of concentration for a constant e.m.f. or potential applied to the indicator electrode.

1.1.2 History

Electroanalytical chemistry may be traced back to 1776, when Cavendish used conductometry to compare saturated brine, a saline solution and rain water. The initial voltammetric studies began with solid electrodes. The classic research of Le Blanc in 1893 on the electrolysis of metal ions provided the impetus for further study. Salomen indicated the existence of limiting currents for

current-voltage curves for the electrolysis of silver ions. Work on limiting currents and diffusion conditions progressed via Nernst, Laitinen and Kolthoff and others. Classical polarography was introduced by Heyrovsky in 1922. The growth from 1950 onwards of publications dealing with solid electrode voltammetry parallels the rapid increase of the general polarographic literature as cited by Kolthoff and Lingane[2].

During the early 1960's, modifications of the basic polarographic technique aimed at overcoming the various problems associated with it began to meet with success. Investigations of such techniques as square wave polarography, pulse polarography and ac polarography began, to appear in the literature. The decade from 1955 to 1965 might be characterised as the one single period during which the greatest advancement in the technical aspects of polarography took place, while, simultaneously the greatest decline in the practical everyday usage of these techniques occured.[3] This was due to the lack of suitable commercial instrumentation. When atomic absorption instruments became commercially viable the growth of polarography was slowed tremendously because the former was less prone to difficulties and offered good advantages in trace metal analysis, e.g. greater sensitivity and wider elemental coverage. The introduction in the late 1960's of operational amplifier based instruments greatly increased the everyday application of electrochemistry in analytical laboratories. Pulse polarography, introduced by Barker in 1960 became a widely available technique, owing to the capability of these instruments to perform this technique. Pulse voltammetric techniques offer significant improvements in detection limits because of the better discrimination against background currents.[4]

1.1.3 Recent Developments

The analysis of metals by polarographic techniques has found its place alongside atomic spectroscopy (i.e. flame, graphite furnace, and plasma), and provides an excellent means of studying trace metal speciation[5]. Detection limits are comparable to atomic absorption and the instruments are relatively inexpensive. The design of the dropping mercury electrode has recently been improved by PAR and Metrohm, the mercury is contained in a sealed reservoir. The drops are dispensed reproducibly by means of a solenoid operated piston or by gas pressure controlled by valves.

The interest in the polarographic analysis of organic compounds increased considerably with the introduction of the improved instrumentation and there are now wide applications of polarographic analysis for organic compounds and more recently adsorptive stripping voltammetry at the static mercury drop electrode.[6]

There has been a radical increase in the use of solid electrodes in electroanalysis over the past decade and this is due to four major factors. First electroanalytical chemists have become increasingly interested in the determination of organic molecules by anodic oxidation. The anodic limit for mercury is about +0.3V vs SCE in suitable media, (in acidic media the anodic limit for glassy carbon electrodes is more than +1.0V vs SCE). Secondly the ability of electroanalytical techniques to yield in-situ information in complex chemical environments, can best be met by solid electrodes. Thirdly, detectors for liquid chromatography and flow injection analysis based on electroanalytical devices are of increasing significance due to their

excellent detection limits for certain important classes of compounds e.g. biogenic amines, phenols, sugars. These detectors are normally operated by personnel who are not necessarily electroanalytical chemists; thus the device needs to be simple and rugged, and solid electrodes are the most suitable. Finally there is more interest in the use of surface-modified electrodes for electroanalytical applications; again solid electrodes are essential in this area of research. Recently increasing interest has also been shown in micro-electrodes. Because of their small size they are an ideal method of obtaining information in-vivo, also they offer advantages of improved signal to noise ratios for dynamic electroanalytical chemistry.

1.1.4 Practical Implementation

Kolthoff once defined electroanalytical chemistry as the application of electrochemistry to analytical chemistry. Such a definition is partially accurate; but it is preferable to consider electroanalytical chemistry as that area of analytical chemistry and electrochemistry in which the electrode is used as a probe, to measure something that directly or indirectly involves the electrode. The desired information is not the fundamental operation of the electrode process, this may be left to the physical electrochemist.

The non equilibrium situation associated with voltammetric techniques is largely controlled by diffusion of the electroactive species to the electrode. Unlike most spectroscopic methods, voltammetric measurements are made on only a minute fraction of the sample close to the electrode surface. The signal obtained from a voltammetric measurement is a function of

the applied potential and is due to transfer of electrons across the electrode solution interface. The electrode behaves in many respects like an ideal transducer between the chemical and electrical domains. The flow of electrons constitute the output of the transducer. In order that this transfer of electrons can take place, there must be ionic conductivity in the solution, thus a medium or electrolyte solution is required in which ions can exist. Voltammetry and amperometry to a lesser extent are capable of a degree of selectivity towards the probed species. This is because for a given potential, the current due to electron transfer of a redox couple depends to some extent on its standard redox potential. As the potential is changed the total faradaic current will reflect the contribution from each redox couple in solution.

Voltammetric and amperometric transducers are relatively simple, the cell consists of two or three electrodes, a working (indicating) electrode , reference electrode and in a potentiostat controlled cell, a counter electrode carries the current. The use of three electrodes is usual because unless trace analysis is done the currents are large enough to cause some polarisation of the reference electrode in a two electrode system. Voltammetric techniques can be used to study anything that directly or indirectly undergoes a reaction involving electron transfer. The target analyte might be the determinand, or the former might modify the behaviour of a monitorand, either by reacting with it or by a heterogeneous reaction with the electrode surface (e.g. adsorption). Specialist texts on electroanalytical chemistry[7-9] should be consulted for further information on voltammetric and related techniques.

1.2 Theory of Voltametry

1.2.1 Fundamental Principles

The text by Adams[10] provides much useful information on voltammetry at solid electrodes. The monograph by Bond[11] covers modern polarographic techniques at mercury electrodes. Some of the more commonly used voltammetric techniques are discussed in the following sections.

When a cathodic potential ramp is applied to an electrode that is immersed in an electrolyte solution containing a redox species (in the oxidised form), a current will begin to flow, rise rapidly to a peak and then gradually decay. For a redox couple to be reversible in voltammetry; the rate of electron transfer between the redox species and the electrode, must be rapid compared with the rate of mass transfer. The redox couple may be represented by the following equation:

$$Ox + ne = Red$$

where:

Red = reduced form
Ox = oxidised form

The concentrations of the oxidised and reduced forms will be in equilibrium at the electrode surface and the ratio of their concentrations at a given potential (E) is given by the Nernst equation:

$$E = E^{o'} + \frac{RT}{nF} \ln \frac{[Ox]}{[Red]}$$

where:

n = number of electrons transferred per molecule

$E^{o'}$ = formal reduction potential of the couple

The other symbols having their usual meanings.

The formal potential is measurable experimentally and it is more convenient to use rather than the standard potential because it avoids the need to convert concentrations into activities (the activity coefficients are often unknown). It varies from medium to medium because the ionic strength affects the activity coefficients. It could also contain factors related to complexation of the redox species.

The current depends on two steps in the overall process, the movement of electroactive species to the surface and the electron transfer reaction. The electron transfer rate constant (k_f) for a reduction process is a function of potential and can be described theoretically:

$$k_f = k^o \exp\left[-\frac{\alpha n_a F}{RT}(E - E^{o'})\right]$$

where:

k^o = standard heterogeneous electron transfer rate constant (its value is a property of the reaction between the particular compound and the electrode surface)

α = transfer coefficient

n_a = number of electrons involved in the rate determining step

The exponential dependence of k_f on the applied potential account for the steep rise in the current. Concomitant with this the concentration of Ox is becoming depleted at the electrode surface by electrolysis. In a still

solution the mass transfer of Ox to the electrode surface will be by diffusion, which is relatively slow. As the rate of electron transfer increases exponentially the depletion zone grows and the mass transport begins to decrease. At the peak the rate of mass transport becomes limiting and the current is at a maximum. After this point the current depends on time rather than potential.

1.2.2 Linear Sweep Voltammetry

The diffusion problem to a planar electrode for a reversible electrode reaction was first solved by Randles[12] and Sevcik[13]. The peak current (i_p) is given by the following equation:

$$i_p = 2.687 \times 10^5 \; n^{3/2} \; A \; D^{1/2} \; C \; v^{1/2}$$

where:

- n = number of electrons involved in the electrode process
- A = area of the electrode
- D = diffusion coefficient
- C = bulk concentration
- v = scan rate

An essential difference between linear sweep voltammetry and polarography is the dependence of the current on the scan rate for the former, whereas in polarography the current is independent of scan rate.

Matsuda and Ayabe[14] determined the relationship between the peak potential (E_p) and half peak potential ($E_{p/2}$) in linear sweep voltammetry for the cases of reversible, quasi-reversible and totally irreversible systems. For a reversible system:

$$E_p - E_{p/2} = \frac{0.057}{n} \text{ V} \quad \text{at } 25^{\circ}\text{C}$$

For an irreversible system the corresponding equations are as follows:

$$i_p = 2.985 \times 10^5 \, n(\alpha n_a)^{1/2} \, A \, D^{1/2} \, C \, v^{1/2}$$

and

$$E_p - E_{p/2} = \frac{0.048}{\alpha n_a} \text{ V} \quad \text{at } 25^{\circ}\text{C}$$

where:

α = electron transfer coefficient

n_a = number of electrons involved in the rate determining step

As αn_a decreases, the voltammograms become more spread out and the peaks tend to be rounded. Anodic oxidation of organic compounds are often irreversible and the voltammograms display these characteristics. For the irreversible situation the i_p is significantly less than the reversible situation, and it decreases rapidly as n_a becomes smaller. E_p and $E_{p/2}$ for irreversible processes vary with scan rate. This differentiates them from reversible processes, but the variation is only about $0.03/\alpha n_a$ V per tenfold increase in scan rate.

1.2.3 Cyclic Voltammetry

Cyclic Voltammetry was apparently first practiced by Sevcik[13]. It is a useful technique for rapidly observing the redox behavior of the species of interest. The technique has been used to study electrochemically

generated intermediates[15-16] and for investigating the overall processes which may occur in a complex electrode reaction.[17-18] Useful introductions to the technique are available.[19-20]

The excitation signal for cyclic voltammetry is a linear potential scan with a triangular waveform. The potential is scanned linearly with time from a starting potential to a switching potential, the scan is then reversed back to the starting potential. (As in linear sweep voltammetry the forward scan in cyclic voltammetry causes a depletion of reactant species at the electrode surface, concomitant with a significant increase in the concentration of product near the electrode surface. Also the current behaves in the same way. When the scan direction is reversed, if the forward scan was cathodic then the product is oxidised back to the original starting material (for a simple redox reaction) and the current for the reverse process is recorded. Fig. 1 is a typical cyclic voltammogram for a reversible redox couple.)

The formal oxidation potential for the redox couple is the average of the forward and reverse peak potentials. This is an approximation which is most accurate when the electrode reaction is reversible and the diffusion coefficients for the oxidised and reduced forms are the same. If the reaction is reversible then the separation in the peak potentials, ΔE_p will be close to the value given by the following equation:

$$\Delta E_p = \frac{0.058}{n} \quad V$$

Redox couples whose peaks shift farther apart with increasing scan rate are categorised as quasi-reversible.

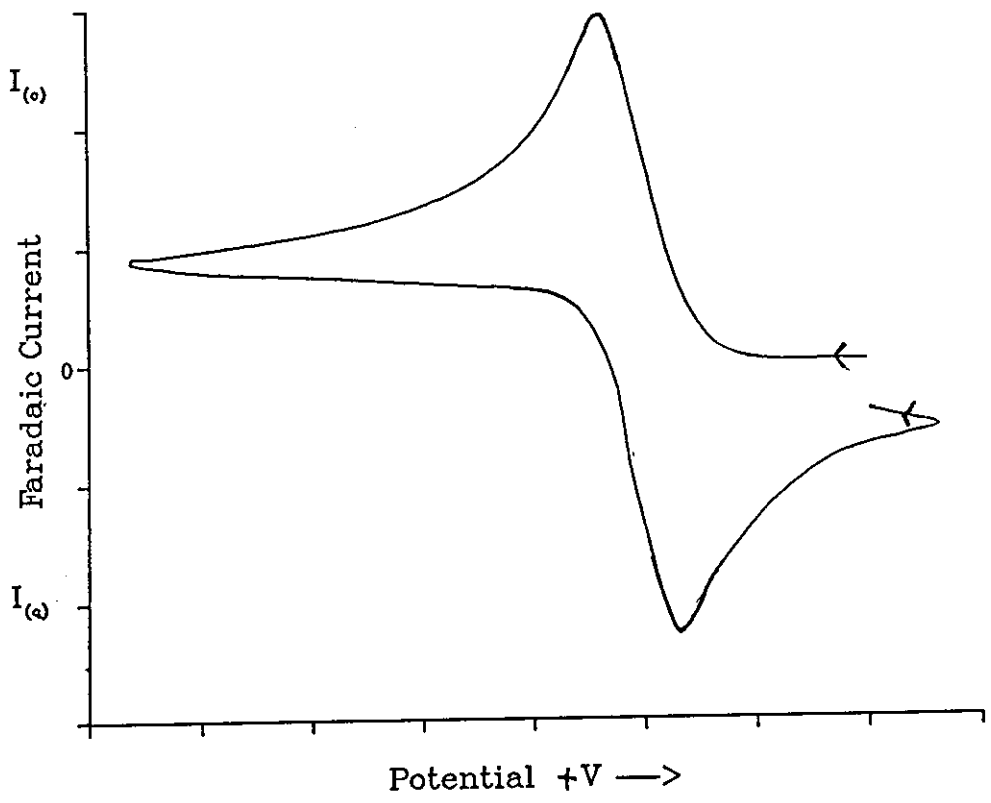

Fig. 1
Typical Cyclic Voltammogram of a Reversible Redox Couple in the oxidised form

For a totally irreversible system, the peaks are so widely separated that no parts of the two peaks overlap on the potential axis at all.

1.2.4 Pulse Voltammetry

Pulse voltammetric techniques tend to give better signal to noise ratios compared with linear sweep voltammetry because the faradaic current is larger and there is better discrimination against charging currents. When a potential pulse is applied to an electrode, the capacitive current that flows is proportional to the magnitude of the pulse, and decays exponentially with time. The faradaic current, on the other hand, decays according to the square root of time. By measuring the current towards the end of the pulse the signal to noise ratio may be improved. This is done in normal pulse voltammetry.

The waveform used in normal pulse voltammetry is shown in fig. 2c; the response (see fig. 2d) is similar in shape to linear sweep voltammetry, or polarography, according to the electrode. The excitation waveform consists of successive pulses of gradually changing amplitude between which a constant base potential is applied. The initial potential is usually chosen to lie in a region where none of the sample components are electroactive. The delay between pulses needs to be sufficient to allow the concentration profile near to the electrode surface to decay.

In differential pulse voltammetry, the current is measured just prior to the application of the pulse and towards the end of the pulse, giving a current which is the difference between the two measurements. The waveform is shown in fig. 2a, the response is peak shaped

Differential Pulse Voltammetry

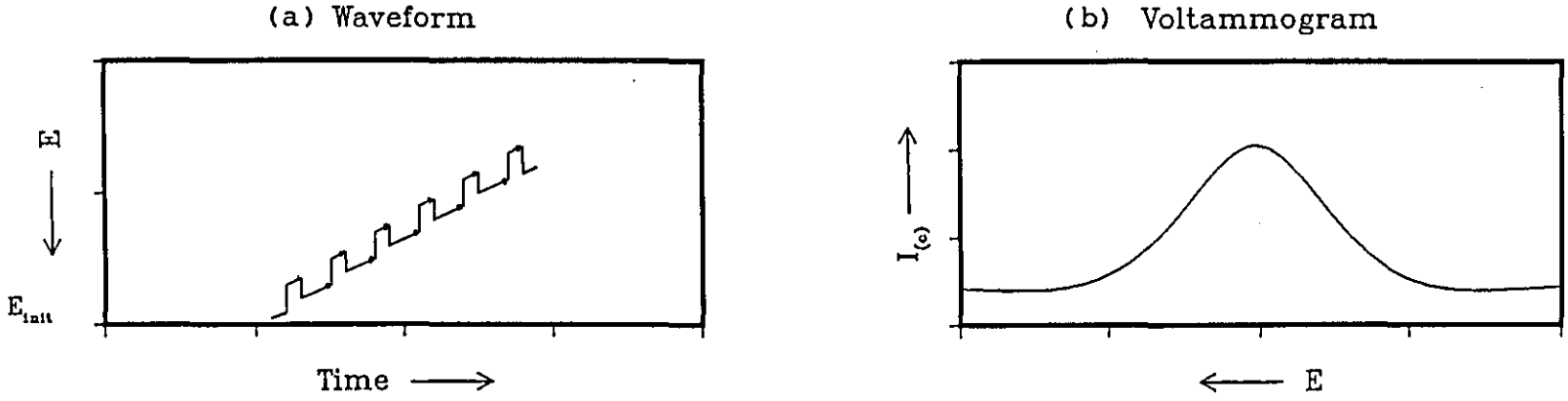

Normal Pulse Voltammetry

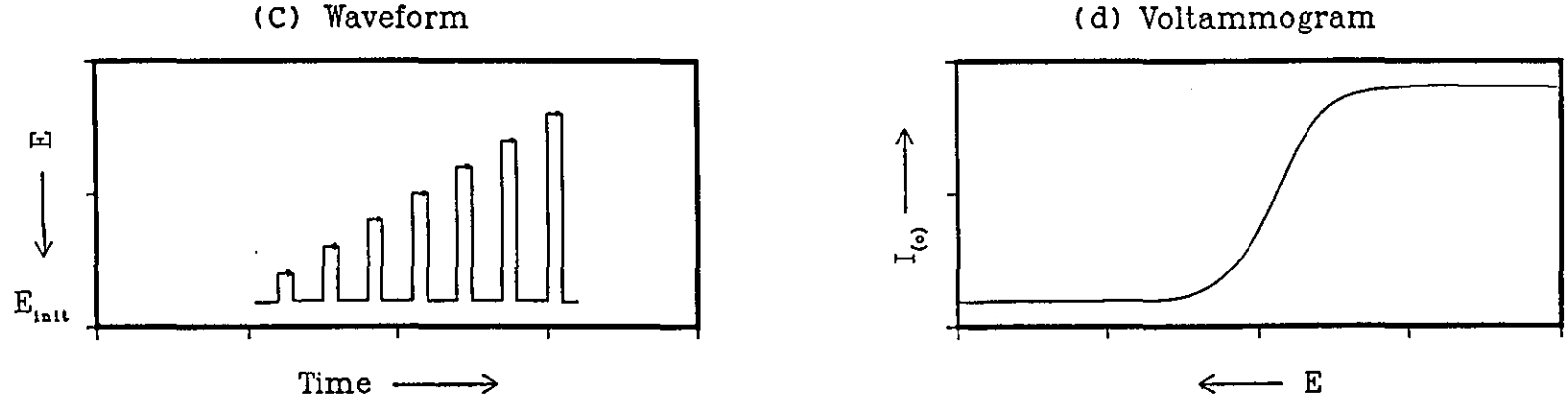

Fig. 2
Potential Waveforms and typical Voltammograms for Pulse Techniques

• = starting point for current measurment

(fig. 2b). The pulse width is often fixed at 50 ms. For most cases a pulse amplitude of 50 mV or less is used. Large amplitudes provide an increase in response which must be balanced against the loss in resolution and the increase in charging current.

The pulse techniques show distinct advantages at the dropping mercury electrode, due to the discrimination against charging current arising from area growth of the drop. At the the stationary mercury drop electrode, where rapid drop growth is possible, the analytical performance and response characteristics of these techniques tend to converge[21], especially for irreversible couples. For solid electrodes the application of pulse techniques may be disadvantageous in some cases. It has been shown by Dieker et al[22] that with the application of normal pulse and differential pulse voltammetry much larger residual currents are observed at glassy carbon electrodes because of chemical transformations of the surface, which are slow to reach equilibrium. Carbon paste electrodes gave satisfactory results in this case. Chey and Adams[23] also found anodic differential pulse voltammetry at carbon paste electrodes analytically useful for trace determination of aromatic amines. The advantage of normal pulse voltammetry is that fouling of solid electrodes by adsorbing electrode reaction products will be minimised as for a large part of the scan time the electrode is at a potential where no electrolysis occurs. For differential pulse voltammetry the resolution of adjacent waves can be useful.

1.2.5 Square wave and AC Voltammetry

AC voltammetry[24] is more commonly used than square wave voltammetry.[25] This is probably because the former is available on some commercial instruments, the added instrumentation is somewhat extensive, and often tends to be inflexible. Anderson and Bond[26] described digital AC polarography, using only a potentiostat, low pass filter and a microcomputer. The response of the two techniques has been likened to each other for the case of an irreversible system.[27] The major advantage of square wave voltammetry over other pulse techniques is the speed of analysis (especially useful for the dropping mercury electrode).[28] Recently Zachowski et al investigated the optimisation of square wave voltammetry at a dropping mercury electrode and compared the results with theory. There is also better discrimination against a wide range of background currents, and this ought to be advantageous when applied to solid electrodes.

1.2.6 Hydrodynamic Voltammetry

In static voltammetry the mass transport to the electrode surface is by molecular diffusion as a result of the depletion of the electroactive species by electrolysis. In hydrodynamic voltammetry the mass transport also includes a convection term, because the electroactive species will be entrained by a moving liquid and transported with it.[29] Levich called the combination of these two processes convective diffusion. He derived equations to describe the mass transport process taking place in stirred or flowing solutions, with various electrode configurations. The principles of current distribution and mass transport in flowing solutions have been reviewed by Newman[30]. Pungor et al[31] comprehensively

reviewed the theory, practice and applications of hydrodynamic voltammetry.

Because of the increased mass transport to the electrode surface hydrodynamic voltammetry is more sensitive than voltammetry in a still solution. Convective diffusion may be achieved by moving the solution relative to the electrode as in flow through cells or stirred solutions, or by moving the electrode in a stationary solution, as in the rotating disc electrode.[32-33]

1.3 Theory of Hydrodynamic Amperometry

1.3.1 DC Limiting Currents for Different Cell Geometries

The most popular flow through cells for hydrodynamic amperometry are the thin layer and wall jet cells, tubular cells have been used for many years, but are somewhat less popular with electroanalytical chemists. One reason is perhaps because the electrode surface is relatively difficult to polish.

Matsuda and co-workers have studied most of the cell geometries of importance, i.e. thin layer and tubular cells[34] and the wall jet cell[35]. Yamada and Matsuda[35] described the construction and the electrochemical response of a wall jet in terms of the hydrodynamic conditions. They derived an equation for the limiting current for a wall jet cell.
The equation is given:

$$i_L = (1.60k)\ n\ F\ C\ D^{2/3}\ v^{-5/12}\ V^{3/4}\ a^{-1/2}\ r^{3/4}$$

where:

C = concentration of electroactive species

D = diffusion coefficient of above
v = kinematic viscosity
V = volume flow rate of the solution issued from the nozzle
a = diameter of the nozzle
r = radius of the electrode
k = 0.86

The value of k was calculated from a large number of experimental results. There has been confusion as to the appropriate theory to apply to cells of the wall jet geometry. Recently it has been demonstrated that the behaviour of the cell depends on whether the size of the cell affects the natural development of the hydrodynamic boundary layer.[36] Gunasingham et al[37-38] have discussed the theory and applications of the large volume wall jet electrode. They concluded that in order to obtain maximum efficiency from the electrode, the body of the jet nozzle should be located well clear of the hydrodynamic boundary layer. They found that the effective cell volume depends only on the order of this boundary layer and separations of the nozzle and electrode up to 10 mm caused no break up of the jet nor any signs of turbulent eddy formation.

For the thin layer cell the following equation[39] gives the limiting current:

$$i_L = 0.68n\ F\ D^{2/3}\ C\ b\ l^{1/2}\ u^{1/2}\ v^{-1/6}$$

where: b = thickness of electrode
l = length of electrode
u = linear flow rate
The other symbols have the same meaning as for the wall jet cell.

The theory describing the current at a thin layer cell

has been reviewed by Weber.[40]

1.3.2 Pulsed Detection

The application of potential pulses of fixed amplitude to a constant base potential is the amperometric equivalent of pulse voltammetry. The current is measured in a similar way to differential or normal pulse voltammetry. The pulse waveforms have been used to improve the selectivity of amperometric detection in flowing systems and in some cases to overcome adsorption of electrochemical reaction products.

From theory the sensitivity of these pulse techniques should be greater than for DC detection and this is generally found in practice.[41,42] The increased sensitivity is greatly offset by increased background currents, these currents are relatively large at solid electrodes compared with mercury.[43-45] The source of the background current is mainly from faradaic surface transformations,[46-48] this is especially true for glassy carbon electrodes where the oxygen containing functional groups behave as redox couples with slow relaxation times.

The detection limits using these pulse techniques are consequently poorer than for DC amperometry.[43-45,49-51] The improved selectivity[52,53] is therefore only useful where the analyte is present at sufficiently high concentrations. The decrease in adsorption of reaction products and impurities present in the carrier have been reported for pulse amperometry applied to glassy carbon[44,54], platinum[55] and mercury film[53] electrodes.

1.3.3 Triple Pulse Detection

Triple pulse amperometric detection (PAD) has been developed by Johnson and coworkers[56] for the detection of analytes not easily detected by oxidation at electrodes by application of DC or pulse potentials. The reaction products from many electrochemical oxidations tend to adsorb onto the electrode surface causing a decrease in response, this is a well known problem for certain classes of compounds e.g. alcohols, amines and sulphur compounds.[57-59] The first step in many of these anodic oxidations is the production of free radicals, which at sufficiently high concentrations, can polymerise and adsorb strongly onto the electrode surface. (see chapter 10 in reference 10)

The application of the PAD waveform to platinum and gold electrodes enables compounds to be detected without loss of electrode activity due to the electrochemical cleaning of the electrode.[60] The method usually relies on the adsorption of analyte onto the electrode surface, where catalysis of the analyte oxidation occurs, by metal oxides. The compounds need not be electroactive in order to be detected, the supression of surface oxide formation enables the analyte to be detected as a negative peak.

A PAD waveform is illustrated in fig. 3. The current is sampled near the end of period t_1 at potential E_1. The cleaning potential E_2 is larger than E_1 to accelerate oxidative removal of all remaining adsorbed radicals or molecules; E_3 is rather negative in order to quickly reduce the oxidised electrode surface, giving clean platinum. Also analyte is adsorbed during period t_3 and is detected following the subsequent application of E_1. In addition there may also be oxidation of analyte reaching the electrode by convective diffusional mass

transport during period t_1.

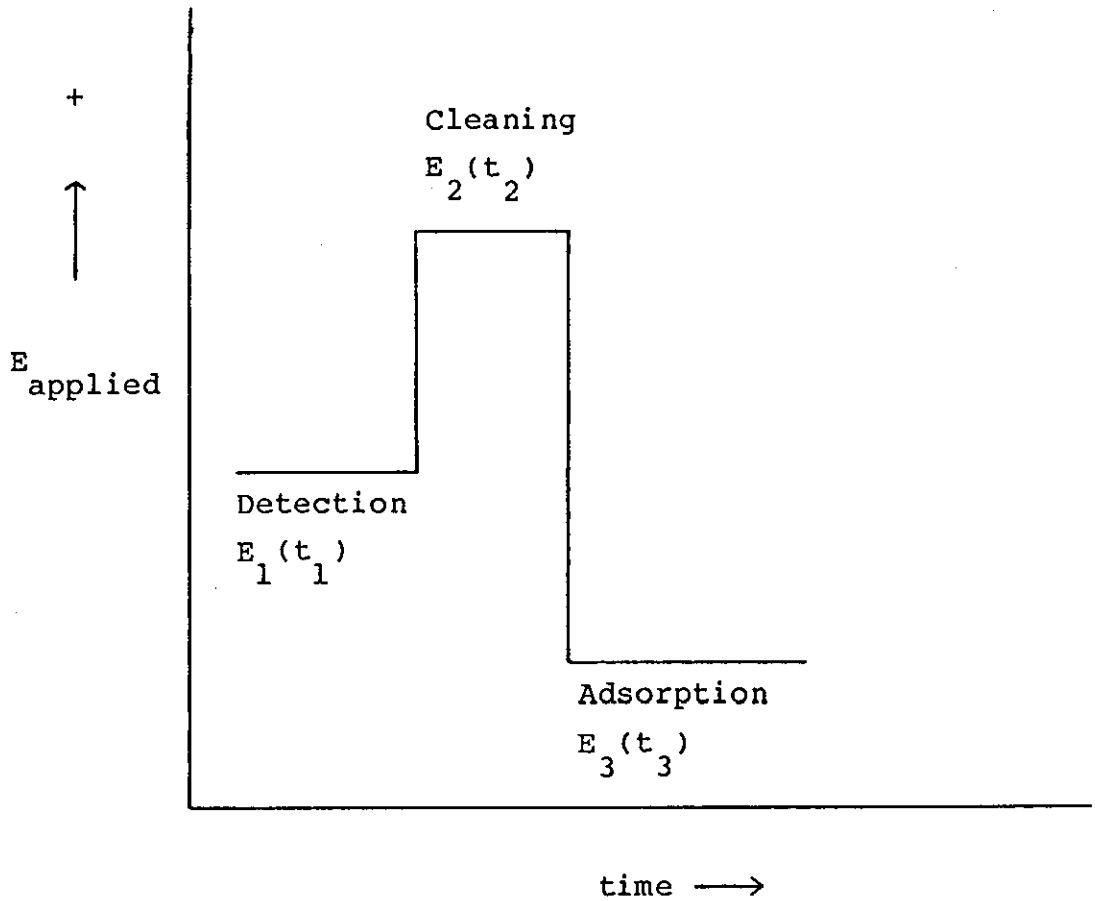

Fig. 3
Triple Pulse Waveform for PAD

A disadvantage of PAD at noble electrodes in flowing streams is that the linear dynamic range is observed in many cases to be rather limited[61]. Because of the surface controlled nature of the detection mechanism, calibration plots of 1/I vs. 1/C have been suggested[61-63] to linearise data over a larger dynamic range.

1.4 Flow Injection Analysis

1.4.1 Introduction to Flow injection Analysis

The term flow injection analysis (fia) first used by Ruzicka and Hansen[64] in 1975 is now widely used and the technique is well established. The acceptance of fia is undoubtably due to its versatility, which allows the method to be used in conjunction with a wide variety of detectors and analytical techniques, and for the assay of many organic and inorganic substances.[65] The essential features of fia may be presented by the following:

unsegmented flow;
direct injection;
controlled partial dispersion;
reproducible operational timing.

The basic scheme of an fia system is shown in fig 4.

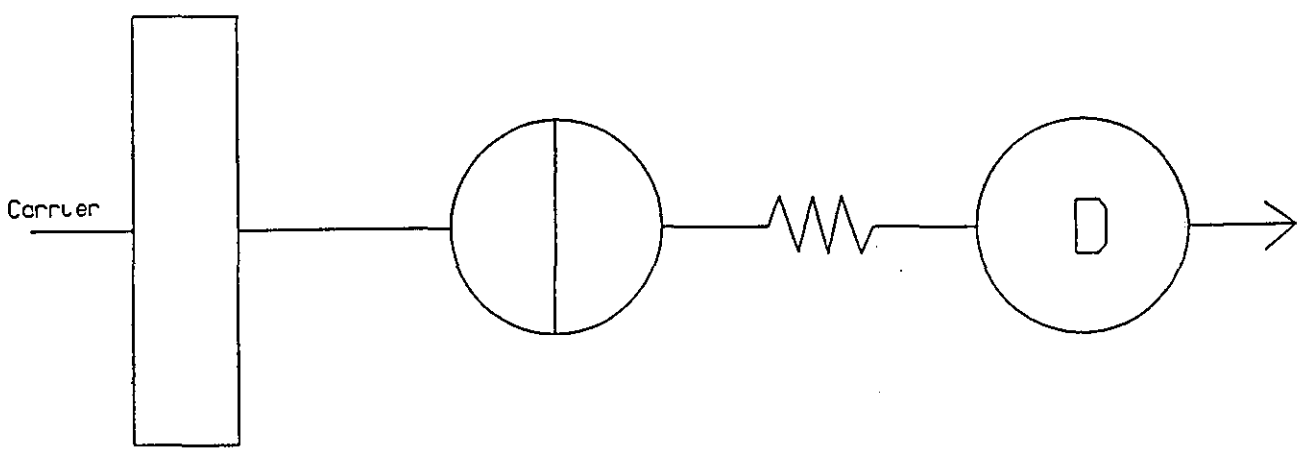

Fig. 4
Schematic Diagram of a typical fia Manifold with a single line

An fia system usually consists of the following units:

a) A propelling unit which should produce a steady pulseless flow of one or more solutions. The solutions may be of dissolved reagents or merely a carrier for the sample plug. The carrier might be a solution of solids, solvents or quite often pure water. The most common method of propulsion is a peristaltic pump, much cheaper methods include gas pressure systems and gravity feed reservoirs.

b) An injection system which allows the reproducible introduction of a volume of sample solution into the flow without stopping it.

c) A length of tubing along which the transport operation takes place, this is often referred to as the manifold. Dispersion of the sample plug into the carrier or reagent takes place as the plug passes along the tube, also there may be chemical reactions occuring.

d) A flow cell, accommodated in a detector which enables some property of the analyte to be transduced into a continuous signal which is amplified and fed to a recorder or a microcomputer.

The signal obtained from fia techniques is transient. A typical fia peak is shown in fig. 5. The parameters affecting the peak shape are :

a) The length and bore of the manifold.
b) The flow rate of the carrier.
c) The volume injected along with the length and bore of the sample loop.
d) The viscosity of the sample and carrier.
e) The detector and recording system time constant.

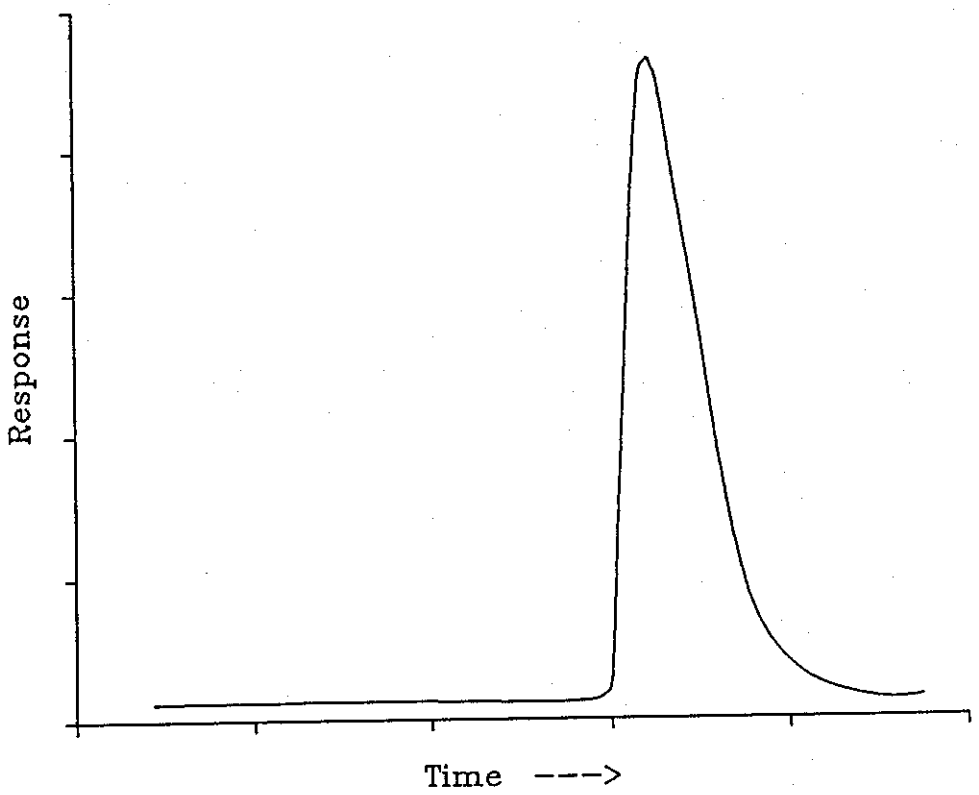

Fig. 5
Typical Output for Flow Injection Analysis

1.4.2 Theory of Flow Injection Analysis

The theory and applications of fia[66-67] are well covered by books and review articles.[68-72] The major advantages

of the technique are its speed of analysis, simplicity and the ability to perform sample manipulation on line. It is fairly easy to apply to traditional static methods using existing equipment and "home-made" manifolds constructed from inexpensive materials.

In fia transmission tubes the transport of liquid is essentially by laminar flow because the flow rates needed for the Reynolds number to exceed 2000 are fairly high and are not normally encountered. As a consequence of this the shape of the sample plug is always well defined.

There are two mechanisms by which the sample plug becomes dispersed. Convective transport tends to give a parabolic velocity profile, the molecules at the tube wall having a negligible velocity due to frictional forces. At the centre of the tube the molecules are least influenced and have the highest velocities. Molecular diffusion occurs wherever a concentration gradient exists.

The diffusion of molecules in the sample plug may take place in two directions, axial and radial. The effect of axial diffusion is minimal. The effect of radial diffusion is more significant. The effect is caused by concentration differences perpendicular to the direction of flow. The effect of convection on the peak shape may be observed immediately after injection of the sample plug. The contribution from radial diffusion becomes more marked with time and by the time the sample plug reaches the detector, for a typical fia experiment the effect will begin to be significant. The molecular diffusion coefficient and tube radius are the important factors determining the contribution from radial diffusion.

For moderate travel times (time elapsed before the first analyte molecules reach the detector), the peak has a

leading edge which rises rapidly to a maximum, and a tail which gradually returns to the baseline: this is the peak shape usually recorded in fia. For long travel times the peak shape becomes almost Gaussian.

The dilution of the sample by the fia system is termed the "dispersion" also "dispersion coefficient".[73] The dispersion is given by the following equation:

$$D = \frac{Co}{C}$$

where:

D = dispersion
Co = concentration of sample
C = concentration of sample at the peak maximum calculated from the peak response of the detector due to analyte.

Various mathematical models have been proposed to relate the dispersion in fia to the characteristics of the system[66]: the theory tending to differ from practice due to unaccountable errors contributing to tailing of the peak, e.g. from connectors, smearing of the sample plug from the injection process. Some authors apply an accommodation factor to allow for these differences.

1.4.3 Flow Injection Analysis with Amperometric Detection

The combination of amperometric detectors with fia is a very convenient method of detecting electroactive species provided that the sample matrix is fairly simple, owing to the moderate resolution of amperometry. Fia is often used to characterise new amperometric detection

principles and previously unstudied chemical systems before application to hplc.

The main strengths of amperometric detection in fia are high sensitivity and simplicity of flow manifolds. The increased sensitivity is due to mass transport to the electrode by convective diffusion. For amperometry at constant potential the background currents are smaller because there is no charging current, which is the most significant contribution to the noise in voltammetry. There is also the advantage over static voltammetric methods of the speed of analysis by fia. Fouling of solid electrodes can be a problem in oxidative voltammetry, fia with amperometric detection tends to be be less prone to this problem because the residence time of the sample at the electrode is much smaller. There is often linearity over several orders of magnitude of analyte concentration as for voltammeric techniques.

The amperometric flow cells used for both hplc and fia have the same requirements of design and performance that is low dead volume in conjunction with maximum signal to noise ratio. The cells need to be rugged, reliable and easily maintained. The cells commonly used are the wall jet, thin layer and tubular configurations, the theory of which is discussed in 1.3.1.

Although the selectivity of amperometric detectors is poor discrimination between electroactive and electroinactive compounds occurs as well as a limited resolution of some electroactive species. Consequently they are often used to enhance the separation by hplc of complex mixtures[74]. The use of pulsed potential waveforms increases the resolution, but also decreases the signal to noise ratio see 1.3.2. The use of dual electrode detectors can add selectivity and overcome the noise

problem. In some instances the removal of dissolved oxygen is unnecessary for reductive detection[75-77]. The use of dual electrode detection is comprehensively reviewed by Shoup in reference (78).

1.5 Electrochemical Cells and Instrumentation

1.5.1 Potentiostatic Control

In voltammetric and amperometric experiments the requirements are for control of the potential of the working electrode and to measure the current due to electrochemical processes occurring at this electrode. A reference electrode is needed for comparison purposes because it is not possible to directly measure the potential between the working electrode and the solution phase, this potential is termed the inner potential. The reference electrode serves to complete the circuit and to provide a second interfacial potential so that the relative potential of the working electrode may be known. If no current is passed, the influence of the applied potential does not extend beyond the diffuse layer (outer part of the electrical double layer).

If the working electrode potential is changed such that a current flows due to electrochemical processes then there will be a potential drop across the bulk solution in addition to the inner potentials. If the current is very small and the solution resistance between the electrodes is small then the inner potential will be close to the applied potential, also if the reference electrode carries a negligible current then its potential is almost constant. This is often not the case and a third electrode termed the auxiliary electrode is used to carry the current. The reference electrode is used only

to sense the inner potential of the working electrode. The device used to control the three electrodes is called a potentiostat. A schematic diagram of an electrochemical cell as an impedance network is shown in fig. 6.

For current flow as above, the potential dropped between the auxiliary electrode and reference electrode is compensated for by the potentiostat using a high impedence feedback loop. This controls the potential between the reference and working electrodes. This potential consists of the inner potential of the working electrode plus a small uncompensated resistance of the solution bulk. The placement of the reference electrode in relation to the working electrode can affect this uncompensated resistance.

A schematic circuit diagram of a potentiostat is given in fig. 7, the device depends on the use of operational amplifiers (op-amps). An op-amp is a special device which has a very high input impedance allowing it to measure voltages without perturbing them. The devices have a high gain enabling a small voltage differential at the input to drive the amplifier to its limit. Normally the amplifier is stabilised by feeding back part of its output to what is known as the inverting input. The way in which the feedback is achieved determines the properties of the op-amp: current or voltage may be followed by feedback of the respective property.

1.5.2 Amperometric Flow Cells

The geometry of the cell body and each electrode, as well as the placement of the electrodes within the cell are important factors contributing to overall cell performance. The time constants of the cell depend on the

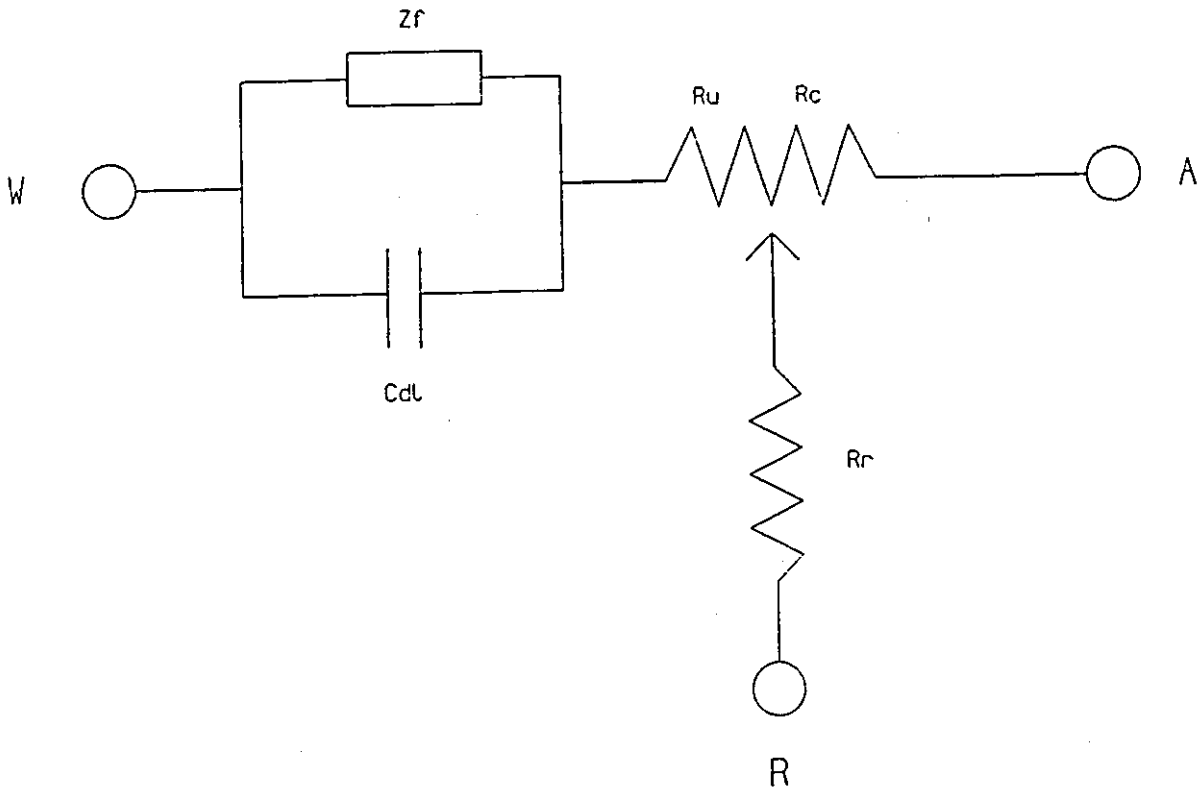

Fig. 6

Equivalent circuit of an Electrochemical Cell

A = auxiliary electrode

R = reference electrode

W = working electrode

R_c = compensated resistance

R_u = uncompensated resistance

R_r = reference electrode impedance

Z_f = faradaic impedance

C_{dl} = double layer impedance

$R_t = R_u + R_c$ (total cell resistance)

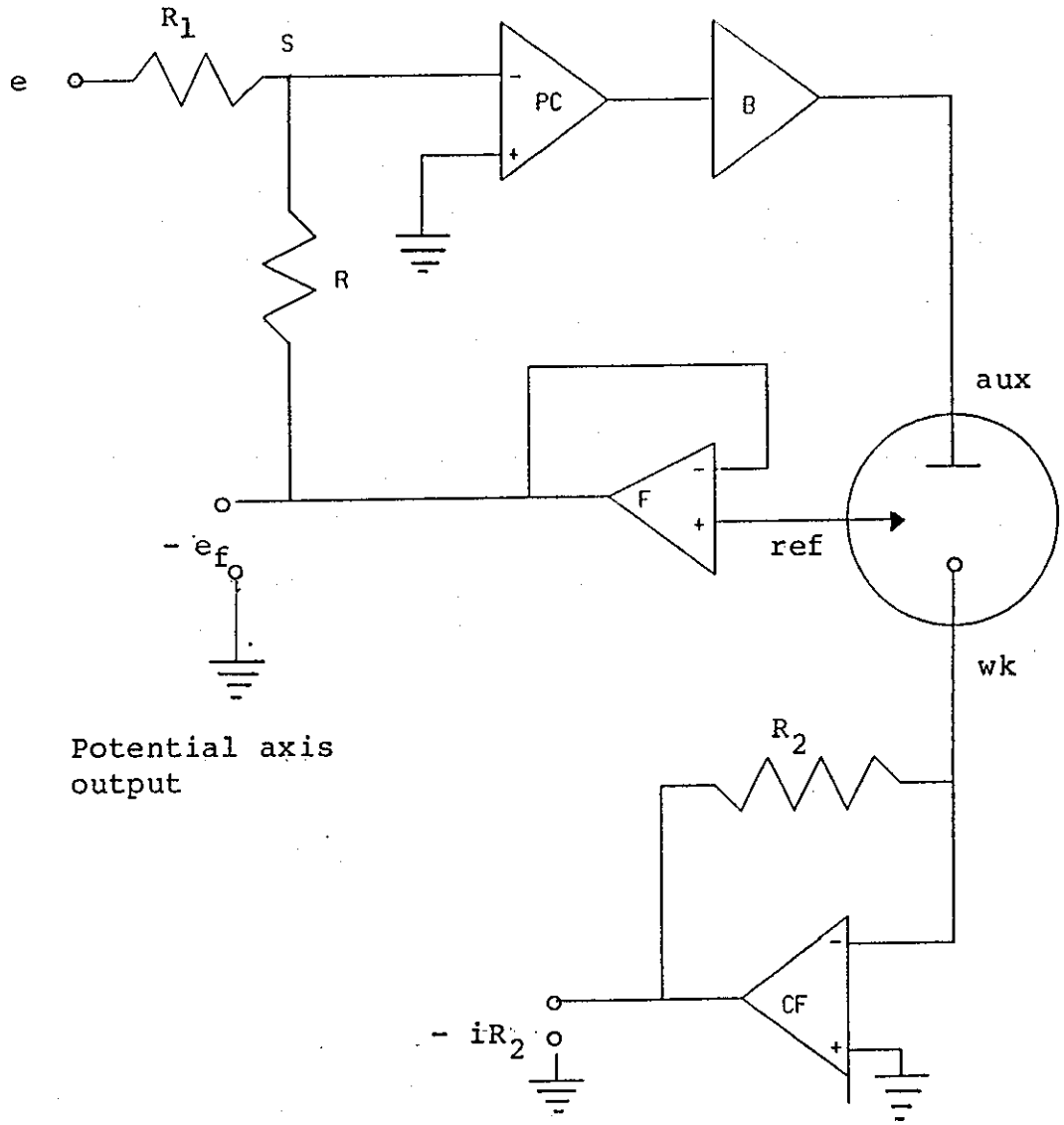

Fig. 7

Schematic diagram of a Potentiostat

PC = adder control amplifier (maintains ref potential - e V vs gnd)

B = booster (for output voltage)

CF = current follower

F = voltage follower (avoids drawing current from ref electrode)

e_f = - e_{wk} (vs ref) (potential axis output to chart recorder

- iR_2 = current axis output to chart recorder

compensated and uncompensated resistances and the double layer capacitance of the working electrode and must be compatible both with the electronics and the electrochemical technique used.

The operation of a potentiostat is described in (1.5.1). For most analytical applications the effect of electrode placement is usually negligible because the iR drop throughout the bulk solution may be 1 mv or less. For pulsed potential measurements the background currents which are offset may be considerable especially for PAD, where large potential pulses are used. In this case it is wise to place the reference electrode opposite the working electrode in order to minimise the uncompensated resistance. The potential drop iR_u is an error in the accuracy of potential control.

Geometry of Flow Through Cells

In order to optimise amperometric flow through cells used for fia and hplc there are many physical factors to be taken into account. The detector only responds to analyte close to the electrode so the mass transport of analyte to the electrode and the cell hydrodynamics determine the response and the dead volume of the amperometric detector cell. The baseline noise is mainly dependant on irregularity of the flow of electrolye, for an electrode of given area. The mechanical finish of the cell probably contributes to this noise by generating a degree of turbulance to the flow. The electrochemical noise mainly depends on the area of the electrode.

The relative merits of various detector geometries have been investigated by several workers[48,79-84], and it seems that the performance of the wall jet and thin layer cells is comparable. Although Kissinger in his book[85]

states that "in contests to establish superior performance, conventional thin layer cells have consistently come out the winner". The detectors most frequently used for detection in fia and hplc are the thin layer and wall jet cells. The applications of channel and tubular electrodes was recently reviewed by Compton and Unwin[86].

The Wall Jet Cell

The wall jet cell has been employed by various workers in two distinct configurations, as a thin layer cell[87,88], and a large volume cell[37,38,89]. It has been shown by Albery and Brett[90], and Gunasingham and Fleet[89] that constricting the cell geometry as a thin layer actually prevents true wall jet behaviour and does not decrease band spreading substantially. This is due to interference of the backwall and nozzle body in the boundary layer.

A summary of the criteria for optimising the geometry of the wall jet cell is as follows.[91]

i) The backwall and nozzle should be well clear of the boundary layer.
ii) The bulk volume outside the boundary layer should be large.
iii) The diameter of the jet impinging on the electrode should be at least ten times smaller than the electrode diameter.
iv) The free jet should be stable and posses laminar flow characteristics.

For typical flow rates i.e. 2-6 cm^3 min^{-1}, the separation between working electrode and nozzle needs to be about 2 to 4 mm.[91] Decreasing the electrode area increases the signal to noise ratio, but in practice there is a minimum

area below which the noise does not decrease. This was estimated to be about 0.1 mm^2 by Elbicki et al[36], and it is because there is a noise term related to the electrode size which is independent of electrode area.

It is difficult to place the reference and auxiliary electrodes close to the working electrode without interfering with the boundary layer, and less thought seems to be given to their placement than the geometry of the cell. The reference electrode is usually placed at the side of a conventional disc type solid electrode; the auxiliary electrode is either placed similarly close to the working electrode or the cell outlet is used as the auxiliary electrode. An advantage of the large volume wall jet cell is that there is interdiffusion of the bulk solution with the jet of analyte. This has been used to add suporting electrolyte to the effluent so that electrochemical detection can be accomplished in normal phase hplc.[37] Similarly anodic stripping voltammetry has been accomplished, without the need to flush out the cell.[91]

Thin Layer Cells

The thickness of the solution layer should be uniform, and in order to minimise edge effects the width of the solution layer should be wider than the electrode area. The thin layer is usually achieved by sandwiching a spacer between two blocks. The thickness of the layer is easily varied by choosing different spacer thicknesses. A cylindrical channel of fixed thickness has also been used. A commonly used cell configuration incorporates the reference electrode directly opposite the working electrode to minimise the uncompensated resistance: stainless steel outlet tubing is used as the auxiliary electrode. The thickness of the spacer is such that the

dead volume is small without making the compensated resistance between the reference electrode and auxiliary electrode too large.

The current paths usually run parallel to the electrode surface and a significant proportion of the iR drop exists along the electrode surface therefore the potential between the working electrode and the solution is not uniform across the face of the electrode. When thin layer cells have been used with non-aqueous solvents the iR drop problem can be severe due to poor conductivity.

The auxiliary electrode is never placed upstream of the working electrode because of the possible interference of products from the former with the later, this can also be a problem when the auxiliary electrode is placed opposite the working electrode in order to make the potential on the working electrode evenly distributed. Ionic separation of the reference electrolyte from the bulk solution may be achieved by means of Vycor glass (Corning 7930 glass) or ion exchange membranes (DuPont Nafion 811).

Thin layer flow through cells are commonly used in hplc, this is because the cells work efficiently at the flow rates typically used i.e. 1-2 $cm^3 min^{-1}$;whereas the wall jet cells are more sensitive at the higher flow rates used in fia, typically 2-6 $cm^3 min^{-1}$.

1.6 Electrodes

1.6.1 Mercury Electrodes

Mercury is widely used as an electrode material in electroanalytical chemistry. There are three important reasons for using mercury electrodes. They are; most importantly a very high overvoltage for the evolution of hydrogen, Mercury is liquid at normal temperatures and also mercury may be obtained in a highly pure state. Potentials as negative as -2.0V vs SCE in aqueous solution are accessible using mercury electrodes. Gold electrodes are only usable to about -1.0V vs SCE and platinum is unusable much below 0.0V vs SCE. Mercury dissolves at about +0.3V vs SCE, for oxidations occuring at potentials more positive than this carbon or platinum electrodes must be used.

The advantage of mercury over solid electrodes is that the surface is renewable in situ. For the dropping mercury electrode (DME) the surface is continuously renewed during the potential scan. A disadvantage of this is the charging current due to the growth of the drop. The static mercury drop electrode is a more recent development than the DME. The scan is performed on a rapidly formed drop at a capillary tip[92], the current measurement being made when the drop is almost completely formed and the charging current due to drop growth is low. If the drop is maintained indefinitely then the the electrode is known as a hanging mercury drop electrode, and is useful for inverse voltammetry (stripping analysis).

Mercury electrodes used for detection in fia and hplc include conventional DME's[93], sessile mercury drop electrodes[88,94] and thin film electrodes.[95,96] The

sessile mercury drop electrode is prepared by placing a mercury drop on a small contact made of metal. This type of electrode was used by Neeb[94], and has been employed by Fogg and workers[88] incorporated into a wall jet cell. The mercury film electrode is most often prepared by coating a glassy carbon electrode[95] electrochemically by means of a plating solution containing mercury (II) salts. Care needs to be taken of the conditions for the plating otherwise the coating is uneven and poorly formed. Gold readily forms an amalgam and has been used for reductive detection in hplc[96]. The electrode is easily prepared by dipping a gold electrode into mercury and scraping off the excess mercury with a straight edge. Bratin and Kissinger[97] found that although glassy carbon has a poorer negative potential limit than the amalgamated gold electrode it was more convenient to use.

1.6.2 Carbon Electrodes

Since about 1950 electrochemistry at solid electrodes has become increasingly popular. A major reason for the use of solid electrodes is that many reactions can be studied which are not accessible at mercury electrodes. The ideal properties of a solid electrode are that it should be stable, be easy to prepare, it should have a large useful potential range, and an easily reproduced surface. Carbon electrodes come closest to meeting these requirements. A variety of different forms of carbon have been used, the most important being glassy carbon (correctly termed glass like carbon), graphite and carbon fibre. Gross and Jordan[98] have reviewed the use of carbon as an electrode material for electroanalytical chemistry.

Spectroscopic Graphite Electrodes

Spectroscopic graphite was one of the first reported uses of carbon electrodes for voltammetry. The material is available in the form of rods. The outside of the rods are sealed with ceresin wax and the electrode surface is prepared by breaking off the tip before each voltammogram is recorded. The background currents tend to be rather large: this may be attributed to the porous graphite structure. The reproducibility of voltammograms is poor due to the crude method of surface preparation. Wax impregnation was used to fill in the pores and thus decrease the background currents.[99] The preparation of the surface was improved by machining in a lathe and wetting the fresh surface with surfactant solution[100], even so the performance of this type of electrode does not compare favorably with other carbon electrodes.

Carbon Paste Electrodes

The carbon paste electrode was introduced by Adams[101], and was subsequently applied to the study of many compounds by Olson and Adams.[102,103] The electrode consists of a thick paste of powdered graphite and an inert mulling liquid. The mulling liquid needs to be free of electroactive impurities, insoluble in the electrolyte medium and be involatile. The mulling liquid is usually bromonaphthalene or liquid paraffin (Nujol). Pungor et al[104] investigated silicone rubber as an alternative mull, the useful potential range of the electrode was -0.5V to +1.5V vs SCE. The paste is placed in a well in the end of a cylindrical holder. The electrode surface is prepared by rubbing the electrode on a clean piece of flat plastic to obtain a flat surface. The surface may easily be renewed by removing a thin layer from the tip of the electrode and replacing it with fresh material.

The small background current in the anodic range is considered advantageous for achieving low limits of detection in hplc with amperometric detection.[105] Very low detection limits for anodic detection in hplc have been reported for catecholamines using a microbore column.[106] . The low background current may result from the organic mull filling in any surface imperfections on the graphite powder hence decreasing the surface capacitance of the electrode. A major disadvantage of carbon paste electrodes are that they may only be used in media with moderate proportions of organic solvents. Marcoux et al[107] incorporated sodium lauryl sulphate into the paste in order to use the electrodes in organic solvents. It was suggested that the surfactant improved the wetting of the graphite by the mulling liquid. Atuma and Lindquist[108] developed a carbon paste electrode which was suitable for use with common solvents used in electrochemistry. The mull consisted of ceresin wax and silicone oil.

Rice et al[109] have studied the effect of differing pasting liquids on the electrode background current and reactivity. They found that the background current and electron transfer rate were both decreased by increasing the proportion of organic mull. Pretreatment of the electrode increased both properties to differing extents. Potential limits for different mulling liquids in various electrolyte media are available[85] . More recently Albahadily and Mottola[110] improved the response of carbon paste electrodes by adding 0.1% aqueous surfactant. The improved response with some species was partly due to adsorption, which was not detrimental. Other authors have noted effects characteristic of adsorption,[111,112] but may be attributed in some cases to dissolution of the electroactive species in the organic mull.

Composite Carbon Electrodes

More recently solid fillers have been used to bind the graphite particles, the fillers being more chemically resistant than the organic mulls. One of the most successful graphite composite electrodes has a filler of polychlorotrifluoroethylene (PCTFE, trade name Kel-F). These electrodes are termed "Kelgraph", the electrodes have a lower response to electroactive compounds than a conventional solid electrode, but the background current is decreased to a larger extent[113]. This behaviour may be attributed to the electrode acting as an array of microfaradaic electrodes. The best signal to noise ratio was obtained with a 15% mixture with respect to graphite. Other solid binders include PVC, chloroprene rubber, ceresin wax, and polyethylene.[114-117] Epoxy adhesive has been used as a filler by Wang[118], but the electrodes suffered from a large background current. Henriques and Fogg[119] described a method for preparing epoxy based electrodes using epoxy cured with hydrofluoric acid. The background currents were comparable to commercial glassy carbon electrodes. Armentrout et al[120] prepared a variety of carbon composite electrodes and the most suitable was found to be a 50% mixture of carbon black and polythene. The surface catalytic activity of the carbon black was suggested as a reason for the enhanced current.

Pyrolytic Graphite Electrodes

Walker has described the preparation, properties and structure of pyrolytic graphite.[121] Its structure is based on graphite like crystal units. The factors affecting the electrochemical performance of pyrolytic graphite and glassy carbon electrodes have been studied

by Panzer and Elving[122]. It was found that the most reproducible surface was produced by cleaving the electrode, rather than by grinding. Heplar et al[123] found the electrochemical properties of Pyrolite (an isotropic pyrolytic carbon) were similar to carbon paste, although it can be used at more negative potentials. They presented potential windows for various types of carbon electrodes in different electrolytes and compared them with pyrolytic carbon. Highly oriented pyrolytic carbon gives extremely flat electrodes after surface cleavage. Advantage of this property was taken in fabricating an amperometric thin layer detector[124] with a small channel thickness. It was rather insensitive because of the poor reversibility of redox reactions at the electrode. This was improved by electrochemical pretreatment but the response tended to fade.

Glassy Carbon Electrodes

Glassy carbon should now be correctly termed glass-like carbon according to IUPAC suggestions[125] for the nomenclature of different carbon materials, but the former term is still invariably used. Glassy carbon electrodes are the most widely used solid electrodes for voltammetry and amperometry. This is largely due to its chemical inertness, and the wide range of usable potentials, both anodic and cathodic. Glassy carbon is a gas immpermeable material which is formed by the heating of phenol-formaldehyde resins in an inert atmosphere. The properties of glassy carbon have been described by Yamada and Sato[126]. The use of glassy carbon as an electrode material in electroanalytical chemistry has been comprehensively reviewed by van der Linden and Dieker[87]. The structure of glassy carbon has been descibed as thin ribbons of graphite like sheets which are oriented randomly and are tangled in a complicated manner.[127]

The surface chemistry of glassy carbon has been likened to that of pyrolytic carbon at the graphite plane edges rather than the basal graphite planes[128]. The existence of redox groups on the surface of glassy carbon was suggested by Laser and Ariel[129] to account for the behaviour of the electrode on anodic and subsequent cathodic polarisation. The nature and number of these surface groups depends on the method of manufacture of the material also subsequent physical treatment and polarisation of the electrode. It is suggested that the high temperature treatment of carbon creates carboxylic groups[130], whereas the anodic oxidation in dilute mineral acid solutions results in the formation of quinone and hydroquinone groups.[131] Vasil'ev et al[132] have studied the influence of the temperature of manufacture on the hydrogen overvoltage for voltammetry at glassy carbon electrodes. They found that glassy carbon heated to 3000 ^{o}C exibits the lowest hydrogen overvoltage.

As a consequence of the surface chemistry the response of the electrode to electroactive species depends very much on the method of preparation of the electrode. The background current at glassy carbon electrodes is larger than at carbon paste electrodes, this has been attributed to increased capacitance of the electrode surface due to the micropores formed during the manufacture of the material. The pores are created by trapped gas bubbles evolved during the carbonisation process. The temperature needs to be steadily increased, otherwise an excessive amount of gas bubbles become trapped.

Gunasingham and Fleet[133] made a comparative study of glassy carbon as an electrode material. Monien[134] made a study of various types of carbon electrodes and concluded that pyrolytic and glassy carbon electrodes had the

largest usable potential range.

1.6.3 Preparation of Carbon Electrodes

Numerous methods for cleaning and activating carbon electrodes have been published, and have been reviewed by Hu et al.[135] The pretreatment usually involves polishing the electrode surface with alumina or fine diamond paste[133,136,137], this is usually followed by either electrochemical[136,138-140], or chemical[141] treatments. Ultrasonic cleaning has been used to remove traces of polishing material from the surface.[142,143] Plasma treatment[142] and laser treatment[144,145] have been used to clean and activate carbon electrodes. These procedures drastically affect the electrode performance. Most pretreatments are intended to improved the reversibility of redox reactions at the carbon electrode, although Wang and Tuzhi[146] have shown that an enhancement in stability (i.e. decrease in electrode poisoning) towards several compounds for glassy carbon electrodes was produced by a simple preanodisation. The stability enhancement was attributed to the formation of an oxide layer on the surface. For certain analytes a catalytic effect was also observed. Hoogvliet et al[147] showed that the degree of adsorption and deactivation of glassy carbon electrodes used for the amperometric analysis of adrenaline may be significantly decreased by an electrochemical pretreatment subsequent to polishing with fine alumina and diamond paste. Recently Poon and McCreeedy[148] described a method for repetitive in situ renewal and activation of carbon and platinum electrodes. A laser was synchronised with the drop knocker pulse from the potentiostat to irradiate the electrode surface prior to each potential step for differential pulse voltammetry. The laser assisted voltammetric experiment provided enhanced resolution and greatly extended

electrode life for several organic species. Van Rooijen and Poppe[149] demonstrated that the application of a voltage pulse waveform for five minutes is effective in restoring the response of glassy carbon electrodes after deactivation by organic compounds.

1.6.4 Metal and Metal Oxide Electrodes

Metal solid electrodes are less popular than carbon as working electrodes for voltammetry and amperometry because they tend to exhibit higher background currents especially at the extremes of potentials. Platinum and gold are the only commonly used metal electrodes.

Platinum is suitable as an electrode material for anodic oxidations, but the formation of platinum oxides at potentials greater than about +0.8V vs SCE gives rise to high background currents and may inhibit the redox reactions of the electroactive species.[10] The overvoltage for hydrogen evolution on platinum is very small, making it unsuitable as an electrode for reductions. Adams[10] recommends cleaning platinum electrodes in chromic acid, followed by electrochemical reduction of the surface oxides in background electrolyte. Any sorbed hydrogen produced during the reduction step is reoxidised by holding the electrode at a slightly positive potential. James[150] and Fetham et al[151] have surveyed activation methods for platinum electrodes together with an appraisal of kinetics and mechanism of electrode mechanisms. Goldstein and Van de Mark[152] described a chemical cleaning method for platinum electrodes and showed that the rate constant for the $(Fe(CN)_6)^{3-/4-}$ redox couple varied by two orders of magnitude according to the pretreatment of the electrode.

Gold has a larger overvoltage for hydrogen evolution and

is used for reductions down to about -1.0V vs SCE. The anodic range is limited by formation of gold oxide at about +0.4V vs SCE, also by substances in solution which form stable complexes with the gold.[153,154]

Palladium and rhodium are of little use as an electrode material because of hydrogen adsorption on palladium[154] and adsorption of oxygen on both rhodium and palladium.[154]

The interest in electrocatalysed anodic detection at metal oxide electrodes is slowly increasing, but is still with limited applications. It is well known that certain metal oxides are good electrocatalysts[155,156], but the limited potential range and poor selectivity make them unsuitable for voltammetric applications. In amperometric detection in hplc, voltammetric resolution is less important and the electrocatalytic activity for certain types of compounds may be useful.[60] Doped lead dioxide electrodes have been shown to have promise for electrocatalysed detection in acid media.[60] Nickel oxide electrodes have been studied by Huber and workers for electrocatalysed detection in fia and hplc[157].

1.6.5 Micro-electrodes

Electrodes are referred to as micro-electrodes when their diameter is less than about 10 μm. Carbon fibre is the commonly used material for this type of electrode, the fibres have diameters in the range 6-12 μm. These electrodes have found applications in clinical chemistry where their small size has been an advantage for in-vivo studies. In analytical chemistry their use is becoming more common. Carbon fibre micro-electrodes are usually formed from the high temperature pyrolysis of polyacrylonitrile (PAN) or pitch. The basic unit of the

fibres is a ribbon consisting of a graphitic layer.[158] Bunches of these ribbons run parallel to each other and are known as microfibrils. The structure of carbon fibres is of longitudinal microfibrils which are packed together as in a tree ring, with voids between them due to poor packing.

The most common method of constructing voltammetric electrodes from a single fibre is by sealing the fibre into a glass capillary. A detailed account of the preparation of these electrodes is given by Anderson and Cushman.[159] Wightman has discussed some of the differences between voltammetry at micro-electrodes and at conventional ones.[160] He showed that micro-electrodes could be used for ultra fast voltammetry in conventional electrolytes, with scan rates up to 20 kVs^{-1}.[161] An improvement in signal to background noise ratio should be possible where there are flow irregularities caused by pump pulsations, because micro-electrodes are insensitive to convection due to the small size of the diffusion zone.[162] Caudill et al illustrated the increased signal to noise ratio of a detector constructed from 100 carbon fibre discs, compared with glassy carbon at high potentials. Composite electrodes consisting of mixtures of graphite and PCTFE[163] termed "Kelgraph" electrodes show increased signal to background noise ratios compared with glassy carbon electrodes when used for the detection of carbamate pesticides separated by hplc.[164] A review of the electroanalytical applications of carbon fibre electrodes is available.[165]

1.6.6 Chemically Modified Electrodes

The area of chemically modified electrodes is one of the most active areas of electroanalytical chemistry. The

subject has been comprehensively reviewed by Murray.[166] More recently a short review article by Murray et al[167] has outlined some of the ground rules for designing chemically modified electrodes for analytical purposes. The understanding of the mechanism of electron transport through the mediator, and transfer between the mediator, and the redox couple in solution is being advanced by further developments in theory.

The use of chemically modified electrodes for analytical purposes is becoming more frequent. Two major advantages are selective determination of species that are poorly electroactive, also selective concentration of components into a film on the electrode and subsequent detection for both metals and organics. The preparation of stable and reproducible modified electrodes remains a problem.

1.7 Detection and Monitoring of Trace Levels of Aromatic Amines (Anilines) in Air

1.7.1 Introduction

Primary aromatic amines are widely used in the manufacture of a variety of industially important substances. They are intermediates in the production of dyestuffs, pharmaceuticals, and photographic and agricultural chemicals, and are used in the processing of rubber.

Many aromatic amines are known or suspected to be carcinogenic towards humans.[168,169] The manufacture or use of certain amines is prohibited by law, also the use of others is controlled, for example 1-naphthylamine. The threshold limit for aromatic amines in most countries is in the low ppm ranges, hence it is important to be able

to detect these trace levels of amines.

1.7.2 Sampling of the Atmosphere

A widely used method of sampling amines in the atmosphere is by passing a metered volume of air through a suitable sorbent, such as silica gel[170] or a porous polymer.[171] The trapped material is thermally desorbed or extracted by a solvent for subsequent analysis in the laboratory. By increasing the volume of air sampled, enrichment of the amine is possible, but the concentration of interferents is also increased because the sorbents tend to be non-selective. The precision of the measurement is decreased, because the trapping efficiency is decreased.

Gas washers and impingers are generally less efficient means of trapping vapour samples, than adsorption by solid material because the rate of dissolution of vapour is lower than that of adsorption. An advantage is that the trapping process can be made semi-continuous by frequently replacing the absorption liquid, whereas adsorption onto solids must be discontinuous, due to the difficultly of releasing the adsorbed sample. Bosset et al[172] described a gas bubbler which could be rinsed out and used repeatedly in situ, by the use of valves and a rotating spray-head. Hrabeczy-Pall et al[173] presented a method for continuously monitoring fluoride in air using a recirculating absorber.

Several methods have been described where the vapour is continuously intercalated with the absorption liquid.[174-176] The plugs of gas sample are entrained by the absorption liquid towards the detector, with dissolution of the gas. A debubbler is required to destroy the gas bubbles. Although efficient, only low

levels of sample enrichment are possible.

More recently diffusion denuders are being used for the collection of gases. The walls of the diffusion denuder need to be coated with suitable agents in order to act as a sink for the gas of interest, for example oxalic acid has been used for ammonia[177], and for aniline.[178] After collection the coating and sample are washed off and the walls are recoated. Dasgupta et al[179] developed a diffusion scrubber in which the collecting element is a membrane tube around which a scrubber solution flows continuously, and it is possible to carry out analysis continuously.

Devices have been developed in which the analyte gas is accumulated by spraying an aerosol of a liquid into the gas stream and condensing the enriched liquid.[180,181] The devices are said to be efficient, give a degree of enrichment and are capable of continuous monitoring.

1.7.3 Measurement Techniques

Colourimetric Methods

If an immediate result is required then the simplest method is to use test papers impregnated with a colour forming reagent. The papers are exposed to a measured volume of air, then compared with colour standards. These test papers can be quite sensitive, but they often suffer from interferences, and instability of the reagents. Meddle and Smith[182] developed a simple field test for primary aromatic amines with a sensitivity of about 10ng, using a test paper impregnated with 4-(dimethylamino)cinnamaldehyde. By incorporating an antioxidant in the reagent formulation the shelf life of

the test papers was extended to seven days.

This reagent has been used to determine primary aromatic amines colourimetrically[183]. The aromatic amine was dissolved in ethanol, then HCl the reagent was added. The colour took about 30 minutes to develop; the absorbance was measured at 520 nm. The limit of detection varied between 0.02 to 0.1 $\mu g cm^{-3}$ according to the amine. Albi and Vioque[184] used the same reagent to determine fatty acid anilides and free aniline in edible oils, with detection limits of about 0.1mg kg^{-1}. Kupfer and Bruggeman[185] investigated the reaction of 4-dimethylaminobenzaldehyde with aniline but the method was not specific or sensitive enough for determination of trace levels of anilines. Bratton and Marshall[186] developed a method for the colourimetric determination of aniline using a coupling reaction with N-1-naphthylenediamine in dilute acid, followed by extraction into an organic solvent. Chrastil and Wilson[187] adapted the method for the determination of aniline in the presence of 4-aminophenol. Disadvantages are the slow reaction rate; the colour intensity takes two hours to become stable, measurement being at 530 nm. More recently Norwitz and Keliher[188] also used N-1-naphthylethylenediamine for the determination of trace amounts of aniline. The detection limits were 0.8 and 0.6 $\mu g cm^{-3}$.

Rowat and Singh's method[189] for the determination of amines was based on a colour forming reaction of the amine with Fe(III) ions and acetyl chloride. Colour formation was faster than for Bratton and Marshall's method but was general for primary amines and was less sensitive.

El-Dib[190] proposed a much faster method for the

determination of aniline derivatives in water, compared with Bratton and Marshall's. El-Dib's method involved diazotisation of the amine in the sample with resorcinol or 1-naphthol and could be used to detect aniline concentrations down to 0.1 ppm, with a coefficient of variation between 0.5 and 6.

Some of the colourimetric methods are quite sensitive but the big disadvantage is the time required for colour development and the considerable sample preparation. The selectivity is adequate for samples with simple matrices.

Spectrophotometric Methods

Mixtures of phenol and aniline were determined in air and solutions[191] by measuring the absorbance at 235 nm in pH 7 buffer where only aniline absorbs and in dilute alkali where both compounds absorb and the aniline λ max. is unchanged. The method was used for determining concentrations down to 0.8 mg m^{-3} of aniline after passage of the air sample through Na_2CO_3 solution at 1 l min^{-1}.

Fluorimetric Methods

Tomkins and Ostrum[192] determined primary aromatic amines in synthetic crude oil by derivatisation with fluorescamine then fluorimetric analysis. The fluorescence excitation was at either 390 or 389 nm and the emission spectrum was scanned between 400 and 600 nm. The detection limit was 0.14 µg cm^{-3} for meta and para toluidine. A sensitive fluorimetric method[193] for the determination of primary aromatic amines was described involving diazotisation of the amino group and coupling with 2,6-diaminopyridine, followed by reaction of the resulting azo dye with ammoniacal cupric sulphate. The

excitation was at 360 nm and the emission was measured at 420 nm. The detection limits were in the range 2 to 6 ng cm^{-3} (2 ng cm^{-3} for aniline) with a precision of 6%.

Electroanalytical Methods

Chey and Adams[23] applied anodic pulse voltammetry to the trace determination of aromatic amines and phenols using a carbon paste working electrode. Good reproducibility and linearity of calibration curves were achieved at the ppm to ppb level, but for some amines e.g. 1-naphthylamine serious filming occurred, and a fresh electrode must be made for each run. The voltammetric determination of aromatic amines (including aniline) at a glassy carbon electrode was investigated by Olabiron.[194] Adsorption at the electrode was found to be the main difficulty, especially at the 10^{-4} M level. More recently the on line voltammetric analysis of aniline[195] was discussed with respect to minimising electrode poisoning.

Fogg et al[196] presented a method for the analysis of aromatic amines by diazotisation followed by reaction with nitrite. The excess nitrite remaining was monitored on-line using a glassy carbon electrode: amine concentrations in the range 1 μM to 0.1 mM were detected by this indirect method. Fogg et al[197] have also described an on-line bromimetric method for the determination of phenol, aniline, aspirin and isoniazid using fia. Bromine was produced by injection of acid into a bromate-bromide eluent and monitored at a glassy carbon electrode. The sample concentration was determined by the decrease in the bromine peak. Concentrations of aniline down to 1 μM were measured with a precision better than 3%. A recent paper[198] describes the electroanalysis of primary amines using carbon paste electrodes modified with $[Fe(CN)_5(L)]^{3-}$, where L is

pyridine 4-carboxaldehyde. The electrode is immersed in the amine solution to be analysed and an imine is formed at the electrode surface. The voltammetric response of the imine is used as the analytical signal. Aniline gave a suitable response at the electrode (imine formation is specific for primary amines).

Amine vapours have been detected directly using electrochemical sensors. Ghoroghchian et al[199] described a novel approach to electrochemistry in the gas phase using a 5 μm carbon fibre micro-electrode in combination with a palladium pseudo reference electrode. The electrode system was used as an amperometric detector for gc and as a gas sensor for a range of compounds including aniline.

Blurton and Stettor[200] designed an amperometric detector suitable for gas chromatography, using a PTFE bonded diffusion electrode. The diffusion electrode consists of a cavity filled with electrolyte in contact with a three electrode system. There is an air access to the counter and reference electrodes, while gas exposure to the working electrode is accomplished by a labyrinth path into the electrode from the outside. Stettor and Tellefson[201] discussed the electrochemical oxidation of hydrazine and methyl hydrazine using the sensor described by Blurton and Stettor.[200]

Gas Chromatography

When more resolution of sample components is required then the techniques of gc and hplc give the necessary separation with good detection limits. Luckas and Lorenzen[202] determined aniline and anilides in oil by both gc and hplc. The sample was saponified, extracted with solvents then extracted into HCl solution. The

absorbance was monitored at 244 nm for hplc and for gc detection was by flame ionisation detector (fid). The detection limits for both methods were 0.1 mgl^{-1}; this could be reduced to 0.01 mgl^{-1} by bromination of the aniline.

The nitrogen phosphorus (N-P) detector is more selective towards aromatic amines and also more sensitive than a fid. Cooper et al[203] determined selected nitrogen-containing pollutants using a N-P detector. Detection limits ranged between 0.5 and 43.7 pg for aromatic amines. Selective detectors were evaluated for gc and hplc methods[204] for the trace analysis of aniline in water.

A good detection limit was established for some amines using hplc with an amperometric detector, but some dinitroanilines were difficult to oxidise. The uv detection was more general but the detection limits were inferior (1 to 10 ng injected). The preferred method was gc with N-P detector. Detection limits for aniline and 18 of its derivatives were in the range 0.1 to 4.6 ng injected (1 to 12 $\mu g\ l^{-1}$ in sample).

The electron capture detector (ecd) is very sensitive and selective towards halogenated compounds, in order to detect aromatic amines precolumn derivatisation is required. Coutts et al[205] determined aniline and aminophenols in aqueous solutions using gc with ecd. The acetyl derivatives were prepared before treatment with trifluoroacetic anhydride. Concentrations down to 0.1 n mol of each analyte were detected in 100 cm^3 of water (on column detection limit 0.33 p mol). Meddle and Smith[206] used gc with ecd to determine the concentration of aromatic primary amines, in atmospheres generated using diffusion tubes. A heptafluorobutyryl chloride derivative

was prepared and purified. Concentrations down to 20 pg per 5µl of solution were easily detected with a coefficient of variation of up to 5%.

High Performance Liquid Chromatography

The polar nature of aromatic amines and their low vapour pressures make their analysis by gc difficult, because the amino groups may be adsorbed on the chromatographic support resulting in severe tailing or losses of components. The use of amperometric detectors in hplc is becoming more common because for certain types of compounds (especially aromatic amines), these detectors offer a sensitive and somewhat selective means of detection compared with spectrophotometric detectors.

Varney and Preston[207] compared a coulometric porous carbon electrode detector with a thin layer amperometric detector fitted with a glassy carbon electrode for the trace analysis of aromatic amines in sea water using hplc. Detection limits were 15 and 1.5 nM resectively for aniline. Lores et al[208] determined some halogenated anilines and related compounds by hplc with amperometric and UV detection. The detection limit was 10 ng to several µg for UV detection at 254 nm. The amperometric detector gave up to 50 times better signal to noise ratios, the detection limit for aniline was 0.23 ng and for 4-chloroaniline 0.38 ng. Concialini et al[209] studied the chromatography and voltammetry of 21 different aromatic amines, with a view to their detection in hplc by amperometry. Detection limits were of the order 0.1 ng for 20 µl injected using a wall jet cell fitted with a glassy carbon electrode. A carbon fibre amperometric detector was used to monitor aromatic amines[210] after separation by hplc. The amperometric detector was substantially more sensitive than a UV

detector connected in series, and the lowest detection limit was a few picograms. There are many other examples where improved detection limits for aromatic amines have been achieved by amperometric detection rather than UV detection in hplc.[211-214]

Stahl et al[215] determined anilines in oil by hplc with fluorescence detection after derivatisation with fluorescamine. The anilines were liberated from the oil by heating with soda lime. The detection limits for aniline and anilides was 1 ng (0.1 ppm). Baumann and Marke[216] determined migrated aromatic amines from plastics in food simulating solutions. The amines were separated by hplc and detected with amperometric and fluorescence detectors. For amperometric detection the detection limit for several aromatic amines was 0.09 ppb (including aniline) to 1.3 ppb (o-dianisidine). By precolumn derivatisation with fluorescamine and fluorescence detection the detecion limits were 0.34 ppb (m-xylyenediamine) to 56 ppb (benzidine).

1.8 Aims of the Work

The need for portable monitors to detect volatile organic species in air is of special importance when highly toxic species are present. Aniline was selected as a suitable species for this study, because it has properties which are similar to those of some toxic chemical agents.

The aim of the research is the development of an electroanalytical device for the measurement of aromatic amines (especially aniline) in air. An evaluation will be made of the instrument's sensitivity and selectivity. From this work it ought to be possible to indicate the feasibility of developing a detector which would have

applications as an on-line monitor for use in the field.

Electrochemical detectors offer operational advantages in terms of selectivity towards the electroactive species of interest. Due to the simplicity of the sensor, miniaturisation of electrochemical detectors should be feasible because the electronic components necessary to operate the device are readily available in miniaturised form.

The development of the electrochemical sensor will be carried out in three phases:

i) the investigation of the electrochemistry of aromatic amines at solid electrodes using conventional voltammetric techniques;

ii) the design and investigation of voltammetric techniques suitable for the detection of anilines using flow through and static cells.

iii) Construction and testing of a gas sensing cell.

CHAPTER 2
INSTRUMENTS, EQUIPMENT AND CHEMICALS

2.1 Instrumentation

Metrohm E 611 VA-Detector

This instrument is a potentiostat module, suitable for amperometric methods. Voltammetric methods were used with this instrument connected to a Metrohm E 612 VA-Scanner module. The Metrohm E 611 VA-Detector was capable of the following methods of operation:

(1) DC Amperometry
(2) DC Tast Amperometry (integrated current measurement over the last 200ms of drop time (t drop))

(3) Differential Pulse 1 (DP1: duration of pulses superimposed on base potential = 60ms; integrated current measurement for 20ms immediately before and at the end of the pulses)

(4) Differential Pulse 2 (DP2: duration of pulses superimposed on base potential = 160ms; current integration as for DP1)

The time constants for the three damping setting are not available.

Metrohm E 612 VA-Scanner

When connected to the above potentiostat the Metrohm E 612 VA-Scanner provided the following addition methods of operation:

(1) Single-sweep voltammetry
(2) Triangular-wave voltammetry
(3) Cyclic triangular wave voltammetry

Dionex Ionchrom / Pulsed Amperometric Detector

The Pulsed Amperometric Detector comprised of a potentiostat which applies a repeating sequence of up to three different, selectable applied potentials (E1, E2, E3) to the cell working electrode. Each potential is applied for a selectable period of time or pulse duration (t1, t2, t3, respectively).

In all modes of operation the potentiostat measures current only during the E1 pulse. Sampling the current occurs 20ms before the end of the E1 pulse. Use of a 1/50 second (20ms) sampling period cancels the 50Hz line noise. The sampled current is amplified and held by a sample-and-hold amplifier which returns the value to the recorder. The following methods of operation were available:

(1) DC Amperometric detection (t1>0, t2=0, t3=0)
(2) Double potential pulsed detection (t1>0, t2>0, t3=0)
(3) Triple pulse amperometric detection (t1>0, t2>0, t3>0)

The durations of each of the pulses are adjustable in

increments of 60ms; the applied potentials are continuously variable. The time constants for the instrument damping were 0.3s, 1.0s, 3.0s.

LKB (Biochrom) Ultraspec II (4050)
UV/VIS Spectrophotometer

The wavelength range is 200 - 900 nm. The type of monochromator was Czerny-Turner configured with holographic diffraction grating (1200 lines mm^{-1}). The accuracy was quoted as $\pm$ 1 nm with a bandwidth of 5 nm.

Chart recorders

The following chart recorders were used in conjunction with the above instrumentation:

Linseis 05.50L
Bryans 28000
Tarkan W + W 600

2.2 Ancillary Equipment

Pumps

A Gilson Minipuls 2 peristaltic pump was used for propelling the carrier in fia. The pump was model HP4, with four channels. The pump head comprised ten metal rollers (Inox/S.S.). Pump tubes of PVC were used throughout the research. The flow rate may be varied by adjusting the potentiometer (from 0.5 to 25rpm), and by changing the pump tube diameter (up to 3.2 mm i.d.). Smooth flow is achieved by applying pressure to the pump tubes by means of adjustable compression cams. The pump is said to be capable of working against up to five bars

backpressure.

An air compressor from Fracmo Motors Hastings was used to supply laboratory air for the experiments on aniline vapour. The gas diffusion cell and connecting tubes was thermostated using a circulating heater pump from Grant Instruments Cambridge Ltd.

Injection Valves

A Rheodyne 5020 manual rotary valve was used as an injection valve for fia and as a stream switching valve. All parts in contact with the eluent are made of PTFE, except the rotor, which is made of PCTFE. The valve has six ports, lengths of PTFE tubing extend from the valve and are terminated by flanged ends and standard 1/4" tube end fittings. Two of the lengths form the sample loop; the volume may be increased by additional flanged tubing.

A Dionex slider valve (used in series 2000i Ion Chromatographs) was used for fia in conjuction with PAD: details of the valve are shown in fig. 8. All the parts in contact with the eluent are inert, the slider being of PCTFE and the port faces are of PTFE. The valve has eight ports, two were connected to a sample loop and the two opposite them were connected to a bypass of smaller diameter and of shorter length. The valve was operated by compressed nitrogen gas, at a pressure of 100 psi. The gas was switched between the actuating pistons at either end of the valve by means of solenoid valves. Two three way mains operated solenoid valves were controlled by a toggle switch in order to alternately pressurise and vent each piston.

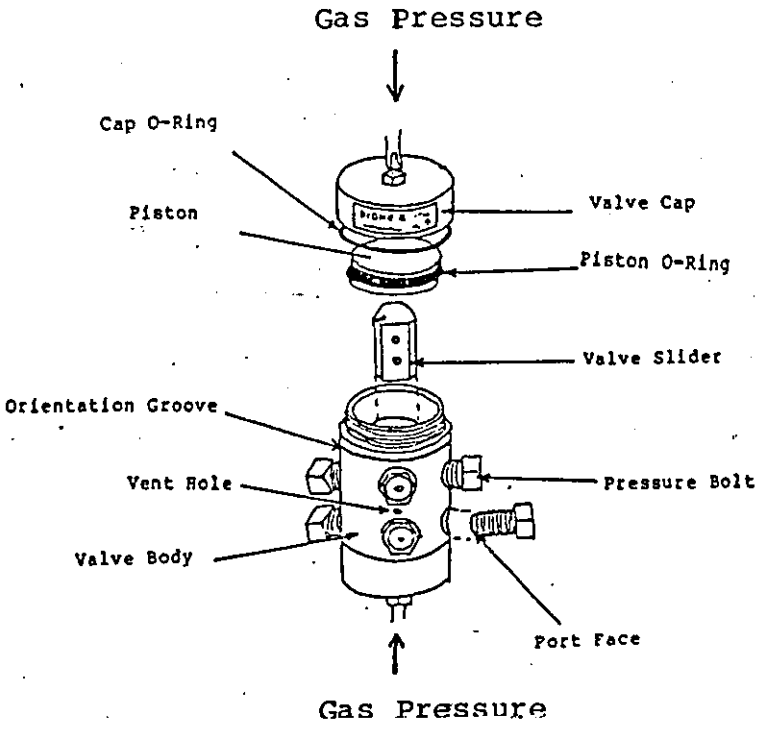

Fig. 8
Details of Dionex Slider Valve

Flow Rate Measuring Devices

The gas flow rates were measured using Gec-Elliott series 1100 rotameters for a maximum flow rate of 1.2 l min^{-1}. The liquid flow rate in some experiments were measured using a device designed by a colleague in this laboratory[218]. It is based on a piezo-resistive pressure transducer (RS 303-337). A schematic diagram is shown in fig. 9.

Flow though Cells

An 8 µl Helma quarz flow cell was used with the UV detector. The path length being 1 cm.

A wall jet cell was built according to the design described by Fogg and Summan[88], for details of its construction see fig. 10. The electrode holder was made from PTFE, but the eluent inlet block was made from glass -filled PTFE, rather than PTFE because of its better machining properties. This improved the finish of the inlet hole, and the flow channels. The electrode holder was designed to accept the Metrohm mini solid electrodes of 7 mm o.d.. This cell is designated WJ1 in the text of this thesis.

A wall jet cell was subsequently designed using the recommendations of Gunasingham and Fleet[89] and Yamada and Matsuda.[35] This was regarding the separation between the nozzle outlet and the electrode and the cell chamber geometry. The cell was fabricated in two halves and could be snapped together in a similar manner to the WJ1 cell. The cell was constructed from PCTFE because of its chemical inertness and good machining properties. For details of its construction see fig. 11. The upper half consisted of the cell chamber and the inlet nozzle. Two

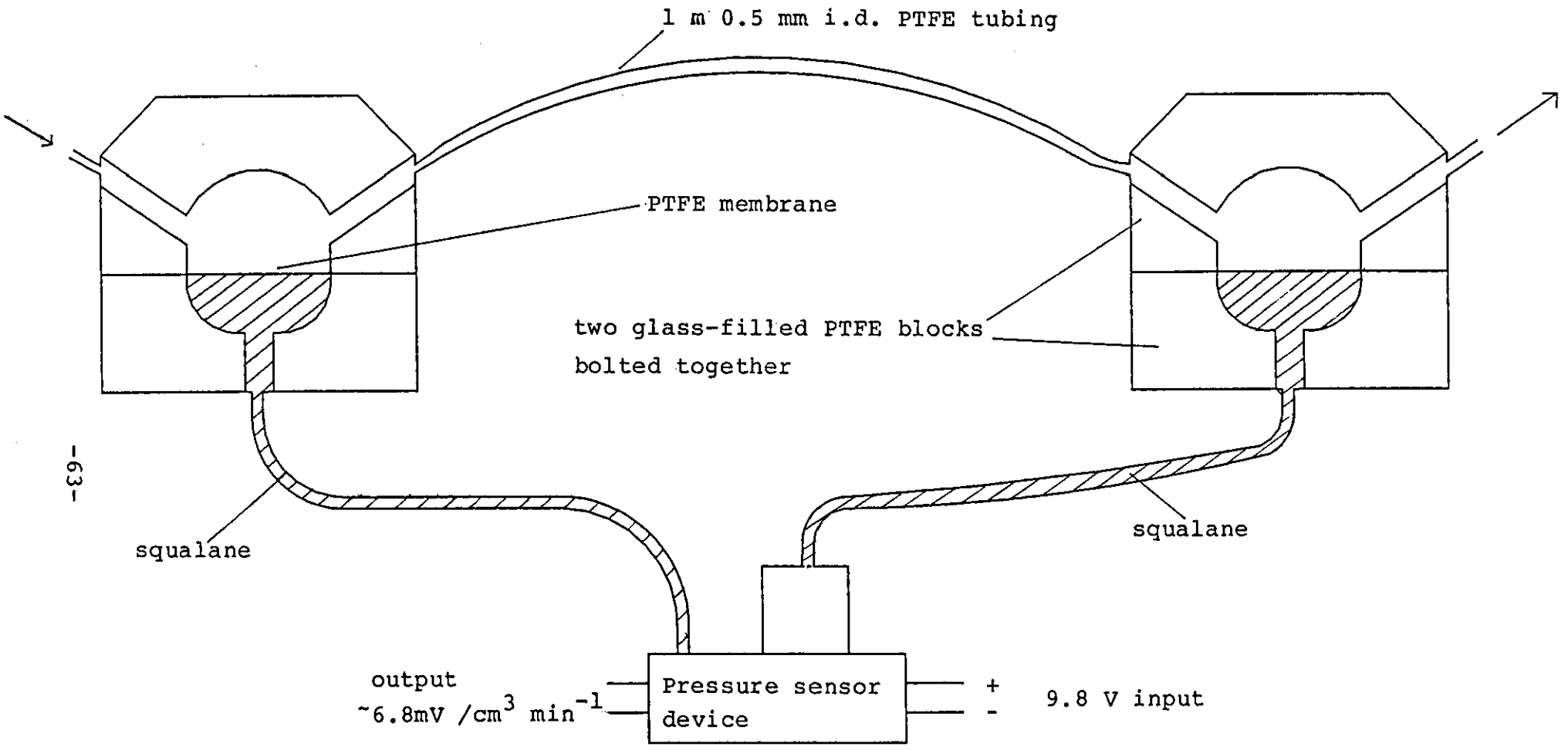

Fig. 9

Flow Rate Device

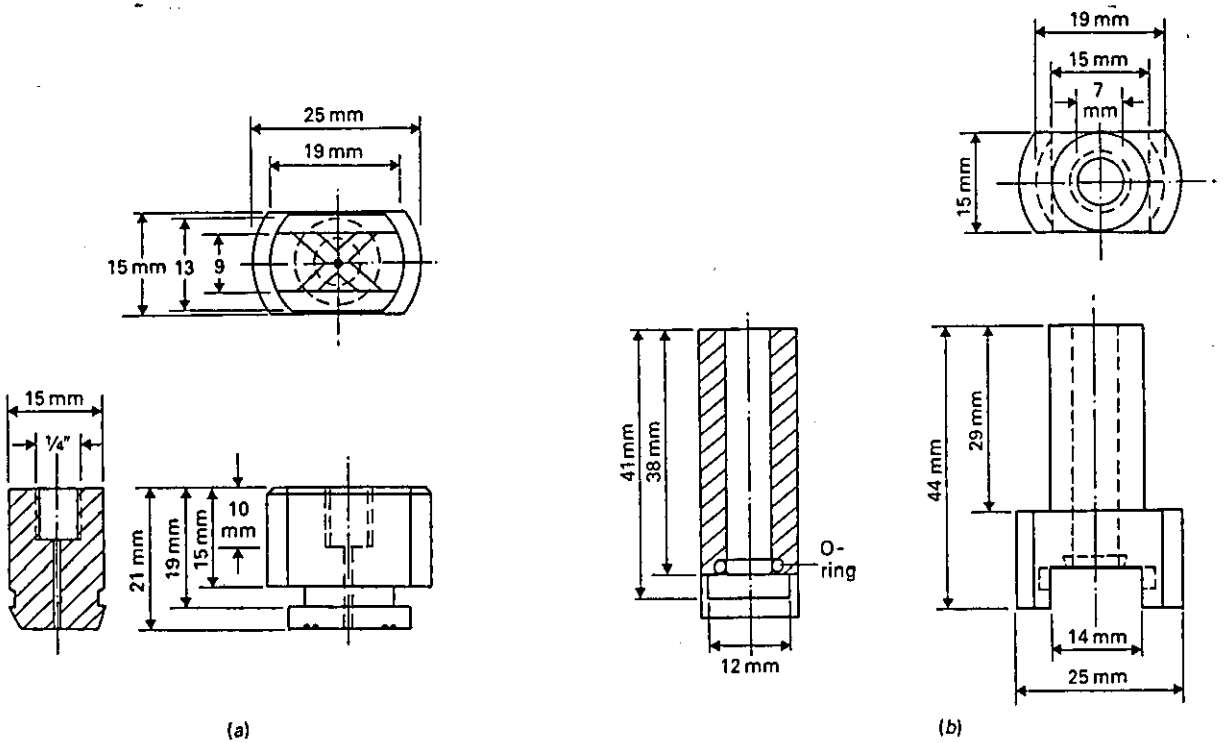

Fig. 10

Details of Wall jet Cell (WJ1)

a) part holding eluent entry port

b) part holding electrode

(from Analyst, 109, 1029, (1984))

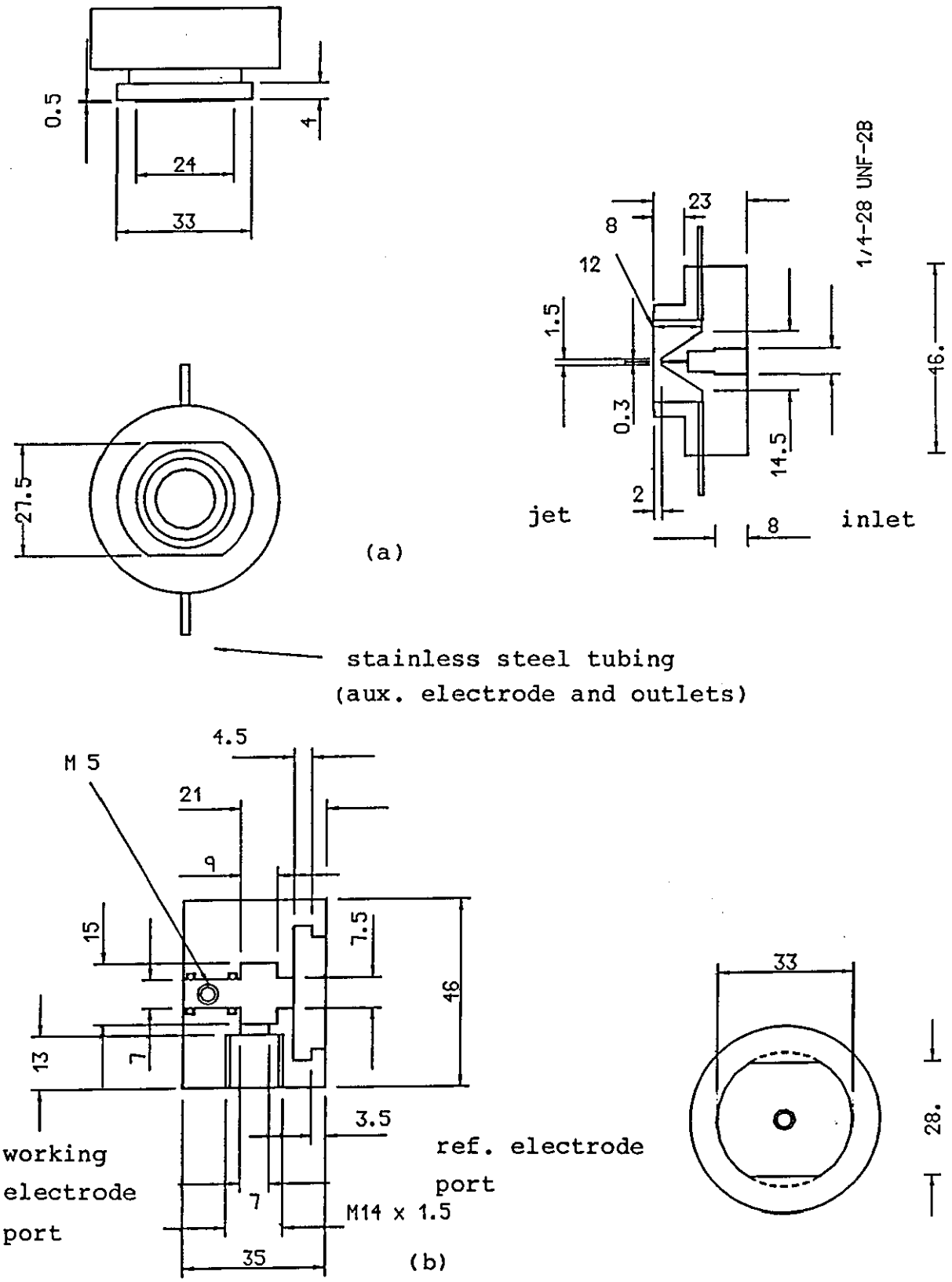

Fig. 11

Details of Wall jet cell (WJ3)

a) part with the cell cavity, inlet and outlet ports

b) part holding the reference and working electrodes

stainless steel tubes were inserted at the top of the chamber to act as the cell outlets and as auxillary electrodes. The lower half of the cell was designed to hold the Metrohm mini solid electrodes o.d. 7 mm. A hole was drilled in the side of the cell and threaded to accept the Metrohm 6.0727.000 mini silver chloride reference electrode. The cell outlets were joined together and connected to about 30 cm of 0.3 mm i.d. PTFE tubing to provide enough back pressure to prevent bubble formation in the cell. This cell is designated WJ3.

A Dionex thin layer cell incorporating a platinum working electrode was used for fia in conjuction with PAD. Details of the cell assembly are shown in fig. 12. The working electrode is permanently mounted in an electrode block. The auxiliary electrode is made of stainless steel and screws into the reference block and is the cell outlet. The cell inlet is another stainless steel fitting which is used to ground the electrolyte. The reference electrode screws into the reference block opposite the working electrode. An ion exchange membrane gives an ionic connection between the reference solution and the eluent. The two cell halves are bolted together with a gasket between them forming the channel. The effective volume of the cell is quoted as 9 µl.

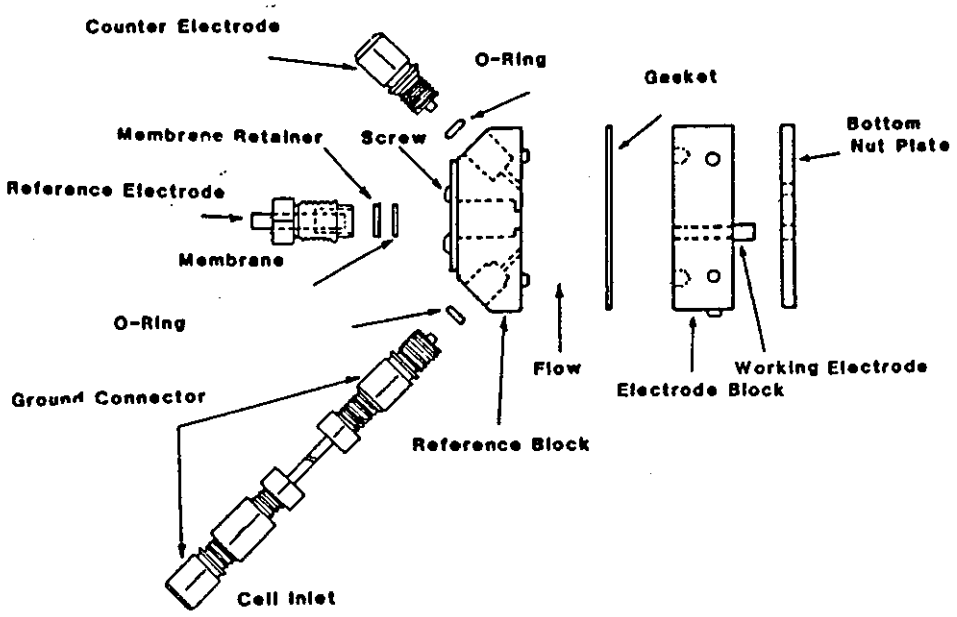

Fig. 12
Details of Dionex Amperometric
Thin Layer Flow Cell

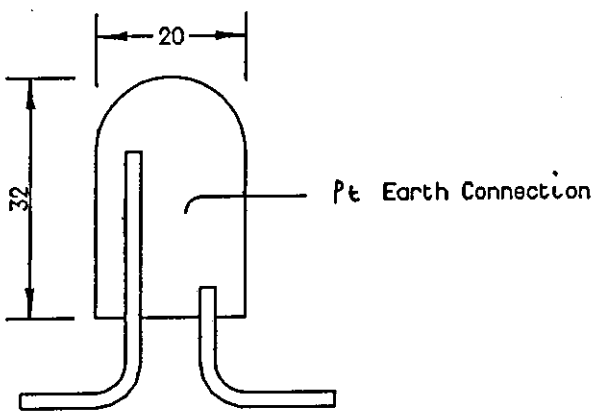

Fig. 13
Glass Pulse Damper for fia

Electrodes

Metrohm 6.0805.010 mini glassy carbon electrode, diameter of active zone: 3.0 ± 0.05 mm, o.d. 7 mm.

The following Metrohm electrodes which were used are now only available for the rotating disc electrode system:

Metrohm glassy carbon electrode (now 6.1204.000), diameter of active zone: 4.8 ± 0.05 mm, o.d. 7 mm.

Metrohm gold electrode (now 6.1204.020), diameter of active zone: as above.

Metrohm 6.1204.050 platinum electrode, diameter of active zone: 3.0 ± 0.5 mm, o.d. 7mm.

Graphite epoxy electrodes were constructed using the method described by Henriques and Fogg.[119] The graphite epoxy was bonded into thick walled glass capillary tubing of nominal dimensions: 2 mm i.d. and 7.1 mm o.d..

Microarray disc electrodes were constructed from reticulated vitreous carbon (RVC), of porosity 100 pores per inch. The RVC was a gift from the following company:

The Electrosynthesis Company Inc.,
P.O. Box 16,
East Amherst,
N.Y. 14051
USA

Pulse Damper

A pulse damper was constructed from glass with a platinum wire ground connection. (fig. 13)

Polishing equipment

Diamond paste for coarse polishing of electrodes was obtained from Winter Diaplast (UK). The paste was grit size D7 (5-10 μM), the carrier is miscible with water, oil and alcohol. Fine alumina for polishing was obtained from BDH in sizes; 0.3 and 0.015 μM. Bhuler polishing pads were obtained from Anachem.

Single String Bead Reactor

A single bead string reactor (SBSR) was made from 0.5 mm i.d. PTFE tubing. One end of the tube was blocked with a piece of porous PVC then glass beads were sucked up into the tube to the desired length. The beads were seived previously to the correct size such that the tube was not blocked by them. The other end of the tube was then sealed with another piece of porous PVC. The glass beads were supplied by Phase Sep.

2.3 Chemicals

Chemical	Grade	Supplier
sulphuric acid	AR	Fisons
aniline	AR	BDH
acetonitrile	HPLC	Fisons
dimethyl sulphoxide	AR	BDH
sodium hydroxide	AR	Fisons
sodium acetate	ARISTAR	BDH
p-toluidine	GPR	Hopkin & Williams
N,N-dimethyl-p-toluidine		Aldrich
di-sodium tetraborate	AR	BDH
methanol	HPLC	Fisons
acetic acid	AR	Fisons
pyridine		Fluka
dimethyl formamide	GPR	BDH
graphite powder	SPECPURE	Johnson Mathey
o-dianisidine		Aldrich
sodium perchlorate	AR	BDH
N,N-diethylaniline	AR	Hopkin & Williams
p-aminophenol	GPR	Hopkin & Williams

CHAPTER 3

VOLTAMMETRIC AND AMPEROMETRIC ANALYSIS OF ANILINES

3.1 Analysis of Aniline

3.1.1 Introduction

Interest in the electrochemical oxidation of amines dates back to the mid-1800's, when the oxidation of aniline was first studied[217] Some of the first data on the voltammetric oxidation of aniline was obtained by Lord and Rogers.[219] They found that in aqueous solution the first step is the production of a cation radical, which is poorly stabilised by the amine group. The cation radical immediately undergoes further reactions. This was substantiated by Mohliner.[220] The mechanism for the anodic oxidation of aniline in aqueous solution pH 0 - 6.5 is thought to be an ECE process[10] and is as follows:

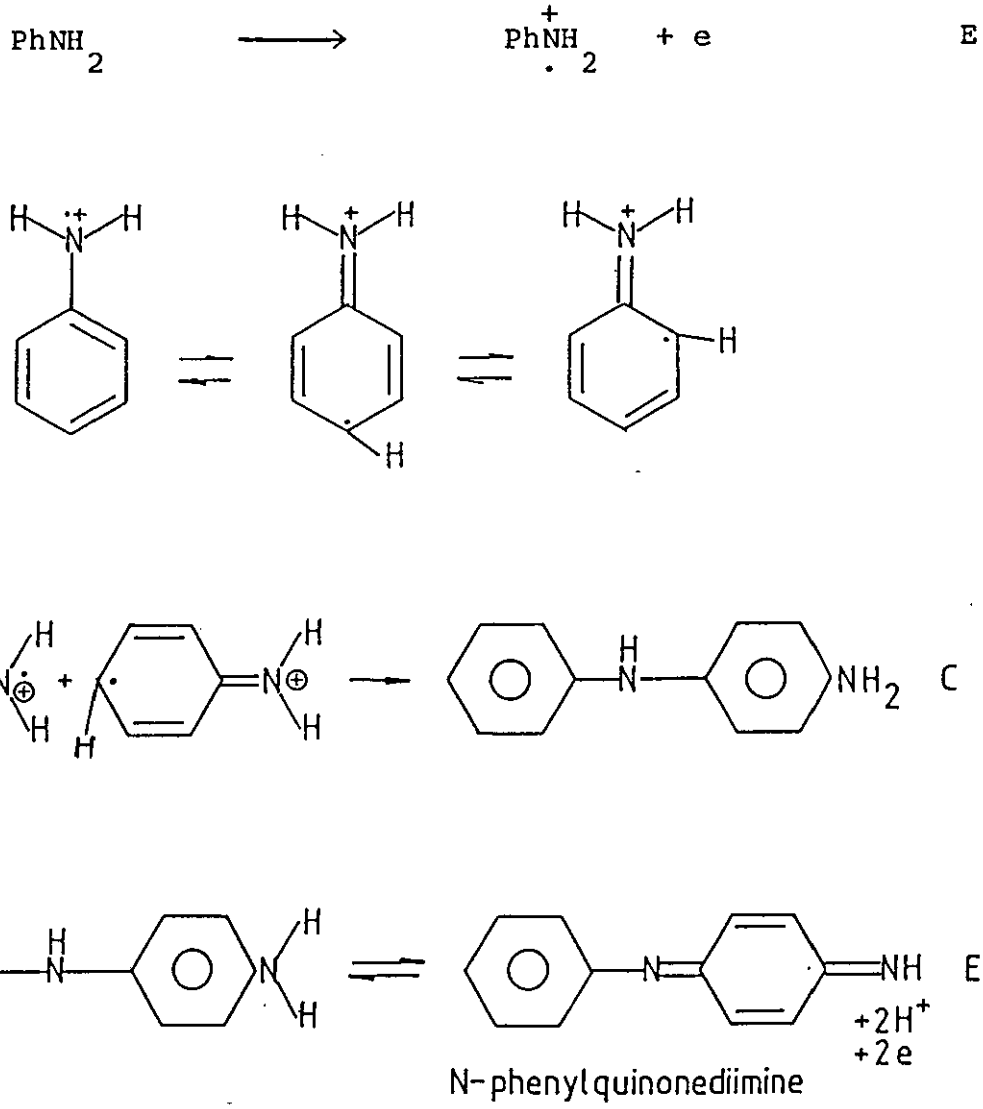

Significant amounts of benzidine are formed in more acidic solutions via tail to tail coupling.
Polymerisation of the p-aminodiphenylamine may be represented by the following reaction scheme:

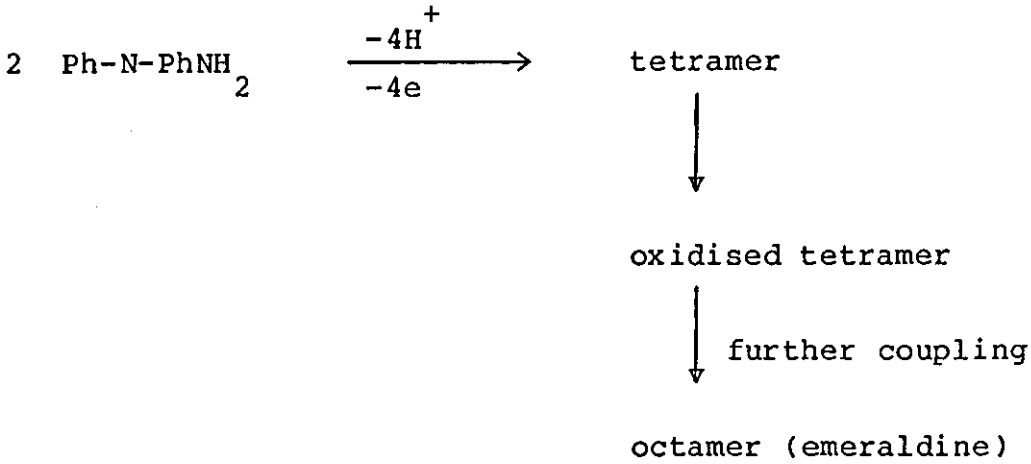

Desideri et al[221] found similar products in alkaline solutions, also significant amounts of azobenzene formed by head to head coupling. The percentage of the latter was found to increase with increasing pH or with the addition of dimethylformamide. These authors suggest that the formation of a poisoning agent is favoured by an increase of aniline concentration and delayed by an increase of the potential scan rate and an increase in the pH.

Breitenbach and Hechner,[222] studied the anodic oxidation of aniline in acetonitrile and water and offered the following conclusions regarding the mechanism of film formation on the electrode. At the beginning of the electrolysis the primary product from the oxidation of aniline reacts to form dimers. The dimer concentration reaches a steady value near the electrode followed by the adsorption of the dimer. When the adsorbed dimer reaches a certain concentration it reacts increasingly with the primary oxidation product to form trimers and larger condensation products. After the coverage of the electrode with polyaniline film further aniline oxidation is inhibited.

Sharma et al[223] deduced that aniline oxidation in

acetonitrile occurs by two successive one electron steps to give a dication. Head to head coupling occurs with a neutral aniline molecule to yield azobenzene. The monocation radical first formed is not thought to undergo any coupling reactions. The reaction scheme for anodic oxidation of aniline in acetonitrile is represented below.

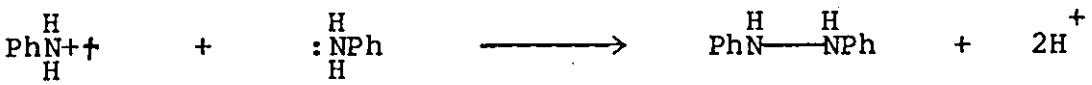

Hydrazobenzene

azobenzene

Secondary aromatic amines are also known to give dimers and higher polymers, when oxidised anodically, e.g. N-methylaniline.[224] Tertiary aromatic amines are thought to give mainly dimers e.g. N,N-dimethylaniline gives mainly benzidine.[10] Substitution in the para position tends to stabilise the initial cation radical produced apart from blocking dimerisation at this position. Consequently it is not surprising to find that N,N-dimethyl-p-toluidine undergoes oxidation in the side chain[225] to give the aldehyde and the acid rather than dimerisation to an orthobenzidine. The oxidation reaction is proposed to follow the following pathway:

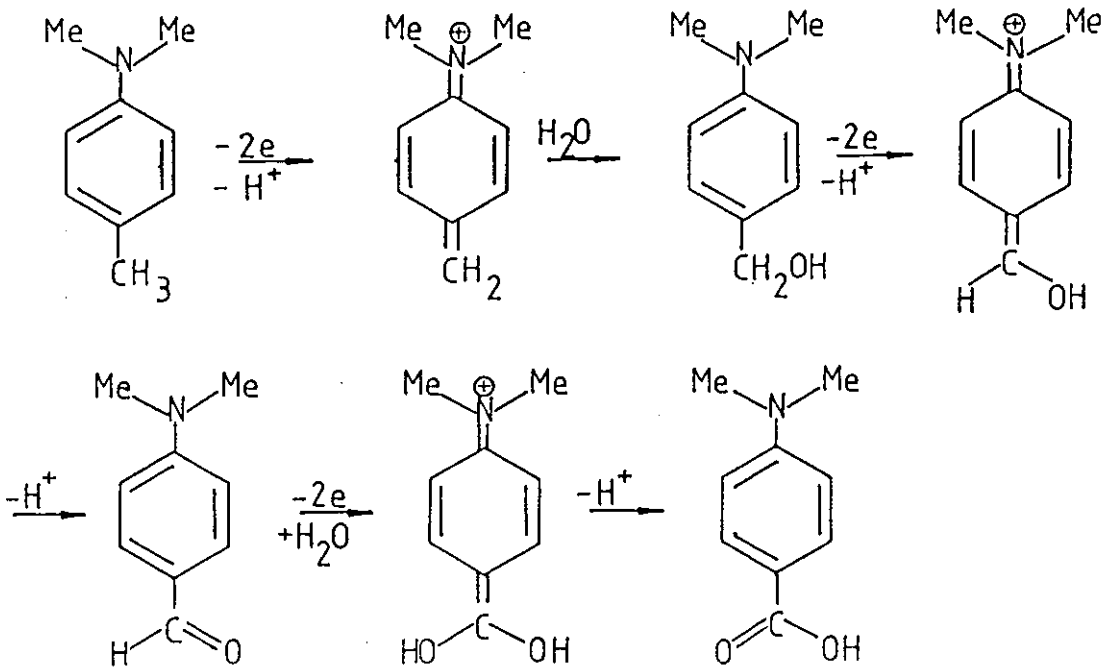

In acetonitrile dimerisation is observed.[226]

3.1.2 Voltammetry of aniline

The effect of pH on Electrode Poisoning

Experimental

The degree of electrode poisoning was investigated in aqueous solutions over the pH range 0.7 - 12, and for methanol pH 0.7. McIlvain buffers of ionic strength 0.1 M were used for solutions with pH values in the range 2 to 11. The solution with pH 0.7 was 0.1 M sulphuric acid and the pH 12 buffer was 0.05M sodium tetraborate plus 0.1M sodium hydroxide. Also a solution was prepared using the pH 12 buffer with 5% dimethylformamide (DMF) added. A stock solution of 10 mM aniline in distilled

water was prepared and aliquots of this were made up to volume with the appropriate buffer in order to prepare a solution of 0.1 mM aniline. One cell was half filled with buffer and the other with 1mM aniline dissolved in the same buffer. Two electrodes were used, a 4.8 mm diameter glassy carbon electrode and a home made graphite epoxy electrode.[119] The electrode was polished using an aqueous slurry of 0.05 μM alumina, rinsed with distilled water before placing it in the buffer solution. The electrode was conditioned by scanning three times between the potential ranges to be used in the experiment, starting from the lower potential. The scan being a linear sweep voltammogram (voltammogram), scan rate 4 mVs^{-1}. The background scan was recorded and then the cell was replaced by the sample cell. Two scans were carried out consecutively. The electrode was taken out of the cell and repolished as before and the process was repeated. Three such voltammograms were recorded. This process was repeated for each buffer solution in turn, for both electrodes, fresh buffer being used for each voltammogram.

Results and Discussion

The percentage decrease in peak height was used to estimate the extent of poisoning of the electrode surface. Typical voltammograms are shown in figs. 14-16. Table 1 shows the mean percentage decrease in peak current for two consecutive scans for a set of three voltammograms.

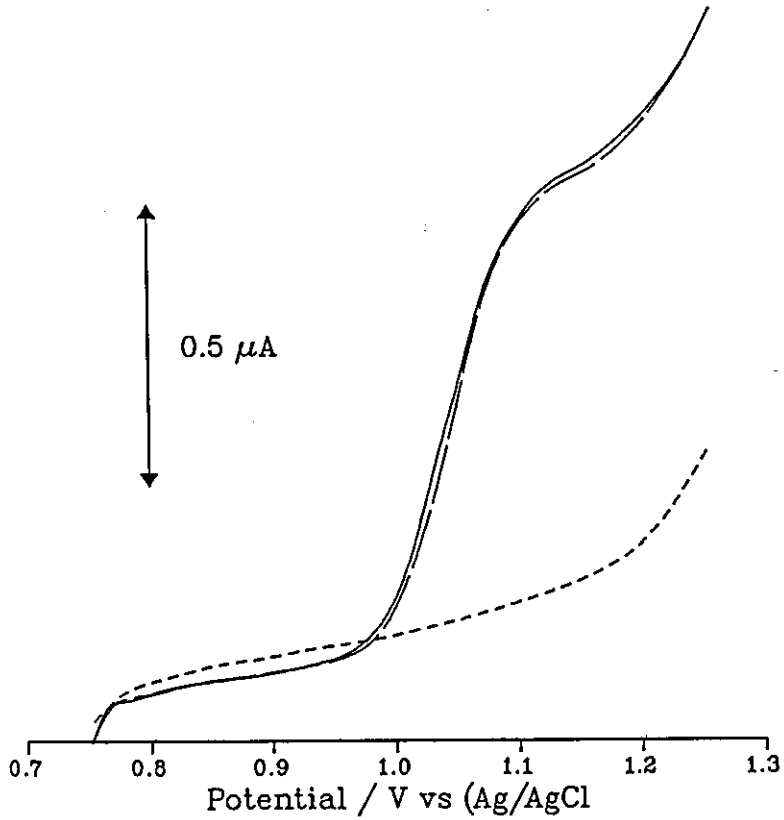

Background
1st scan
2nd scan

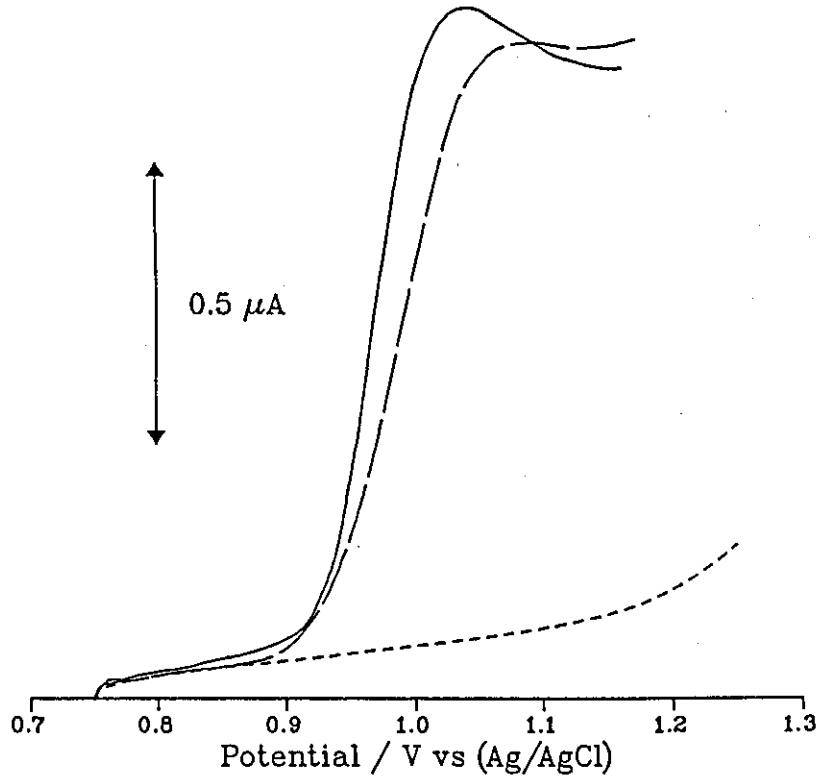

Fig. 14
Linear Sweep Voltammograms of Aniline (0.1 mM)

Conditions: Background =
0.1M sulphuric acid / 100% methanol
electrode = glassy carbon (4.8 mm dia.)
ν = 3mVs^{-1}

Background = 0.1 M sulphuric acid (pH 0.7)
electrode = glassy carbon (4.8 mm dia.)
ν = 3 mVs^{-1}

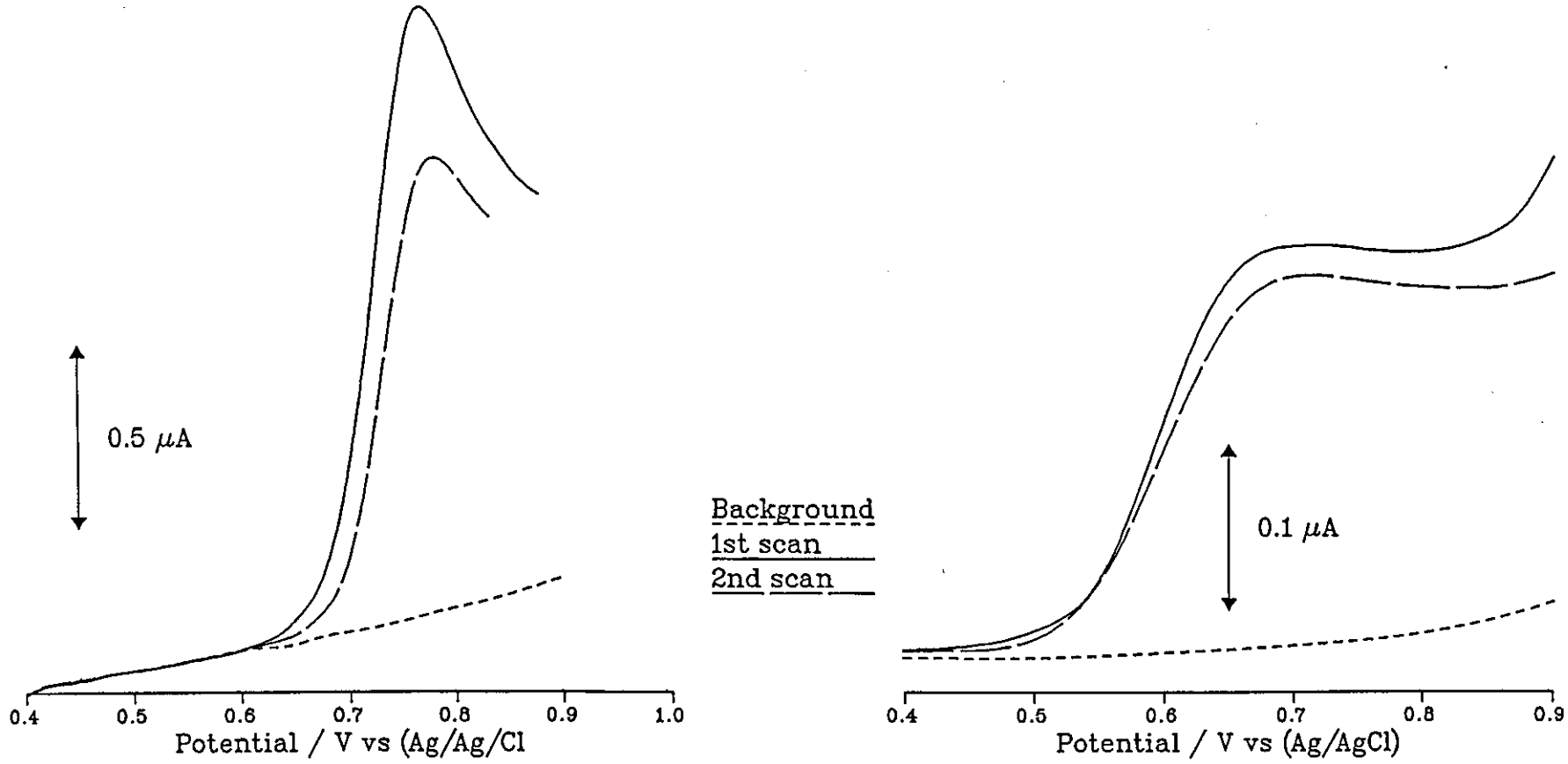

Fig. 15

Linear Sweep Voltammograms of Aniline (0.1 mM)

Conditions: Background =
pH 7.0 buffer (0.1 M)
electrode = glassy carbon (4.8 mm dia.)
$\nu = 3 mVs^{-1}$

Background = pH 11.0 buffer (0.05 M)
electrode = graphite epoxy (2mm dia.)
$\nu = 2 mVs^{-1}$

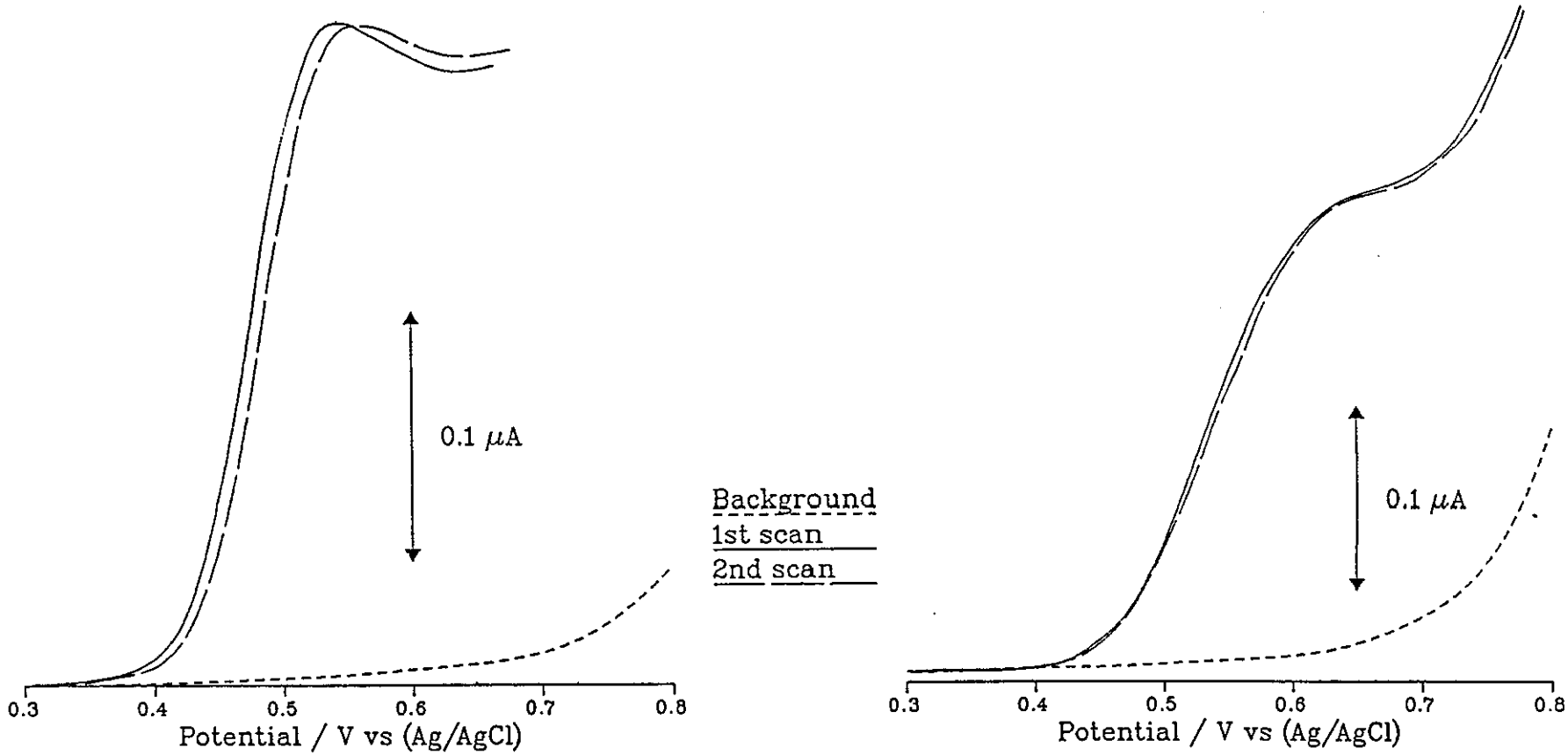

Fig. 16

Linear Sweep Voltammograms of Aniline (0.1 mM)

Background = pH 12.0 buffer (0.05 M)
electrode = graphite epoxy (2mm dia.)
ν = 2 mVs^{-1}

Background = pH 12.0 buffer (0.05 M)
+ 5% dimethylformamide
electrode = graphite epoxy (2mm dia.)
ν = 2 mVs^{-1}

Table 1

The effect of pH on Electrode Poisoning for Linear Sweep Voltammetry of 0.1 mM aniline

Decrease in Peak Current (mean) / %		
pH	Glassy Carbon Electrode	Graphite Epoxy Electrode
0.7/MeOH	2	
0.7	7	10
2.0	15	19
3.0	18	25
5.5	21	27
7.0	24	26
9.0	19	21
11.0	12	7
12.0	7	3
12.0 + 5% DMF		1

The results illustrate the general trend only as the deviation was large. One reason is the poor reproducibility of carbon electrodes after polishing. The decrease in response is attributed to the amount of polymer film adsorbed onto the electrode surface. The polymer film has been shown to be conductive in a limited potential range[227] and at the potential required to oxidise the aniline the film is thought to be insulating.[228] As the film builds up the current decreases: this is because the rate of diffusion of aniline through the film is rather slow compared with the bare electrode.

The electrodes were poisoned least at either high or low pH values. Poisoning was lowest in aqueous solution with the graphite epoxy electrode using pH 12 buffer with 5% added DMF, although it is difficult to be conclusive about the relative merits of the two electrodes. It was discovered that some degredation of the electrode occurs at pH 12 because the background current increases with repeated scans in background electrolyte and this was a major drawback. An explanation for the lower poisoning at high pH values was proposed by Desideri et al[221]. They found that as the pH was increased the yield of azobenzene also increased, also adding dimethylformamide increased the yield. The latter was attributed to the basicity of dimethylformamide. The azobenzene is much less susceptible to further polymerisation than the other dimers as the nitrogen atoms are no longer a reactive centre.

The hydroxyl ions are said to compete for the cation radical produced by the initial one electron oxidation of aniline, a proton is abstracted and dimerisation of the resulting radical is thought to be the preferred reaction. The reaction scheme is described:

$$2\ Ph\dot{N}H_2^+ + OH^- \longrightarrow Ph\dot{N}H + H_2O$$

$$2Ph\dot{N}H \xrightarrow{-2e} Ph{-}N{=}N{-}Ph + H_2O$$

The reason the poisoning is decreased in acid solution is not clearly understood. Condensation of the dimers may be less favourable at lower pH values, a competing reaction is possibly the hydrolysis of some of the imino dimers.

The glassy carbon electrode was poisoned less for the

methanolic solution than the aqueous solution at pH 0.7 but this still was not acceptable. The methanol probably stabilises the cation radicals, allowing a further one electron oxidation to the neutral radical. This would give more azobenzene and therefore decrease the poisoning.

The effect of Non aqueous Solvents on Electrode Poisoning

Experimental

The apparatus was the same as for the aqueous solvents. The solvents were as follows:

1) 0.1M sodium perchlorate dissolved in;

i) pyridine, ii) acetonitrile, iii) acetonitrile plus 0.1 M pyridine.

2) 50% aqueous methanol plus 0.1 M w.r.t sulphuric acid and pyridine.

The concentration of aniline was 5 mM, the reason for the use of this high concentration was to provide a large enough signal to give a good s/n ratio in the presence of the high background current for the electrolytes. The aniline samples were prepared by pipetting the appropriate quantity of aniline into a graduated flask; either a weighed amount of sodium perchlorate was added and this was made up to the mark with the correct solvent or the flask was half filled with solvent then sulphuric acid was added by pipette and made up to the mark. The reference electrode was silver/silver chloride. (Ag/AgCl)

Results and Discussion

Table 2

The Effect of Solvent on Electrode Poisoning for Linear Sweep Voltammetry of 5 mM Aniline

Solvent and Electrolyte	Decrease in Peak current (mean) / %
Acetonitrile / 0.1M $NaClO_4$	45
Acetonitrile 0.1M pyridine / 0.1M $NaClO_4$	25
Pyridine / 0.1M $NaClO_4$	50
50% methanol 0.1M pyridine 0.1M H_2SO_4	80

Table 2 shows the results of the anodic oxidation of aniline in organic solvents. The lowest poisoning was observed for the system; acetonitrile, 0.1M pyridine and 0.1M sodium perchlorate as electrolyte (fig 17). In acetonitrile the oxidation mechanism is known to be two one electron transfer stages[223] resulting in a di-cation radical, although in these experiments a second peak was not detected. Filming of the electrode still occurs, presumably polymerisation also takes place in non aqueous solvents although the major product is known to be azobenzene. Adding pyridine decreased the poisoning significantly and this favours azobenzene formation.

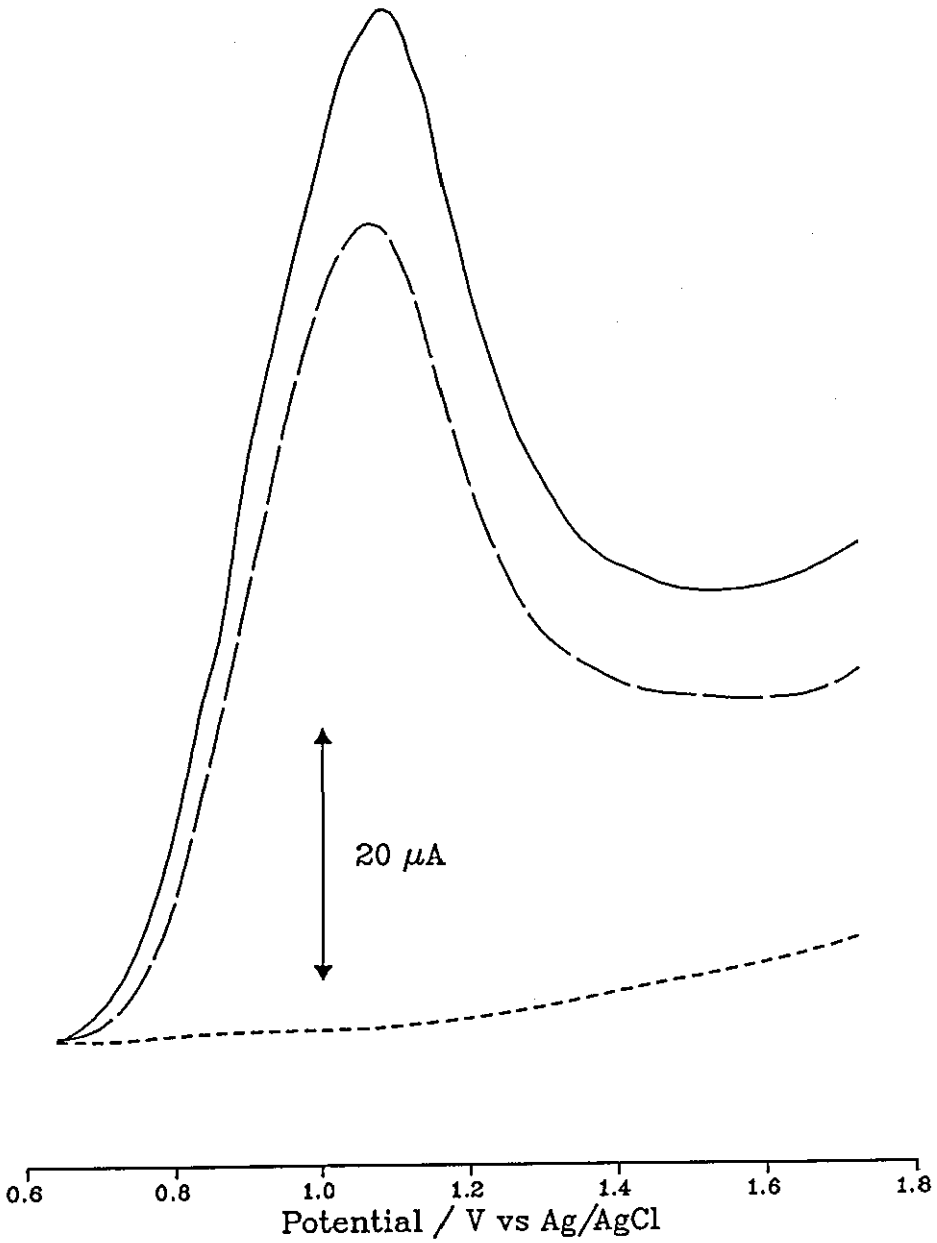

Fig. 17
Linear Sweep Voltammogram of Aniline (5.0 mM)

Conditions: solvent =
1 M pyridine in acetonitrile, electrolyte =
0.1 M sodium perchlorate, $\nu = 3$ mVs^{-1}
electrode = glassy carbon (4.8 mm dia.)

Background
1st scan
2nd scan

in pure acetonitrile, the coupling reactions competing with azobenzene formation are probably responsible for the polymerisation. It seem that it is not possible to prevent polymerisation occuring at the electrode surface because the solvent effects do not completely prevent the coupling reactions of dimers, but it appears to be beneficial to increase the production of azobenzene.

3.1.3 Analysis of Aniline by fia with Amperometric Detection

Experimental

The potentiostat was a Metrohm E 611 detector which was used in the DC mode or in the pulse mode with a choice of two pulse widths according to the charging currents generated. A pulse of fixed height is generated from a preselected base potential. The potentials were chosen according to the hydrodynamic voltammogram for aniline (fig. 18). The measuring potential for DC amperometry was +1.1 V and for pulse amperometry the base potential was +0.85 V with a pulse height of 0.2 V.

A glassy carbon electrode (3 mm diameter) was used in a wall jet cell (WJ1)[88]. The cell was immersed in a beaker containing electrolyte of the same composition as the eluent (0.1 M sulphuric acid). The counter and reference electrodes, platinum and Ag/AgCl respectively were placed either side of the cell, held in position by clamps. The injection valve (Rheodyne 5020), with loop volume about 60 µl was connected to the cell by means of 0.8 mm i.d. PTFE tubing. A Gilson Minipuls 2 peristaltic pump was used to propel the eluent at a flow rate of 4.0 $cm^3 min^{-1}$. A simple pulse damper was constructed from a small glass tee-piece, with a piece of pump tubing (about 5 cm)

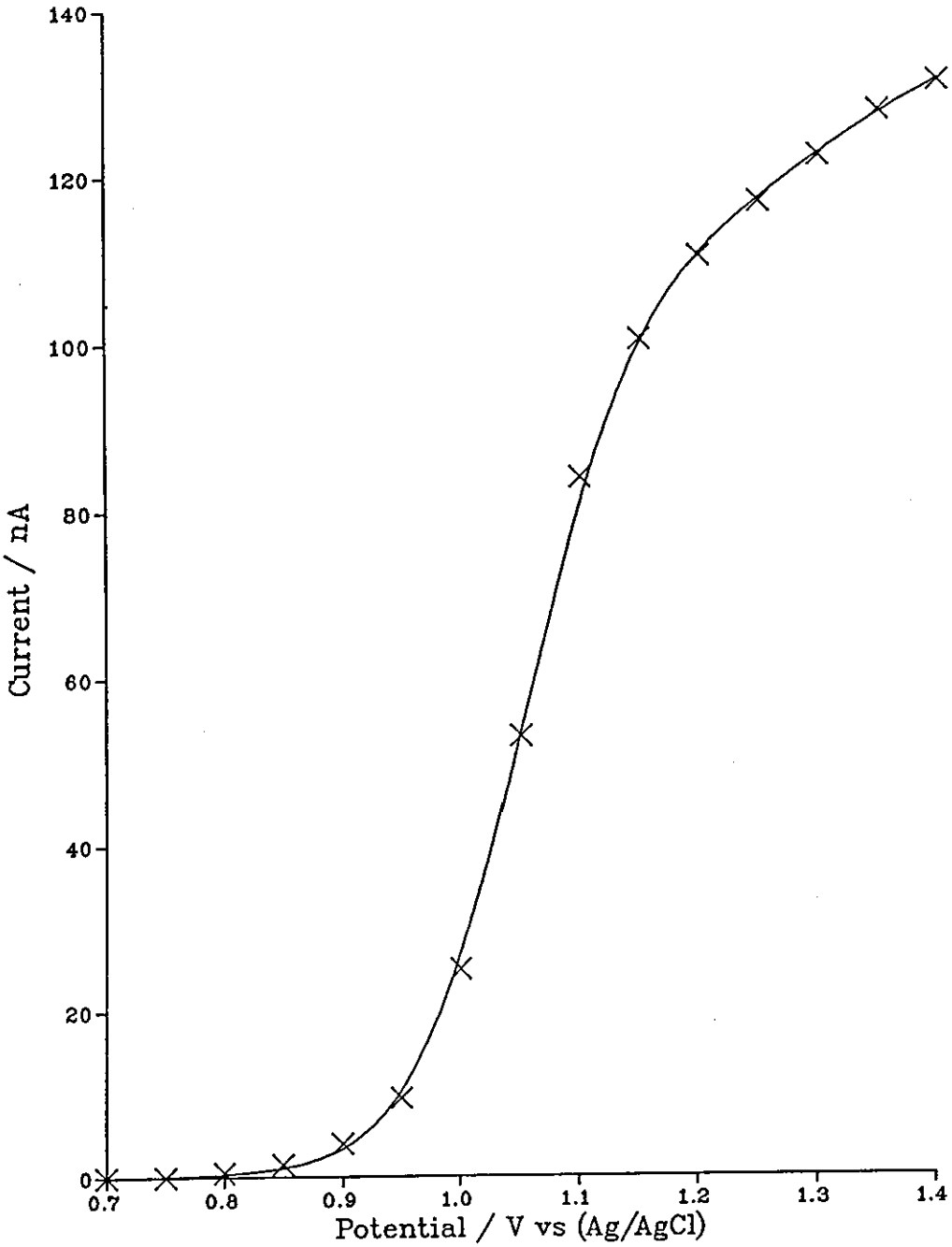

Fig. 18
Hydrodynamic Voltammogram of Aniline (10 μM)

Conditions: cell = wall jet (WJ1)
flow rate = 6.0 cm^3 min^{-1}
background = 0.1 M sulphuric acid
electrode = glassy carbon (3.0 mm dia.)

attached to one arm. The end of the pump tubing was blocked with a column of air trapped in the tube. The damper was inseted between the pump and the valve. It was found necessary to insert an earth guard after the pump because the detector was affected by the static electricity generated by the action of the rollers on the pump tubes. The earth guard consisted of a short length of stainless steel tubing connected to the instrument earth.

Results and Discussion

Fig. 19 shows a comparison of peaks obtained for concentrations of aniline of 0.1 and 0.2 mM. The peaks obtained for DC detection decreased visibly with each injection. The peaks for pulse detection decreased less, but after several injections the decrease in peak height was noticable. The background current generated by the potential pulse is fairly large and the instrument was incapable of offsetting the background current for current sensitivities less than about 0.1 μA f.s.d.. The base potential and pulse potential were compromised because of this. The current due to the slow relaxation of redox couples on the glassy carbon electrode surface after the potential pulse is applied, constitutes a significant proportion of the background current.

Ideally pulsing should be from a potential of electrochemical inactivity, where desorption of products might occur, to a potential where the analyte species is strongly active. This required a pulse amplitude of about 0.3 V, but the pulse amplitude was limited to about 0.2 V by overloading of the instrument. A detection limit of about 10 μM could possibly be achieved, but a detection limit more than one order of magnitude better than this was required.

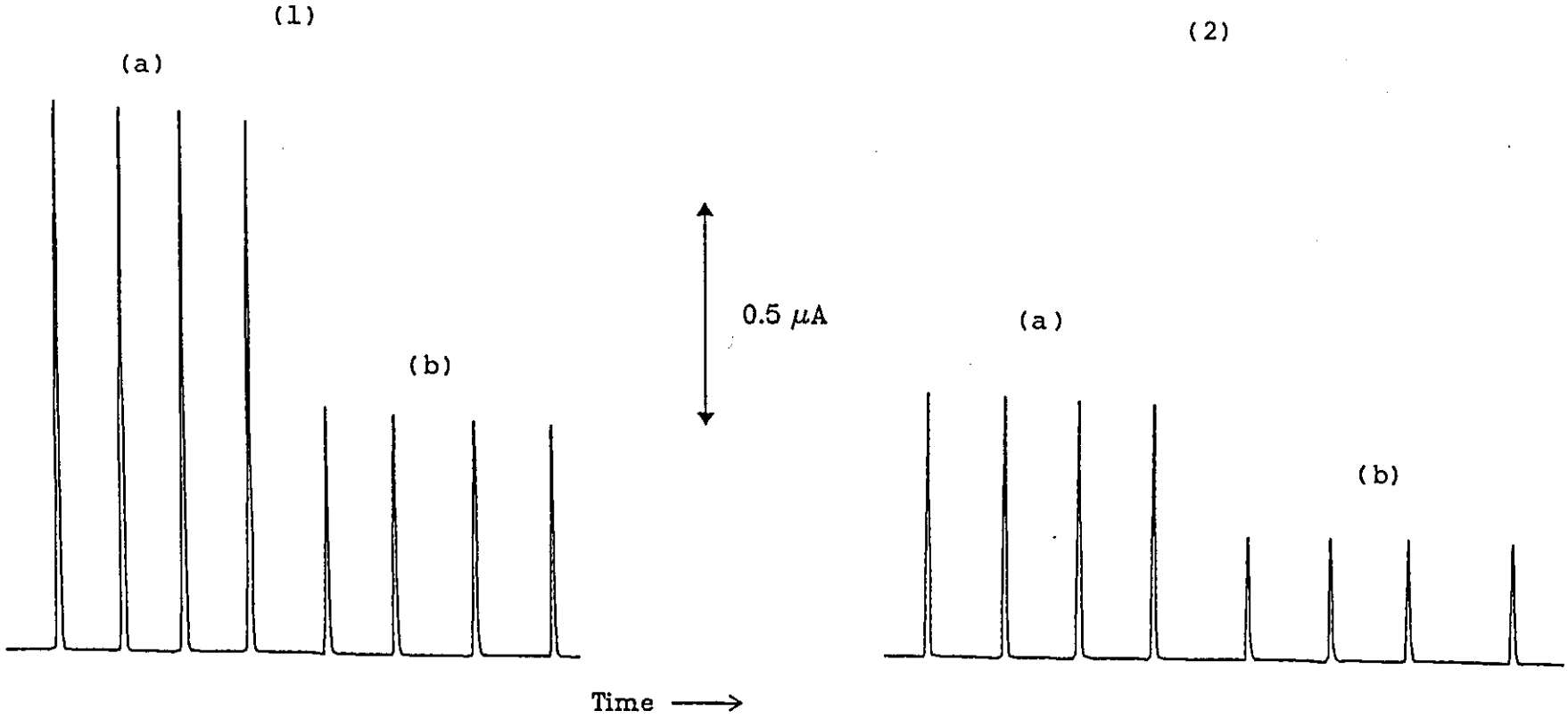

Fig. 19
Typical fia Peaks for the Amperometric Detection of Aniline by DC and Pulse Modes

Conditions: Background = 0.1 M sulphuric acid, electrode = glassy carbon (3.0 mm dia.)
Loop vol. = ~ 60 μl, flow rate = 4.0 $cm^3 min^{-1}$
1) DC detection, E = +1.1 V, baseline offset = +0.15 μ
2) Pulse detection, E_{base} = +0.85 V, ΔE = +0.2 V, baseline offset = +1.1 μA
Aniline conc. x 10^4M: a) 2, b) 1

3.2 Electroanalysis of Substituted Anilines

3.2.1 Voltammetry of Substituted Anilines

Experimental

The same apparatus and preparation of solution was employed as for section 3.1.2 (aqueous solvents). The concentration of amines prepared was 0.1 mM. The background electrolyte was 0.1 M sulphuric acid unless stated otherwise. The electrode was glassy carbon (3 mm diameter). Compounds selected for further investigation were as follows:

Primary Anilines; p-toluidine

Tertiary Anilines; N,N-diethylaniline,
N,N-dimethyl-p-toluidine

Results and Discussion

p-toluidine

The electrode was badly poisoned in alkali, in 0.1M sulphuric acid the poisoning was less than for aniline (fig. 20a). Adding pyridine reduced the poisoning to about 1% for two consecutive voltammograms.

The mechanism for the follow up reactions for anodic oxidation of p-toluidine is proposed to be head to head coupling by Sharma et al[223], giving dimers which tend not to give further coupling. Desideri et al[229] suggest exclusive ortho coupling by either a one or two electron pathway. The latter mechanism would account for the polymer film formation. The effect of adding pyridine is known to promote head to head coupling by proton

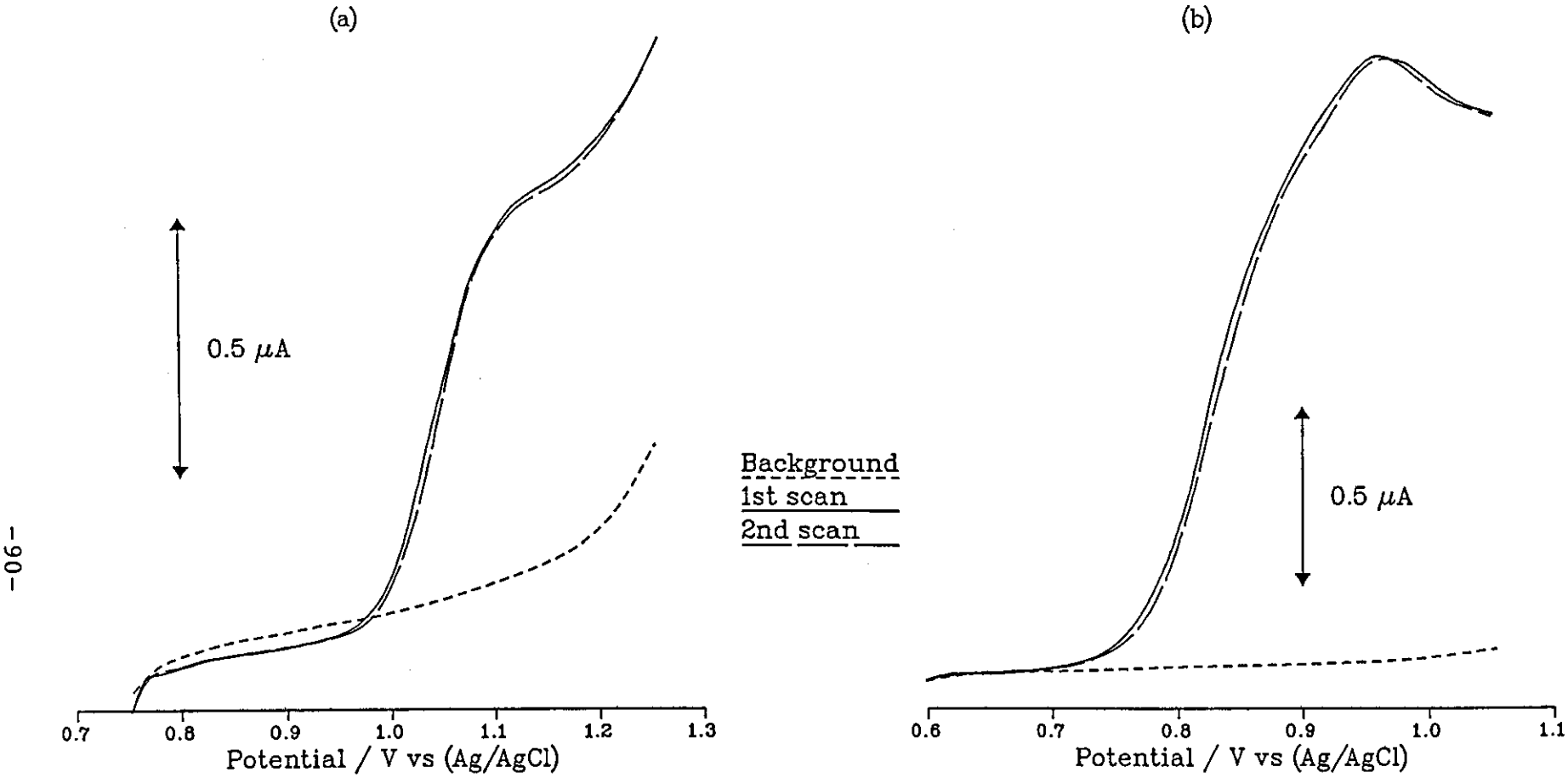

Fig. 20

Linear Sweep Voltammograms of Substituted Anilines

a) p-toluidine (0.1 mM)
Conditions: Background = 0.1M sulphuric acid, electrode = glassy carbon (3.0 mm dia.), $\nu = 2$ mVs^{-1}

b) N,N-dimethyl-p-toluidine (0.1 mM)
Background = 0.1 M sulphuric acid
electrode = glassy carbon (3.0 mm dia.)
$\nu = 3$ mVs^{-1}

extraction from the cation radical, hence less poisoning is observed, but this compound was unsuitable for analytical use.

N,N-diethylaniline

The voltammogram was irreversible and gave rise to variability of the peak current. The electrode was poisoned less than for aniline, but the electrode poisoning was too severe. The poisoning may be attributed to a small proportion of tetramers formed by coupling of tail to tail dimers which are the major product of the initial radicals.

N,N-dimethyl-p-toluidine

The voltammogram was reasonably reversible (fig. 20b), and the reproducibility of the peak current was good. The poisoning of the electrode was low (less than 0.5% for two consecutive voltammograms).

The oxidation is said to occur without initial radical formation in acid solutions. The oxidation is said to proceed via the side chain to give the aldehyde and acid rather than dimerisation to an ortho benzidine.[225] The N,N-dimethyl-p-toluidine showed promise being of similar volatility to aniline giving low electrode poisoning and being fairly easily oxidised ($E_{\frac{1}{2}}$=0.85V) and was investigated further by using fia / DC amperometry.

3.2.2 Analysis of Dimethyl-p-toluidine by fia with Amperometric Detection

Experimental

Hydrodynamic voltammetry was used to find the most suitable potential for hydrodynamic amperometric measurements. The background electrolyte (0.1 M sulphuric acid) and sample (10μM dimethyl-p-toluidine in 0.1 M sulphuric acid) were propelled using seperate pump tubes, sample and background being switched alternately through the detector. The waste line from the valve was of similar dimensions to the tubing connecting the detector to the valve in order to keep the flow rates the same. A glassy carbon electrode (3 mm diameter) was placed in a wall jet cell WJ1 and immersed in a beaker containing background electrolyte. A platinum counter electrode and Ag/AgCl reference electrode were placed either side of the cell. The cell was connected to the valve with a 100cm length of 0.8mm i.d. PTFE tubing. The peristaltic pump was a Minipuls 2 pump.

The baseline was recorded on a chart recorder, the switching valve (Rheodyne 5020) was turned to introduce sample to the detector until a steady reading was obtained. This was repeated for potentials of 0.6 to 1.2V in increments of 0.1V. The flow rate was initially 1.0 $cm^3 min^{-1}$ for the first set of potentials, it was increased to 2.0 $cm^3 min^{-1}$ and the current voltage relationship was measured as before, flow rates up to 6.0 $cm^3 min^{-1}$ were employed. The flow rates were measured by collecting waste eluent overflowing from the beaker for a measured time and weighing this on a balance. The potentiostat was a Metrohm E 611 detector box.

The apparatus for fia was based on the above equipment, a

loop was fitted to the Rheodyne valve, making the volume injected about 75 µl. A pulse damper (fig. 13) incorporating a piece of platinum wire to earth the solution, was placed between the pump and valve. The flow rate was 6.0 $cm^3 min^{-1}$. The measuring potential for D.C. amperometry was +1.0V and for pulse amperometry +0.85V with a pulse amplitude of +0.2V. The DP2 mode (see 2.1) was selected with a drop time of 0.4s. The detector was calibrated over the range 1 to 10µM dimethyl-p-toluidine for the D.C. mode. Each standard was injected three times, starting with the lowest concentration.

A comparison of the Metrohm E 611 detector with a Dionex PAD detector was done by injecting 10 µM of dimethyl-p-toluidine. (The Dionex detector was only available towards the end of the project) The peristaltic pump and damper were the same as above. A Dionex slider valve with a loop of about 70 µl was connected to the wall jet (WJ3), fitted with a glassy carbon electrode (3 mm diameter), by a 60cm length of 0.55mm i.d. PTFE tubing. The flow rate was 3.0 $cm^3 min^{-1}$. The base potential was 0.85V with a pulse amplitude of 0.2V. The Metrohm detector was used as above i.e. the pulse width was 160ms, with the current measured for the last 20ms and the frequency of the waveform was 2.5Hz. The pulse width for the Dionex instrument was 180ms, the current was measured for the last 50ms and the frequency was 2.38Hz.

Results and Discussion

The hydrodynamic voltammogram (Fig. 21) is mass transport controlled and tends towards a current plateau at higher applied potentials. The curve for a flow rate of 6.0$cm^3 min^{-1}$ differs in that there appears to be a second wave with $E_{\frac{1}{2}}$ = 1.1V. The conditions chosen for amperometric detection were 1.0V and 6.0$cm^3 min^{-1}$, the

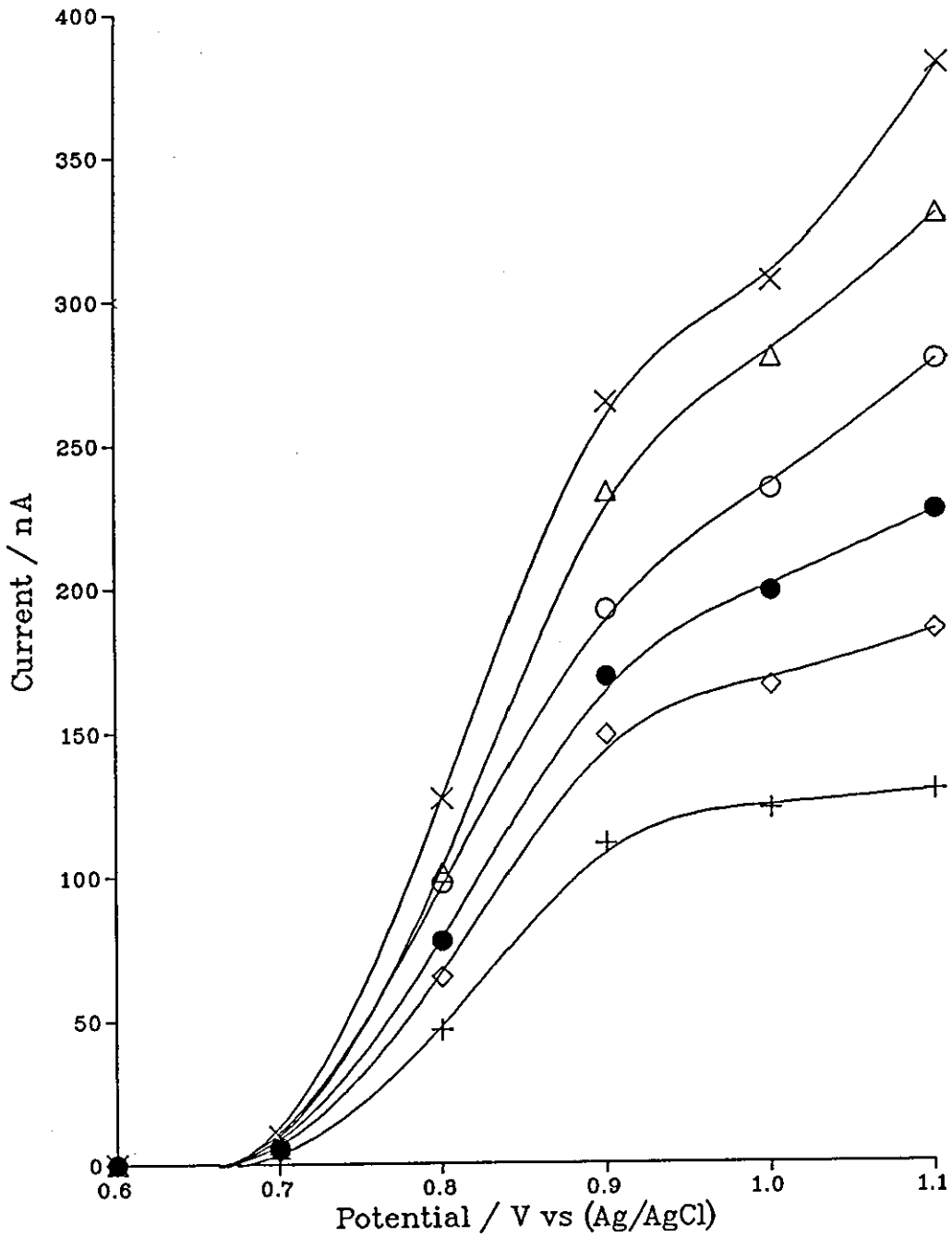

Fig. 21
Hydrodynamic Voltammogram of
N,N–dimethyl–p–toluidine (0.1mM)

Conditions: cell = wall jet (WJ1)
background = 0.1 M sulphuric acid
electrode = glassy carbon (3.0 mm dia.)

potential is on the first plateau and the flow rate was optimal for signal to baseline noise ratio and reagent consumption.

Fig. 22 shows two typical calibration curves for concentrations of dimethyl-p-toluidine in the range 0 to 10 μM for fia with D.C. amperometric detection. The calibrations were prepared consecutively. The decrease in sensitivity for the second calibration was unacceptable. The decrease in sensitivity between consecutive calibrations varied between 4% and 20% for 10 calibrations.

The pulse mode was not capable of detecting concentrations of dimethyl-p-toluidine much below 10μM, because the potentiostat became overloaded with the background current and it was not possible to offset the background current for sensitivities higher than about 0.1 μA f.s.d. The base potential and pulse amplitude were compromised because of this. This problem was encountered previously. The pulse mode was not pursued any further because the detection limit was not low enough for the levels of amine anticipated in the intended application for the sensor (see 1.8). The pulse mode should minimise poisoning of the electrode by reaction products where the electrode reaction is reversible and might have offered a solution to the detection of this amine if the background current could be decreased.

Fig. 23 shows peaks obtained using the Metrohm and Dionex detectors in the pulse mode. The signal to noise ratio for the Dionex detector was far superior and it was possible to offset much larger background currents. The Dionex instrument is specifically designed for the application of complex waveforms and seems to employ superior electronics to avoid overloading the

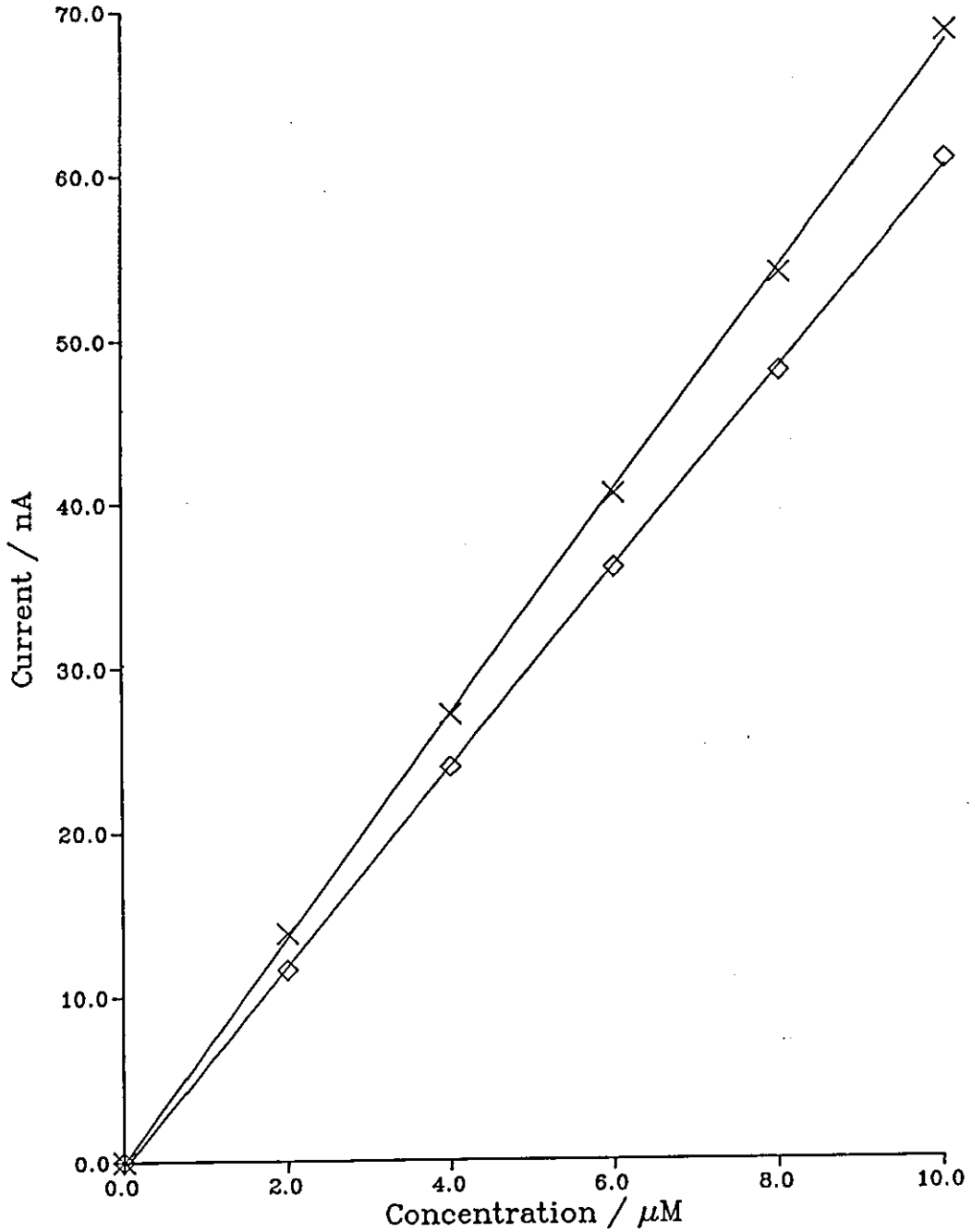

Fig. 22
Typical Calibration Curves for the determination of N,N-dimethyl-p-toluidine by fia

Conditions: background = 0.1 M H_2SO_4
Cell = wall jet (WJ1), vol. injected = ~ 75μl
Electrode = glassy carbon (3.0 mm dia.)
Flow rate = 6.0 cm^3 min^{-1}, E = 1.0 V

× 1st calibration
◇ 2nd calibration

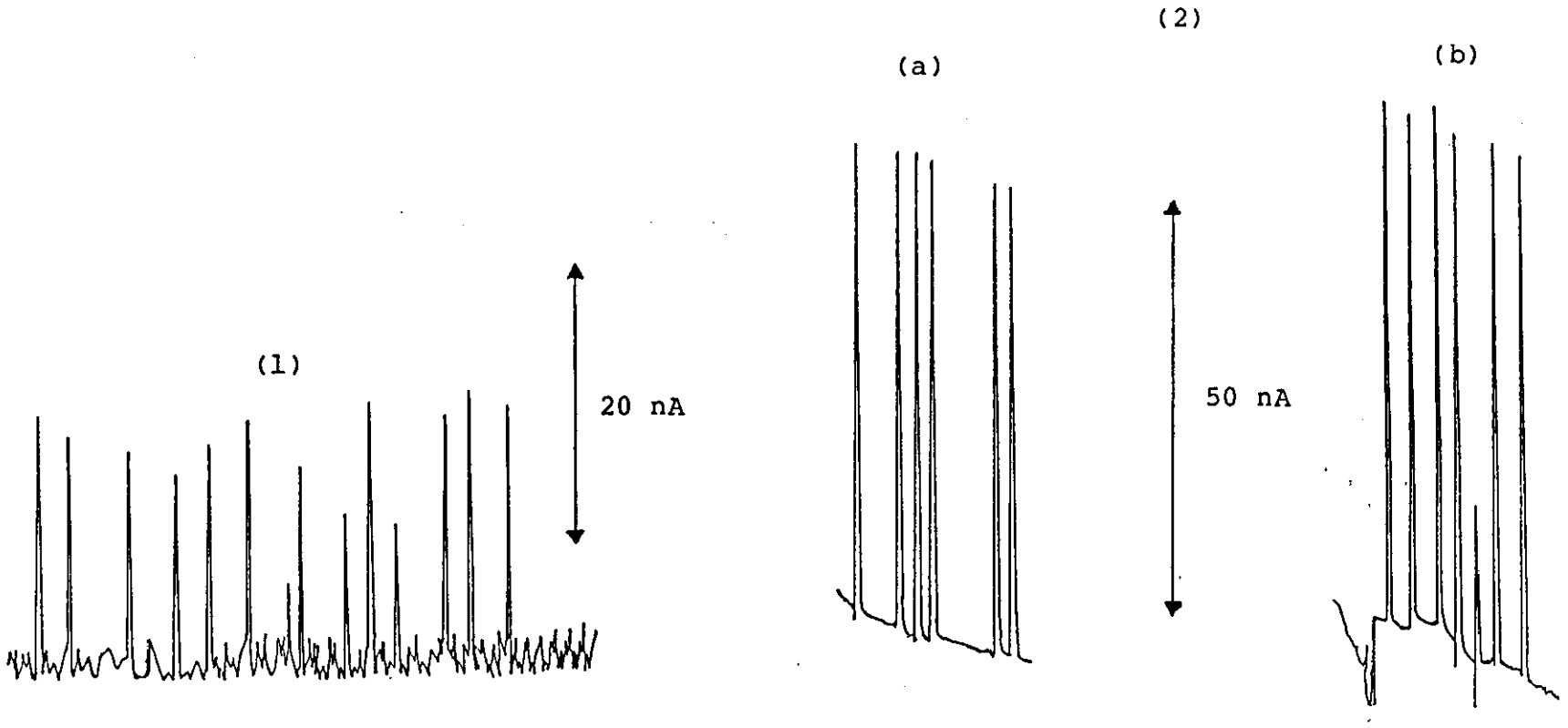

Fig. 23
Comparison of two Detectors for Pulsed Detection of N,N-dimethyl-p-toluidine (10 μM)

Conditions: cell = wall jet (WJ3), flow rate = 3.0 cm^3 min^{-1}, loop vol = ~70 μl, carrier = 0.1M sulphuric acid
1) Metrohm E 611, mode = DP2, E_{BASE} = 0.65 V, ΔE = 0.2 V, t_d = 0.4 s
2) Dionex PAD a) E_1 = 0.65 V, E_2 = 0.85 V, T_1 = 3, T_2 = 4, t(resp) = 0.3 s: b) E_1 = 0.6 V, E_2 = 0.9 V, T_1 = 3, T_2 = 4, t(resp) = 0.3 s

potentiostat circuits. A lower base potential might be used with this instrument, and this potential could be applied for a longer fraction of each cycle: offering the advantage of improved desorption of reaction products from the electrode surface, yet maintaining a good detection limit. The effect of higher concentrations might still be a problem.

CHAPTER 4

PULSED AMPEROMETRIC DETECTION OF ANILINE

4.1 Introduction

The technique of pulsed amperometric detection (PAD) has primarily been developed to detect species which adsorb at a platinum electrode. Their detection is based on the faradaic signal for oxidative desorption.[60] Advantage might be taken of the potentiodynamic cleaning of the PAD waveform to detect organic compounds which foul electrodes when detected by conventional amperometric techniques. PAD waveforms have been established for detection of aliphatic amines in alkaline conditions[62], but for aromatic amines, anodic detection is considered to be successful at constant potential.[60]

The aim of the work in this chapter was to develop a PAD waveform to detect aniline in acidic solution and to then develop a method for the measurement of aniline vapour in air. A simple system was required to generate aniline vapour. The vapour collection device needed to be efficient and readily interfaced to the detector.

4.2 Initial Investigations of PAD of Aniline

4.2.1 Preliminary Voltammetry

Experimental

An acidic solution was used as the absorption solution to ensure efficient trapping of the aniline vapour. The same solution was used as the background electrolyte (0.1 M sulphuric acid) to avoid high blank values because the

PAD response is sensitive to solution pH.[230] It would seem more straightforward to monitor the sample continuously rather than by fia, but that would not permit the background signal to be readily measured. Baseline drift is often a problem in hydrodynamic amperometry at high sensitivity and is overcome by using fia.

Cyclic voltammetry was carried out on a platinum electrode in 0.1M sulphuric acid, and for a solution of 1 mM aniline in the same electrolyte. The scan rate was 10 mVs^{-1}.

Results

The cyclic voltammogram fig. 24 shows the formation of surface oxides on the platinum electrode as the potential is scanned anodically, with an exponential rise in the current for potentials greater than about +1.2 V vs Ag/AgCl. This sharp rise in the current is due to the onset of the electrolysis of water and an increase in the rate of oxidation of the platinum electrode. The reduction of the oxide layer occurs for potentials less than +0.6 V on the cathodic cycle. Oxidation of aniline by diffusion control occurs with Ep = +1.05 V.

Discussion

The information obtained from the cyclic voltammogram may be used to give a starting point for the PAD waveform, according to the following guidelines established by Johnson and workers. In order to achieve efficient desorption of adsorbate the cleaning potential needs to be set close to or even beyond the onset of significant breakdown of water, which was found to be about +1.4 V. The adsorption potential needs to be fairly negative, the

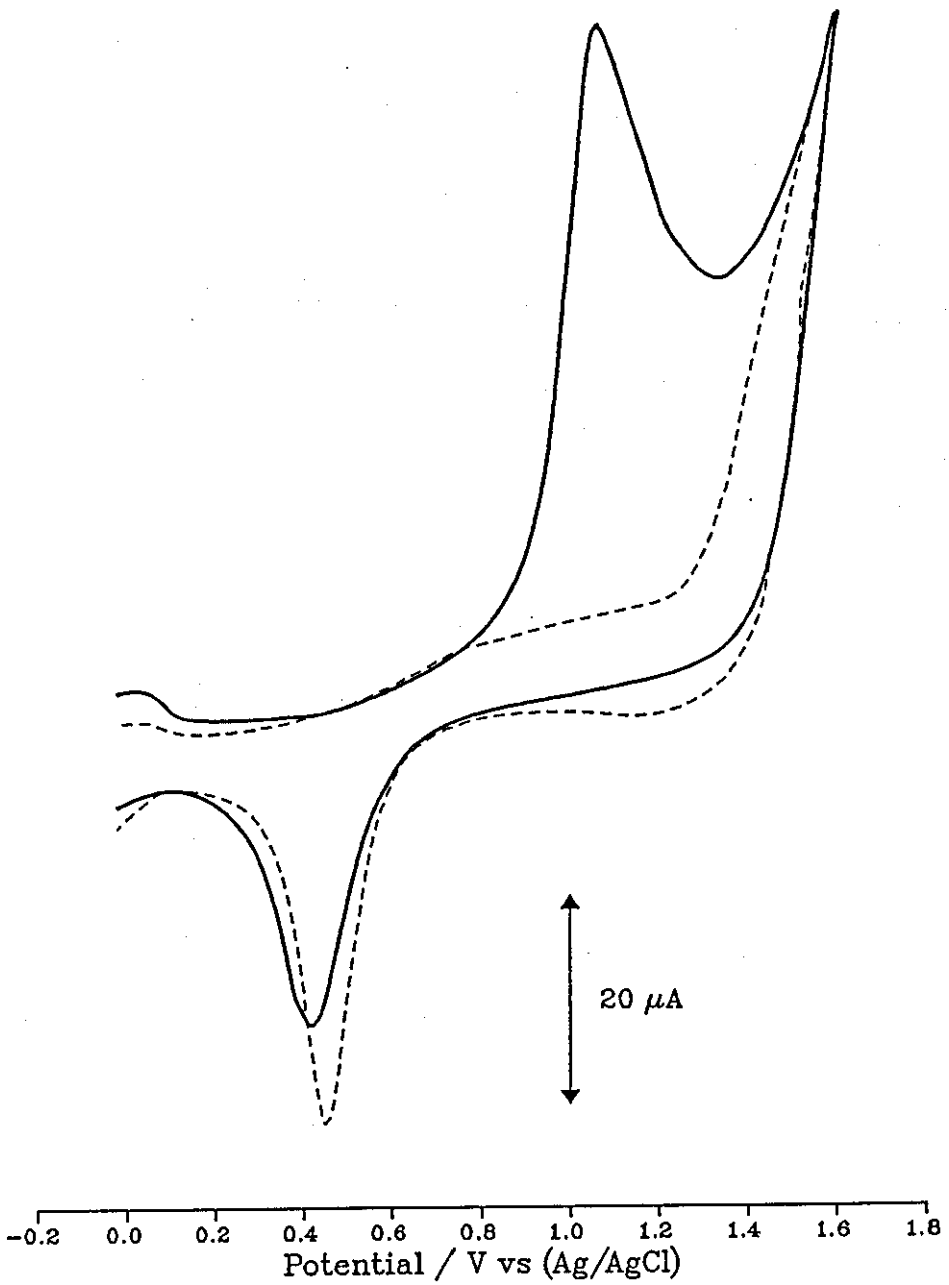

Fig. 24
Cyclic Voltammogram of Aniline (0.5 mM)

Conditions: Background =
0.1 M sulphuric acid, $\nu = 10\ mVs^{-1}$
electrode = platinum (4.8 mm dia.)

Background
Sample

cathodic cut-off being the lower limit. The measuring potential may be adjusted according to the faradaic response obtained. The pulse widths tend to be found empirically because the times and potentials are interdependent. Once a suitable response is obtained (good peak shape), then the pulse widths may be optimised systematically.

4.2.2 Simplex Optimisation of the PAD Waveform

Experimental

A simplex program[231] for optimising atomic absorption instruments was available and so this was used to optimise the PAD fia system. One of the criteria of the simplex method is that all the factors are continuous variables. In the case of the PAD, the pulse widths are only adjustable in steps of 60 ms, and so a compromise was made to round up the values provided by the program to integer values. The flow injecton system consisted of the Gilson Minipuls 2 peristaltic pump to propel the carrier, the home made pulse damper (fig. 13), the Dionex injection valve (fig.8), flow cell (fig. 12) and detector module.

A schematic diagram of the fia system is shown in fig. 25a. The amount of air in the pulse damper was adjusted to give the lowest noise level when monitored using the flow rate device (fig. 9), which was installed after the flow cell. The manifold tubing was 0.5 mm i.d. PTFE, 60 cm long. A short length of 0.3 mm i.d. tubing was placed after the flow cell as recommended, in order to prevent degassing of the eluent and to pressurise the oxygen bubbles which are formed as a result of the cleaning potential. The volume of the loops was approx 100 µl. The injection loop was flushed by pumping the sample from the

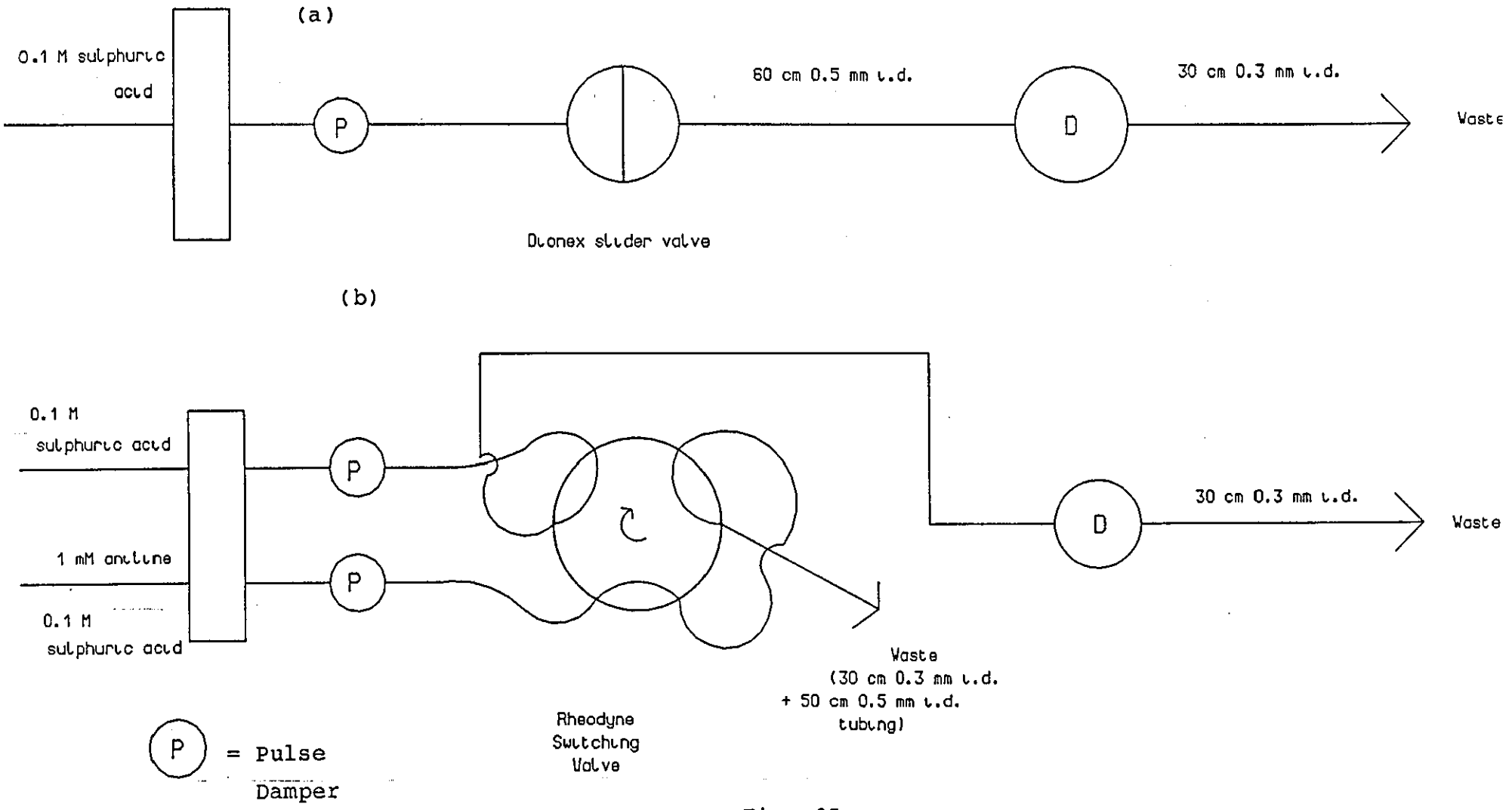

Fig. 25

Schematic diagrams of Flow Manifolds used for fia and Continuous Flow with PAD

graduated flask through the loop, to waste. The flow rate was 1 $cm^3 min^{-1}$ as recommended in the instruction manual. A stock solution of 0.01M aniline in 0.1M sulphuric acid was prepared and diluted to give a sample solution of 1mM aniline in sulphuric acid.

The program asks for the number of variables, the range of each, and the precision required to finish the program. The ranges for the three potentials were based on cyclic voltammetry at a platinum electrode in sulphuric acid. The response factor was defined as the ratio of signal to baseline noise. The response factors were determined experimentally for the initial vertices provided and a reflection of the vertex with lowest response was generated. The response factor was again determined and so on. After a reasonable number of repetitions it was decided to terminate the program because the response factors did not show any trend of increasing in value.

Results

A typical set of results is shown in table 3 for optimisation of the PAD waveform using 1 mM aniline in 0.1 M sulphuric acid.

Table 3

Simplex Optimisation of PAD Waveform

Vertex Number	E1	E2	E3	T1	T2	T3	Resp. Factor
1	0.30	1.29	-0.50	1.0	1.0	1.0	47.7
2	0.99	1.45	-0.34	2.74	2.63	2.55	0
3	0.50	1.87	-0.34	2.74	2.63	2.55	7.35
4	0.50	1.45	0.15	2.74	2.63	2.55	10.1
5	0.50	1.45	-0.34	8.4	2.63	2.55	37.0
6	0.50	1.45	-0.34	2.74	8.29	2.55	0
7	0.50	1.45	-0.34	2.74	2.63	8.2	31.5
			Reflection Vertices				
	0.59	1.53	-0.23	4.0	2.67	4	0
	0.52	1.47	-0.32	3.25	5.33	3.25	0
	0.6	0.98	-0.23	4	3.11	4.08	0
	0.52	1.64	-0.32	3.27	3.02	3.27	12.1
	0.58	1.44	-0.25	3.83	1	3.83	0
	0.53	1.46	-0.31	3.39	4	3.39	9.3

Discussion

The most important feature of the simplex method is the choice of the initial simplex, but its size is said not to be important if it can be expanded or contracted as the method proceeds.[232] The simplex method used here was capable of these features, but the choice of pulse widths is very critical as regards the stability of the electrode and the peak shapes. From observation of the cyclic voltammogram (fig. 24) the rate of formation of

surface oxide is much faster than the rate of reduction to the metal and so it would be reasonable to assume that T3 > T2, in order to keep the effective electrode area constant. The value of T1 can affect both the magnitude and the sign of the signal.[56]

The method failed because the reflection of the lowest vertex and subsequent rounding to an integer tended to change some of the pulse widths by more than 60 ms which had a dramatic effect on the electrochemistry at the electrode. The change in potentials had a much smaller effect, and it might be reasonable to suggest that a weighting factor for the pulse widths would have improved the advance of the simplex program to a maximum. This approach is suggested by Miller and Miller[233] and could be incoporated into the program.The major advantage of the simplex over other methods is that an optimum may be reached with the minimum of experiments, and there are various modifications being made to allow for its weaknesses.[234]

4.2.3 Manual Optimisation of the PAD Waveform

Experimental

Values for E2 and E3 taken from cyclic voltammetry were applied along with specimen times for T1, T2 and T3 taken from the table of PAD waveforms presented in reference (56). By adjustment of E1 it was possible to get a response from the detector. The peak shapes obtained from the initial waveforms were not as commonly associated with fia (see fig. 26a, 26b). These abnormalities in shape were caused by deficiencies in the applied waveform and were used to guide the optimisation of the applied waveform. The apparatus was the same as in section 4.2.2.

Results and Discussion

Table 4 shows the waveforms which were developed using the peak shapes as a guide to optimisation.

Table 4

Triple-step Potential Waveforms for the Detection of Aniline at a Pt Electrode in 0.1 M Sulphuric Acid

W/form	Applied Potential/V			Pulse Width / ms		
W	E1	E2	E3	T1	T2	T3
A	0.6	1.85	0.1	180	120	120
B	0.6	1.85	0.1	180	120	240
C	0.6	1.85	0.2	180	120	240
D	0.6	1.77	0.2	180	60	120
E	0.6	1.78	0.18	120	60	120
F	1.0	1.78	0.18	120	60	120

E1 = measuring potential
E2 = cleaning potential (oxidation of surface and desorption of products)
E3 = activation potential (reduction of oxidised surface and adsorption of analyte)

One of the the preliminary waveforms (WA), (fig. 26a) gave a faradaic response but both the leading edge and tail dipped below the baseline. T3 was increased from 120 to 240 ms (WB), to ensure electrode stability, but the peaks were negative, (fig. 26b). It was eventually found that by increasing E3 from 0.1 to 0.2 V (WC), the peaks

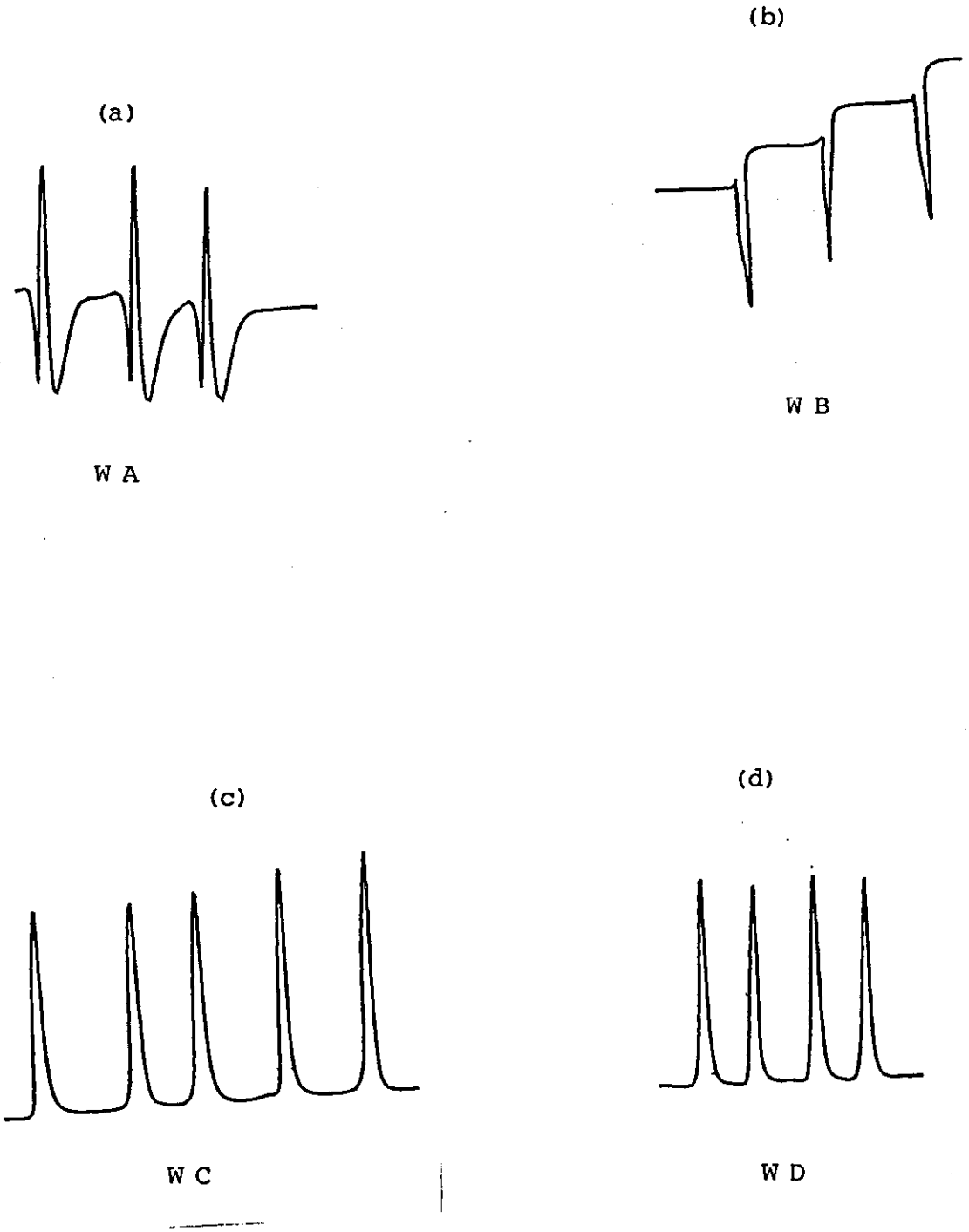

Fig. 26
Typical peaks obtained for fia with PAD for optimisation of some of the Preliminary Waveforms

See table 4 for details of the waveforms.

became positive and well shaped (fig. 26c) but were not stable. By varying T2 and T3 a stable response was obtained (fig. 26d) (WD), with a small decrease in E2 also required.

It must be emphasised that a great deal of trial and error was involved in obtaining the stable and responsive waveform (WD). For the the preliminary investigations it was often impossible to relate the peak shape and height to the applied waveform, e.g. fig. 26a (WA).

4.3 Further Optimisation of PAD of Aniline

4.3.1 Optimisation of the Adsorption Time

Experimental

The adsorption time (T3) was optimised by varying it from 120 to 240 ms in 60 ms steps and recording the peak current and the baseline noise over a period of time for each setting. The apparatus was the same as previously, but 10 μM aniline was injected. The waveform was as (WE), with T3 varying.

Results and Discussion

The results are shown in table 5, it is clear that as T3 was increased the signal to baseline noise was decreased. The faradaic current was increased but the noise was increased to a greater extent. The measuring time T1 was not optimised at this stage and was fixed at 120ms, but it was noted that increasing T1 decreased the peak current. An increased response is not usually obtained for T3 > ca. 200ms for many carbohydrates and amines[235] and so increasing T3 beyond this value tends to decrease

the frequency of the current measurement without a significant increase in the faradaic current.

Table 5
The effect of The Adsorption Time (T3) on the Signal to Baseline Noise Ratio

Adsorption Time /ms	Mean Signal to Noise Ratio	Standard Deviation
120	7.3	1.9
180	4.3	0.5
240	2.9	0.3
300	2.4	0.4

4.3.2 Optimisation of the Measuring Time

Experimental

The time T1 was optimised for waveform (WF) using the wall jet detector (WJ3). The apparatus was set up as in fig. 25a. The flow rate was 3 $cm^3 min^{-1}$ of 0.1M sulphuric acid eluent, E1 was adjusted to 1.0V. The analyte was 10 μM aniline in 0.1M sulphuric acid. T1 was varied between 60 and 180 ms and the peak current and baseline noise was measured over a period of time. The current is measured for the last 20 ms of the measuring time (E1).

Results and Discussion

The signal to baseline noise ratios are given in table 6. The peak current decreased with increasing Tl, but the charging currents decreased at a faster rate initially. The dependence of the faradaic current on the delay before measurement is made is given in reference (56).

If t = time and I_{mt} = mass transport limited faradaic current then at short t i_{mt} is proportional to $t^{-1/2}$ as described by the Cottrell equation. For long t i_{mt} deviates from the Cottrell equation and approaches a non-zero value which is a function of geometry and the rate of convection. The current due to formation of surface oxide (i_{ox}) is proportional to t^{-1}. It follows that at short t the resulting current (i) will be small, possibly negative but for long t it will be enhanced.

The delay time of 40 ms is too short to allow i_{ox} to have decayed significantly more than i_{mt}. The optimum delay was 100 ms i.e. Tl=120ms. This optimum is probably caused by the pump noise from the fia system becoming significant. At longer t the i_{mt} to i_{ox} ratio becomes favorable. On increasing t further, the signal (i) to noise ratio begins to decrease because i is slowly decreasing but the noise due to pump pulsations remains much the same as it depends on the current measurement time (20 ms).

Table 6

The Effect of The Delay in the Measuring Time (E1) on the Signal to Baseline Noise Ratio

T1 /ms	Delay Time /ms	Mean s/n Ratio	Standard Deviation
60	40	2.1	0.23
120	100	7.6	0.46
180	160	7.1	0.37
240	220	6.5	0.58

The waveform (WF) was used in all further applications, only the measuring potential E1 being varied. For the purposes of optimisating the waveform it was assumed that the two flow cells behaved in a similar way when operated at proven flow rates.

4.3.3 Optimisation of the measuring potential E1

Experimental

The experimental set up is shown in fig 25b. The background and sample were pumped using seperate pump tubes for convenience, sample and background being switched alterately through the detector. The waste port from the valve was connected to a length of tubing of similar dimensions as the detector plus backpressure coil. This was to match the flow rates of the two lines. The eluent and sample were 0.1 M sulphuric acid and 1 mM aniline in 0.1 M sulphuric acid respectively. The potential ranges were 0.3V to 1.1V for the dionex cell and 1.0V to 1.2V for the wall jet cell (WJ3). The flow

rates were as used previously. The baseline noise was recorded over a period of time, the valve was then switched to introduce the sample to the detector until a steady reading was obtained. It was noticed that at potentials greater than +0.9 V prolonged passage of sample lead to a steady decrease in signal. The valve was returned to allow eluent to pass to the cell. When the signal had returned to the baseline the potential was changed to the next setting and the electrode was allowed to reach equilibrium before more measurements were made.

Results and Discussion

Table 7 shows the effect of the measuring potential on the signal to noise ratio for the Dionex and wall jet cells (WJ3) respectively.

Table 7
The Effect of the Measuring Potential (El)
on the Signal to Baseline Noise Ratio

	DIONEX CELL		WALL JET CELL (WJ3)	
El / V vs Ag/AgCl	Current / μA	Mean s/n Ratio	Current / μA	Mean s/n Ratio
0.3	13.3	600		
0.4	9.5	650		
0.55	6.5	5400		
0.9	4.0	4000	41.2	
1.0	13.6	17900	108.5	1100
1.1	22.4	14500	140.5	1250
1.2			166	1250
1.3			188.5	

There are two distinct regions of potential (E1), where electroactivity of aniline is observed. The faradaic current observed in the potential region 0.3 - 0.6 V is proposed to be due to oxidative desorption of aniline adsorbed during time T3. The faradaic current observed in the potential region greater than 0.9 V is proposed to be mainly due to diffusion limited electron transfer of aniline during current measurement (the last 20 ms of time T1). For more details see (4.3.6)

The effect of E1 on the signal to noise ratio was first investigated with the Dionex cell. The region (0.3 - 0.6 V) gave a significantly poorer signal to noise ratio than the region beyond 0.9V. The wave for reduction of molecular oxygen falls within the adsorptive region and leads to a high baseline noise. For the region beyond 0.9V, the faradaic currents are of the same order as for the adsorptive region but the noise is much less, being due to oxidation of water and surface oxide formation on the platinum electrode.

The baseline for the adsorptive region (0.3 - 0.6 V) was very noisy and only the higher potentials were optimised. The signal to noise ratios for different potentials in the region (1.0 - 1.2V) were similar, the noise seems to increase at about the same rate as the faradaic current with an increase in potential.

The signal to noise ratio of the Dionex cell is significantly better than for the wall jet cell. The cell geometries must clearly be a major factor. Also it was found that the waste eluent from the wall jet cell contained gas bubbles, increasing the backpressure on the cell seemed to decrease them and decreased the baseline noise. The amount of backpressure which could be applied to the cell was limited by leakage of it. The amount of

bubbles in the waste from the Dionex cell was quite small as more backpressure could be applied, also the electrode area is smaller and so most of the oxygen formed at the working electrode is dissolved by the eluent. Smaller platinum electrodes were not available to fit the wall jet cell.

4.3.4 The effect of the Measuring Potential on the Selectivity of the Detector

Experimental

An atmospheric sample was trapped in a bubbler in order to investigate the interference of pollutants on the response of the PAD to aniline and the selectivity towards aniline afforded by employing different measuring potentials. About 150 l of air from the analytical laboratory were drawn through a dreshel bottle containing 100 cm^3 0.1M sulphuric acid, by means of a water pump. The experimental set up for fia and conditions used was the same as previously. Sample were taken from the bubbler and injected into the fia/PAD, along with an aniline solution for comparison (10 μM in 0.1M acid). The detector was operated at 0.5V and 0.9V.

The infra red spectrum of the trapped air sample was measured but the concentration was too low to give a satisfactory signal. A diazo-coupling test was carried out by acidifying the sample with dilute HCl, cooling to 4 ^oC and adding 2 cm^3 of 0.1% of aqueous sodium nitrite. To this was added 1 cm^3 of 0.1% solution of 2-naphthol in ethanol.

Results and Discussion

The peaks obtained are shown in fig 27. At 0.5 V the atmospheric sample gives a peak height 1.4 times that for 10 μM aniline standard, also the sample peak is much broader. At 0.9 V the sample peak height is 0.2 times that for aniline, the sample peak is slightly more broad. At 0.9 V the detector shows an enhanced response for the aniline standard compared with the trapped air sample. At 0.5 V the current is larger for the trapped air sample. At this potential the current is mainly due to oxidative desorption of adsorbed analyte and might be expected to show a more general response to electroactive adsorbates.

The result of the coupling reaction was negative. The concentration of the unknown substance in the trapped air sample might be at the limit of detection for this test. There was no other more sensitive method available e.g. gc with N-P detector and so the composition of the trapped air sample is unknown.

4.3.5 The effect of Flow rate on the Faradaic Current for the Wall Jet Cell (WJ3)

Experimental

The measuring potentials chosen were E1 = 0.45 and 1.0V, the flow rate was between 1-5 $cm^3 min^{-1}$. A Gilson minipuls 2 pump was used to propel the background (0.1 M sulphuric acid), and the sample (1mM aniline in 0.1 M sulphuric acid). Flow rates were calculated from the volume collected from the cell outlet into a 10 cm^3 measuring cylinder for a period of time measured using a stopwatch. The apparatus is shown in fig 25b.

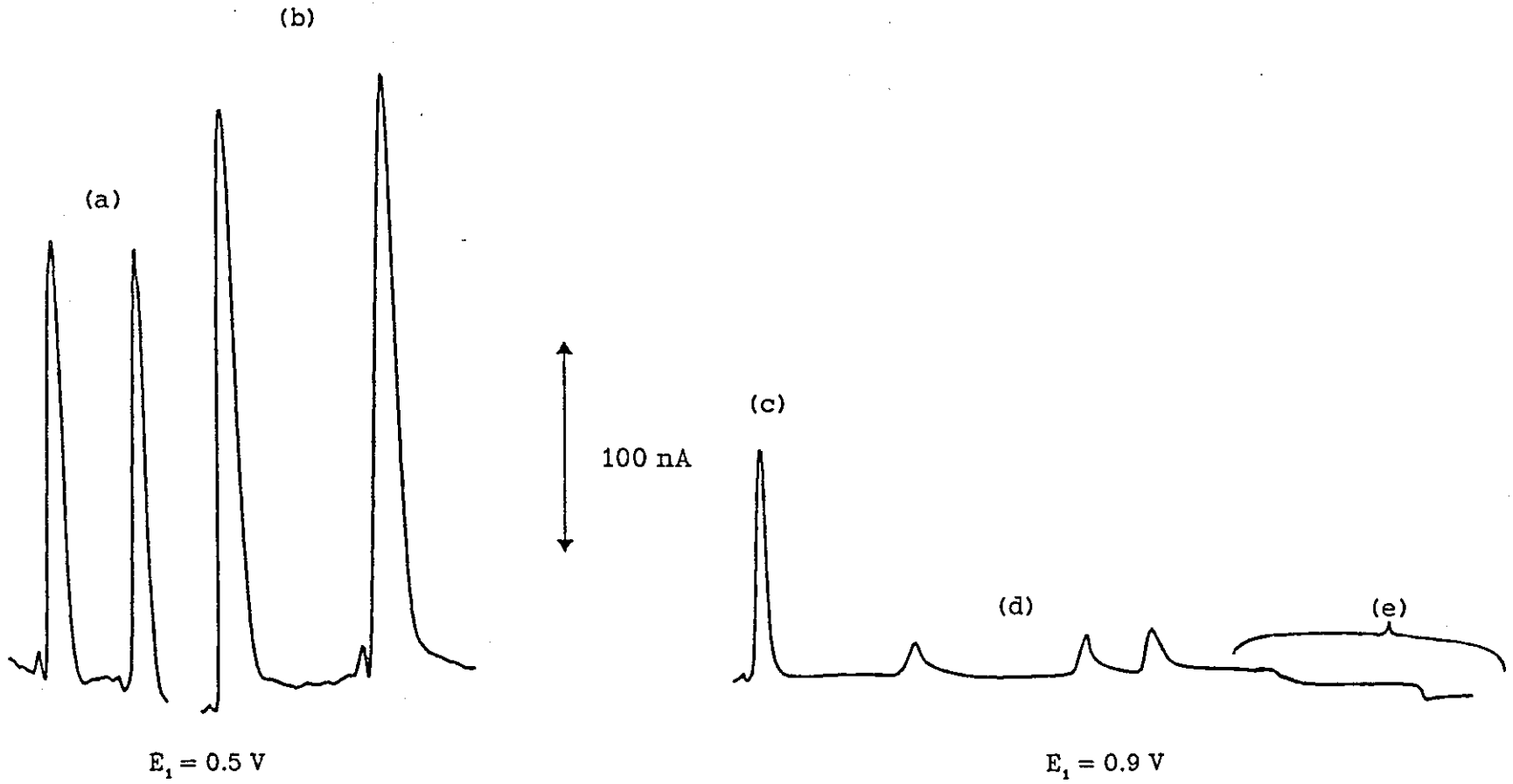

Fig. 27
Peaks for PAD of Trapped Aniline Vapour
at two Measuring Potentials

Conditions:
a) 10 μM aniline, b) Atmospheric Sample (150 dm^3 / 50 cm^3 0.1M H_2SO_4)
c) 10 μM aniline, d) Atmospheric Sample, e) Blanks

Results and Discussion

Typical results are shown in fig. 28.

E = 0.45V

The response of the cell showed a maximum value for low flow rates, as the flow rate was increased further a plateau was obtained. The faradaic current is probably mass transport limited up to the maximum, then the current becomes limited by the rate of the adsorption process as the flow rate is increased. Most often in electrode processes the slowest step is mass transport of the electroactive species to or from the electrode surface by diffusion. By increasing the mass transport by convective diffusion, the current may be increased until the rate of electron transfer becomes limiting. This condition is not usually encountered because electron transfer rates are high for most amperometric processes at solid electrodes, compared with the mass transfer rates available using conventional flow cells. The response normally observed is a gradual increase of the current to a plateau as the flow rate is increased.

In this case, increasing the rate of mass transport beyond the point of maximum current leads to a decreasing response. The kinetics of aniline adsorption are probably rather slow, this is thought to be the case for carbohydrates and amines.[235] This could give rise to adsorption with no concentration polarisation. That is the concentration of aniline at the electrode surface is the same as in the bulk solution. The driving force for diffusion to the electrode surface is usually the concentration gradient, but in this case may be due to the attractive forces of the adsorption sites. The attractive forces would be opposed by the momentum of the electroactive species leading to a decreased current.

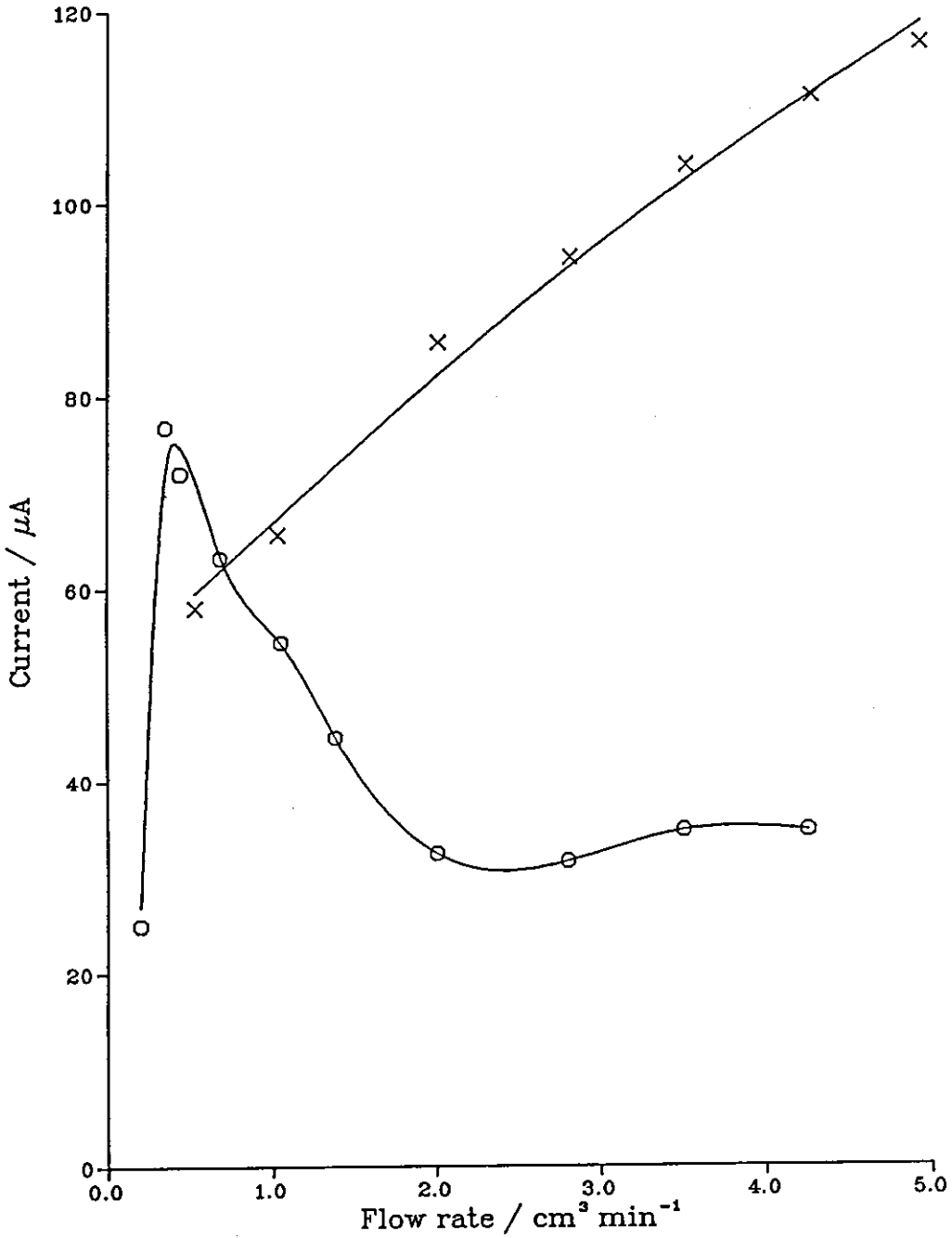

Fig. 28
Flow Rate vs Current for Wall Jet Cell (WJ3)

Conditions:
background =
0.1 M sulphuric acid
conc. aniline = 1 mM

× E1 = 1.0V
o E1 = 0.45V

Another effect of the stream velocity might be to increase the rate of desorption of aniline during the measuring period, hence a smaller number of adsorbed aniline molecules would remain when the current is sampled for the last 20 ms.

El = 1.0V

The response of the cell was similar to that for typical of that for mass transport controlled hydrodynamic electrode process. The rate of the electrode process must therefore be much faster than for El = 0.45V. A second electrode process is proposed to occur for El > 0.7V, data from hydrodynamic voltammetry and calibration plots seem to confirm this and an explanation is given. (see 4.3.6)

4.3.6 Hydrodynamic Voltammetry

Experimental

Hydrodynamic voltammetry was carried by varying the measuring potential El over the range 0.0 - 1.4V. The apparatus was the same as used previously (fig. 25b). Flow rates were 1.0 and 3.0 $cm^3 min^{-1}$ for the dionex and wall jet cells (WJ3) respectively. The background signal was measured by passing the 0.1M sulphuric acid carrier through the cell. The valve was turned to allow the sample stream to the detector (1 mM aniline in 0.1M sulphuric acid) until a steady signal was obtained, then the valve was returned to the carrier stream. When the signal had returned to baseline, then the potential was changed to the next setting and the electrode was allowed to reach equilibrium before the sample was introduced again.

Results and Discussion

Wall Jet Cell

Two regions of activity are observed (see fig. 29). The region between 0.0 V and 0.6 V has a maximum at about 0.35 V. The baseline noise began to increase rapidly below 0.4 V, which is due to the reduction of molecular oxygen. As aniline is not active in this region when employing DC and pulse hydrodynamic voltammetry: then the faradaic current must be due to charge transfer of adsorbed aniline. As the potential is increased beyond the maximium, the decrease in reponse must be due to more rapid electron transfer of the adsorbed aniline along with platinum oxidation during the delay before the current is sampled. Consequently when the current is sampled, less unoxidised aniline remains and so the measured faradaic current is decreased.

The mechanism of electron transfer in PAD is thought to be via oxygen-transfer catalysis;[56] with the adsorbed hydroxyl radical (i.e. PtOH) as the most common designation of the active oxide at platinum. In 0.1M sulphuric acid most of the aniline exists as the anilinium cation and so the mechanism of adsorption is uncertain. Johnson reports that compounds having the same electroactive functional group have very similar response patterns.[60]

The region from 0.7 V to 1.2 V is similar to the response observed for DC and pulse hydrodynamic amperometry. It would be reasonable to suggest that the majority of the response is due to the electron transfer of aniline in the solution phase. This occurs at the electrode during Tl. A small contribution from surface controlled

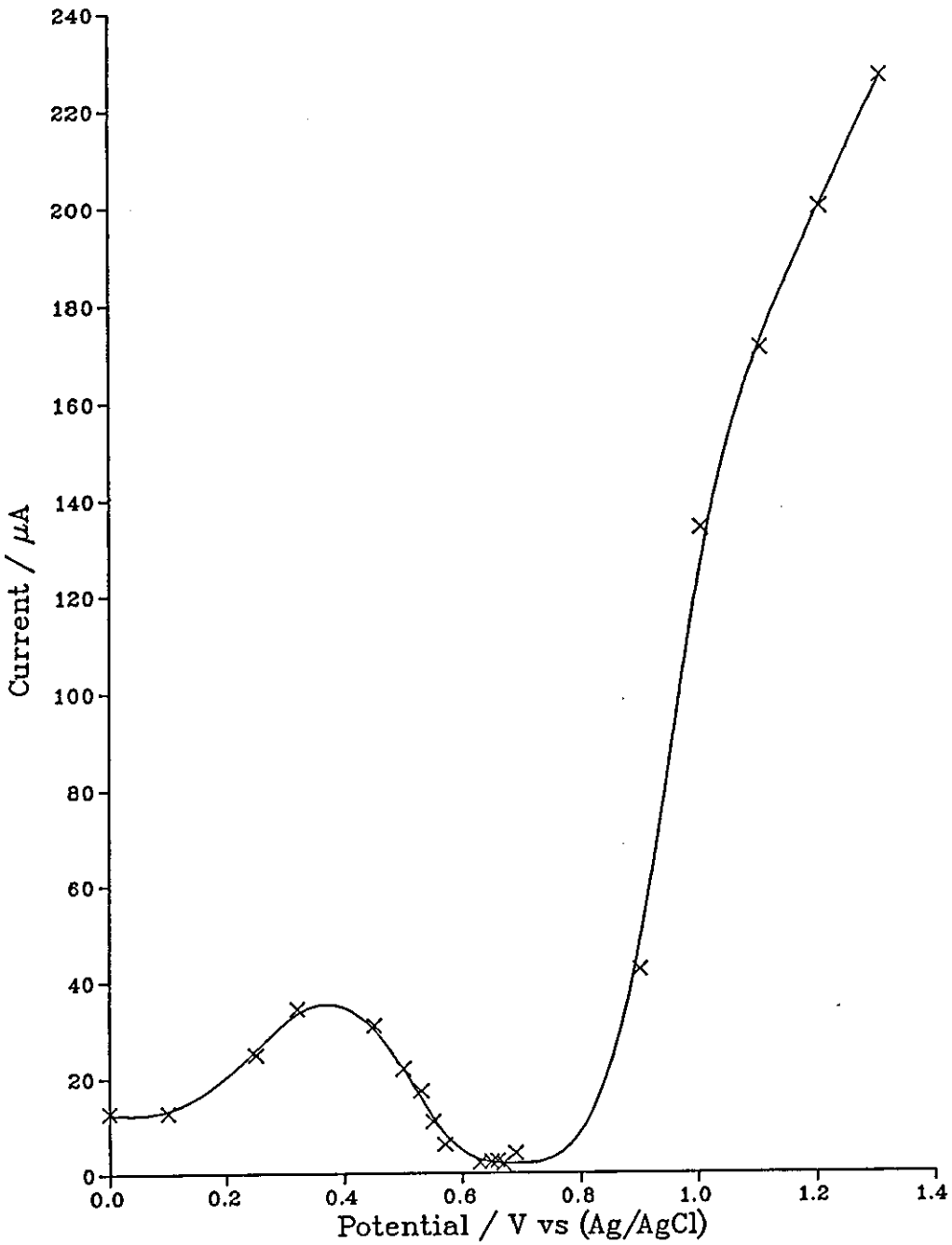

Fig. 29
Hydrodynamic Voltammogram for the
Wall Jet Cell (WJ3)

Conditions: Aniline conc. = 1.0 mM
Flow Rate = 3.0 cm^3 min^{-1} (Continuous Analyte flow)
Background = 0.1 M sulphuric acid

oxidation of aniline adsorbed during T3 is also possible.

Dionex Cell

The hydrodynamic voltammogram is shown in fig. 30. There are two regions of activity as for the wall jet cell. The shapes and sizes of the two regions differ somewhat, the differences in cell geometry and electrode area are probably responsible for this. There is a region between 0.65V and 0.8V where the measured current is negative. This is not a reduction current but results from the measured current in the presence of aniline being less than the background current. This negative current is probably a function of the delay in the measuring period and the measuring potential. If all the adsorbed aniline undergoes electron transfer during the delay in the measuring period, then when the current is sampled only oxidation of platinum and water occurs. If some of the platinum sites remain blocked by reaction products then oxide formation is inhibited there, and the current is less than for the bare electrode.

4.4 Calibration of the PAD Response

4.4.1 Development of a Curve Fitting Program and Characterisation of the PAD Response

Experimental

A computer program was developed[236] from a polynomial least squares fitting program[237] to fit an equation derived from the Langmuir isotherm,[56] to the calibration data. This equation was also modified with an additional term as it was suspected that the response was not controlled soley by the adsorption isotherm. A mass

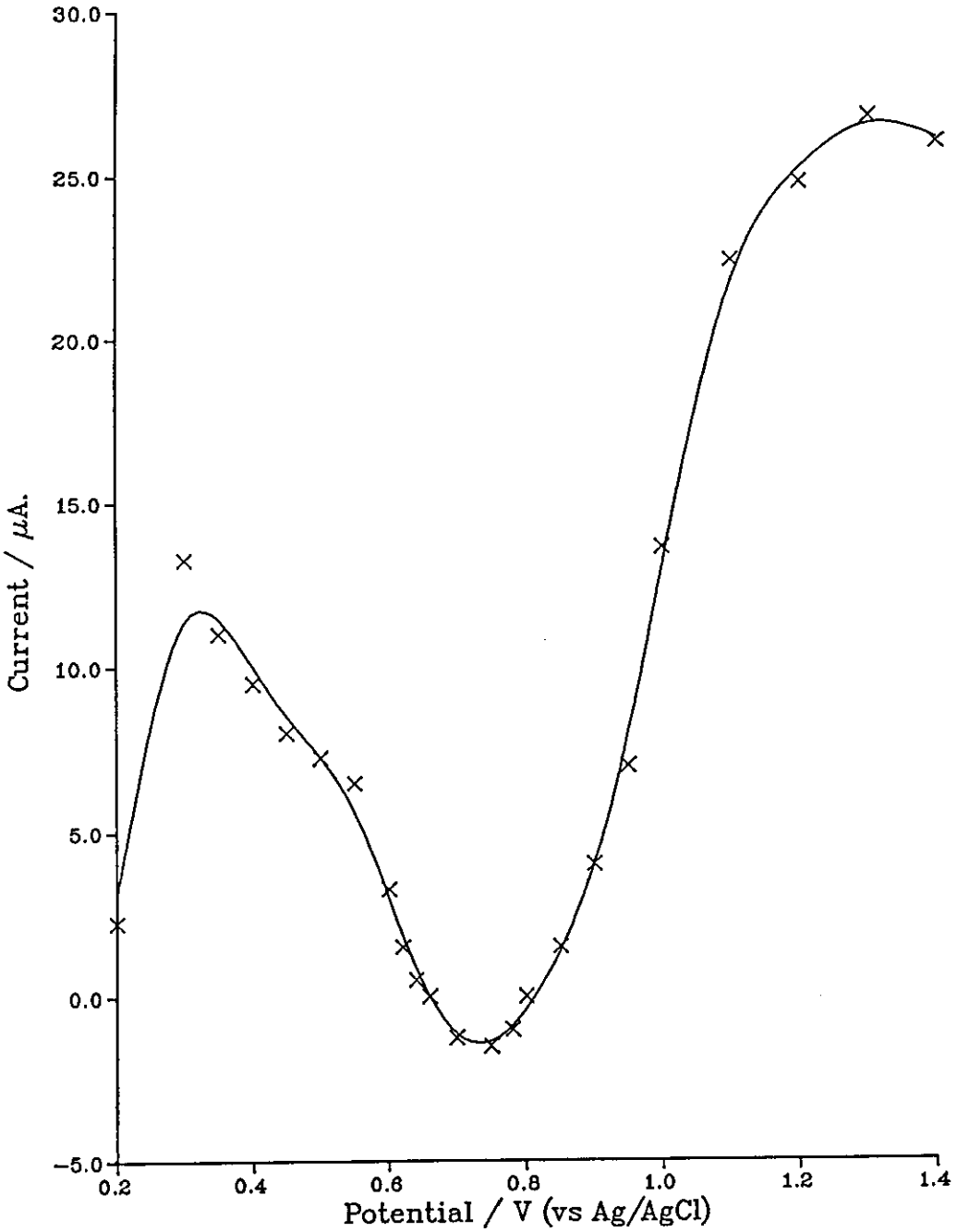

Fig. 30
Hydrodynamic Voltammogram for Dionex Cell with PAD Detection

Conditions: - Continuous Analyte Flow
Aniline conc. = 1 mM, flow rate = 1.0 $cm^3 min^{-1}$
background = 0.1 M sulphuric acid

transport component was suspected to be in addition to the adsorption isotherm limited response. A further term was added to allow for non - zero intercepts. These equations were rearranged into a polynomial form and used in the computer program. The program calculates the coefficients for each term and the correlation coefficient using least squares analysis, and the coefficients of the original rational equations are calculated from the former. A listing of the computer program may be found in appendix (ii).

Experimental

The PAD fia systems for the two cells were as used previously, including the flow rates. E1 was varied for waveform (WF). The concentration of aniline injected was in the range 10 - 1000 μM. Each standard was injected at least five times. The results obtained for E1 = 1.0V were for the wall jet cell.

Results

Fig. 31 show typical curve fits for typical calibration data obtained using the described method. Table 8 illustrates the goodness of fit of the equations and the errors in the calculated concentration. A typical sample of the signals obtained from the calibrations of the PAD fia is shown in fig. 32.

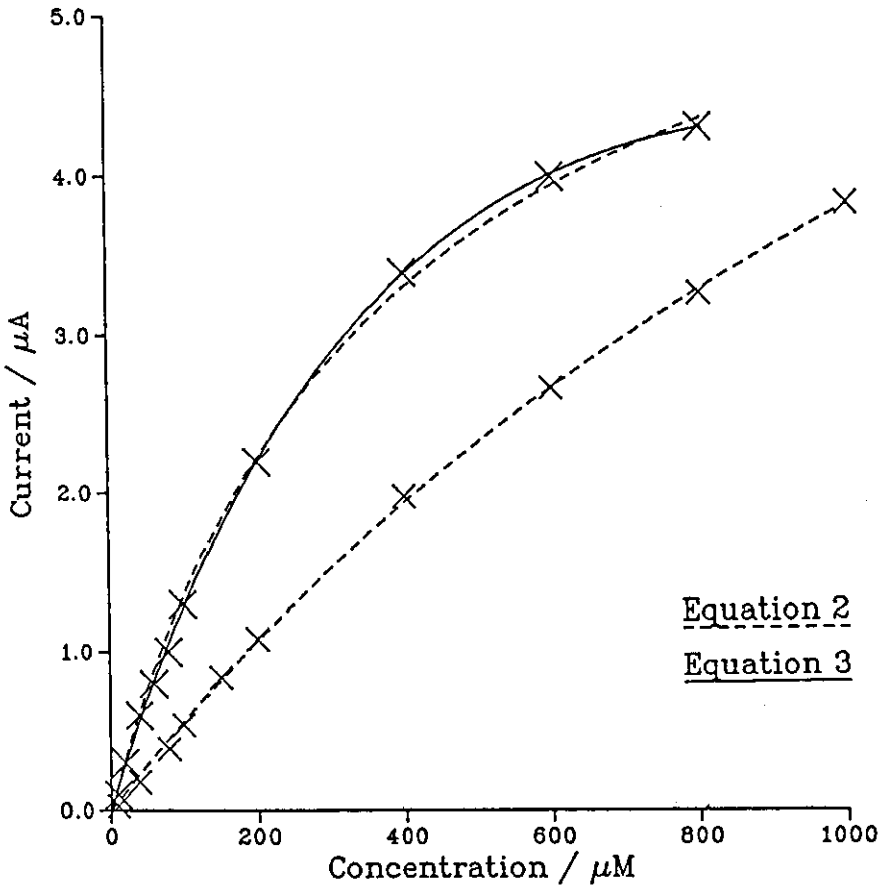

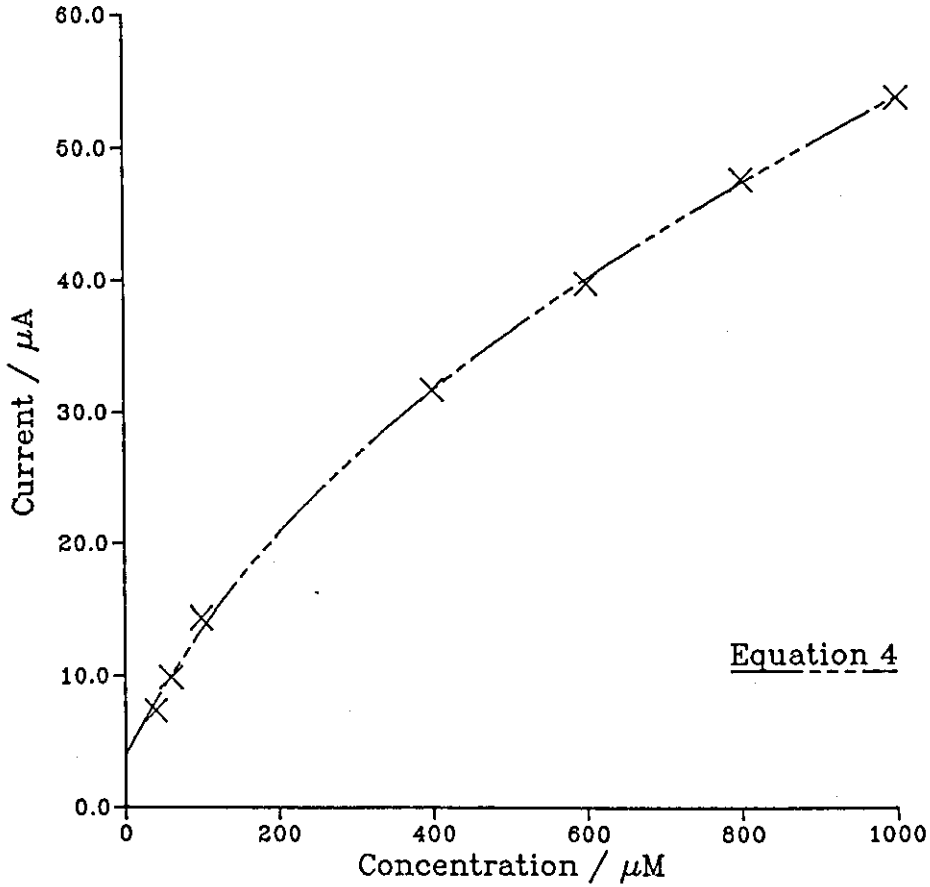

Fig. 31
Calibration Curves for Aniline using PAD

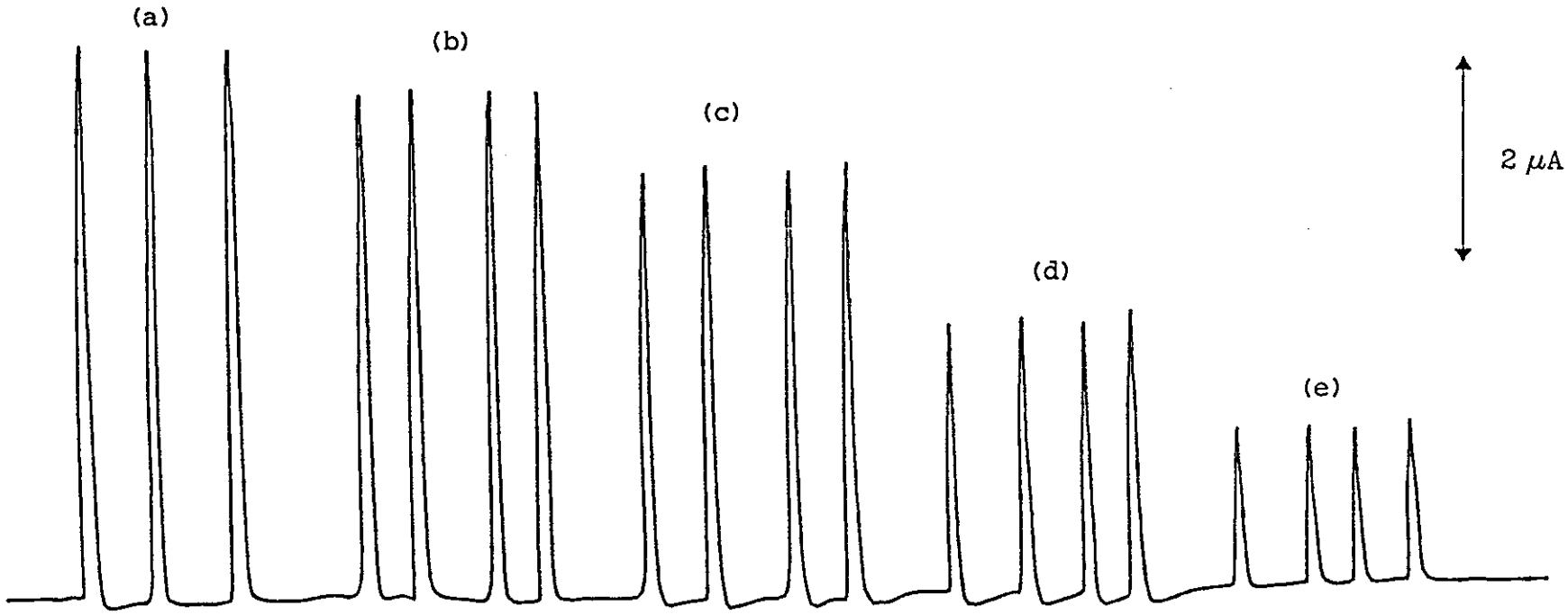

Fig. 32
Typical Peaks obtained for the Calibration of PAD for Aniline

Conditions: Cell = Dionex Flow rate = 1.05 cm^3 min^{-1}, E1 = 0.45 V
Background = 0.1 M sulphuric acid
Concentrations $x10^4$ M: a) 8, b) 6, c) 4, d) 2, e) 1

Table 8

Data obtained from Least Squares Curve Fitting of Calibration Data

El /V	Conc Range /μM	No. of Equatn.	Conc Given /μM	Conc Found /μM	Error / %	Corre. Coeff.
0.45	10-800	1				0.9841
		2	40	38.9	-2.8	0.9832
			200	197	-1.7	
			800	770	-3.9	
		3	40	43.1	+7.8	0.9998
			200	200	+0.0	
			800	805	+0.6	
0.6	10-100	1				0.9961
		2	100	96.2	-3.8	0.9996
			400	410	+2.4	
			800	791	-1.1	
1.0	40-100	1				0.9703
		4	100	111	+11	0.9993
			400	402	+0.4	
			1000	998	-0.2	

Discussion

Fitting equations for calibration data

$$1/I = 1/I_{max} + (1/I_{max}.K_1)(1/C) \quad \ldots\ldots\ldots 1$$

$$I = \frac{K_1 C}{1+K_2 C} \qquad \ldots\ldots\ldots 2$$

$$I = \frac{K_1 C}{1+K_2 C} + K_3 C \qquad \ldots\ldots\ldots 3$$

$$I = A + \frac{K_1 C}{1+K_2 C} + K_3 C \qquad \ldots\ldots\ldots 4$$

Where I_{max} = the theoretical current for maximum surface coverage by analyte.

From the Langmuir isotherm, $\theta = KC/(1+KC)$
where θ = fractional surface coverage
and $K = K_{ads}/K_{des}$
The faradaic current for PAD/fia is expected to be proportional to the surface coverage by analyte.
i.e. $I = \kappa\theta$
$\therefore$ for equation 2
K_1 = K (Lang) * κ (PAD)
K_2 = K (Lang)
For equations 3 and 4 the physical meaning of the coefficients becomes more uncertain. The polynomial equations derived by linearising the rational functions are given in appendix (i).

From table 8 it may be seen that plots of 1/I vs 1/C (equation 1) were non linear for values of El from 0.45 to 1.0V. There are two reasons for the curvature, failure of the Langmuir isotherm to model the adsorption

behaviour and mass transport of analyte either partly sharing control of the adsorption or occuring during the measuring period. The use of reciprocal plots to linearise data was suggested by Johnson and co-workers,[61,63,238] but a recent paper by Neuberger and Johnson[239] no longer recommends this practice.

A paper by Blomgren and Bockris[240] describing the adsorption of aromatic amines on mercury, concluded that aniline is adsorbed predominantly as the anilinium cation, lying flat upon the electrode surface, and the principle adsorption forces arrise from a pi-bond orbital interaction with the mercury. Adsorption isotherms indicated strong repulsions in the adsorbed layer, this was interpreted in terms of coulombic and dispersive interaction potentials between the adsorbed ions. A point of interest is that they found little variation of adsorption of aniline with potential. The adsorption of aromatic hydrocarbons on platinum and other metals has been predicted to occur, from calculations, with the plane of the hydrocarbon ring parallel to the electrode surface. (reference 57 p. 908)

The adsorption of neutral organic substances on mercury has been found to deviate from the Langmuir adsorption isotherm,[241,242] a fact which has been interpreted in terms of Temkin's adsorption isotherm. From this evidence and the experimental results it might be suggested that the use of the Langmuir isotherm to model the adsorption of aniline on platinum is a rather crude simplification. Also the use of the Langmuir isotherm as a model for other compounds becomes questionable, but its advantage is its simplicity.

The non linearity of the reciprocal plot is attributed to mixed control of the adsorption process by mass transport

and the adsorption isotherm.[235] The authors state that the values of K (Lang) for carbohydrates and amines are small compared with thiourea. Also the consequence of calibration for compounds with small K is that response is frequently under mixed control by mass transport and the adsorption isotherm even for very dilute solutions.

The fit of equation 2 to the calibration data was not too successful and may be explained in terms of the reasons given for non linearity of the reciprocal plot as the same mechanism is applied, although the fit was better than for the latter, probably due to the flexibility afforded by the coefficients.

The fit of equation 3 to the calibration data was reasonably satisfactory for E = 0.45 and 0.6 V, although unacceptable errors occured at the lower end of the calibration range. This is most probably because the least squares analysis is unweighted and renders the lower fifth of the calibration curve inaccurate. The term for mass transport in this equation may well correct for inadequacies of the adsorption isotherm.

For El = 1.0 V a satisfactory fit was only obtained using equation 4. The oxidation of analyte reaching the electrode by convective-diffusional mass transport during the measuring period accounts for a significant proportion of the total current. This changes the response characteristics considerably, an acceptable fit to the data was only achieved by introducing a term for a non zero intercept. The fit of this equation to the data is rather uncertain and needs further investigation.

4.4.2 Determination of the Detection Limit for PAD of Aniline using the Wall Jet Cell

Expermental

The optimum conditions for signal to noise ratio determined previously were used to find the detection limit for aniline. The wall jet cell was employed because it was to be used to measure the samples from the bubbler. The appararatus for PAD with fia was as previously. Concentrations of aniline in the range 0.3 to 1.5 μM were prepared in 0.1 M sulphuric acid. The measuring potential El was set to +1.2 V.

Results and Discussion

The calibration curve for the range 0.5 to 1.5 μM aniline is shown in fig. 33. Because of the uncertainty at this level of concentration, the calibration data was weighted according to the standard deviation of the signal for each standard. A regression line was therefore fitted by eye. The baseline noise was measured over a period of time on several separate occasions. The noise was averaged for each occasion and the largest value was used to estimate the detection limit. It is recommended to use the error in the blank value to estimate the detection limit,[243] but in this case the blank value was indistinguishable from the baseline noise. In this case the detection limit was defined as the concentration corresponding to twice the baseline noise. This was about 0.6μM (fig 33). The shape of the fitting line does not agree with that for higher concentrations, but it is difficult to draw any conclusions due to the degree of uncertainty of the measurements. At low concentration the current concentration relationship would be expected to approach linearity.

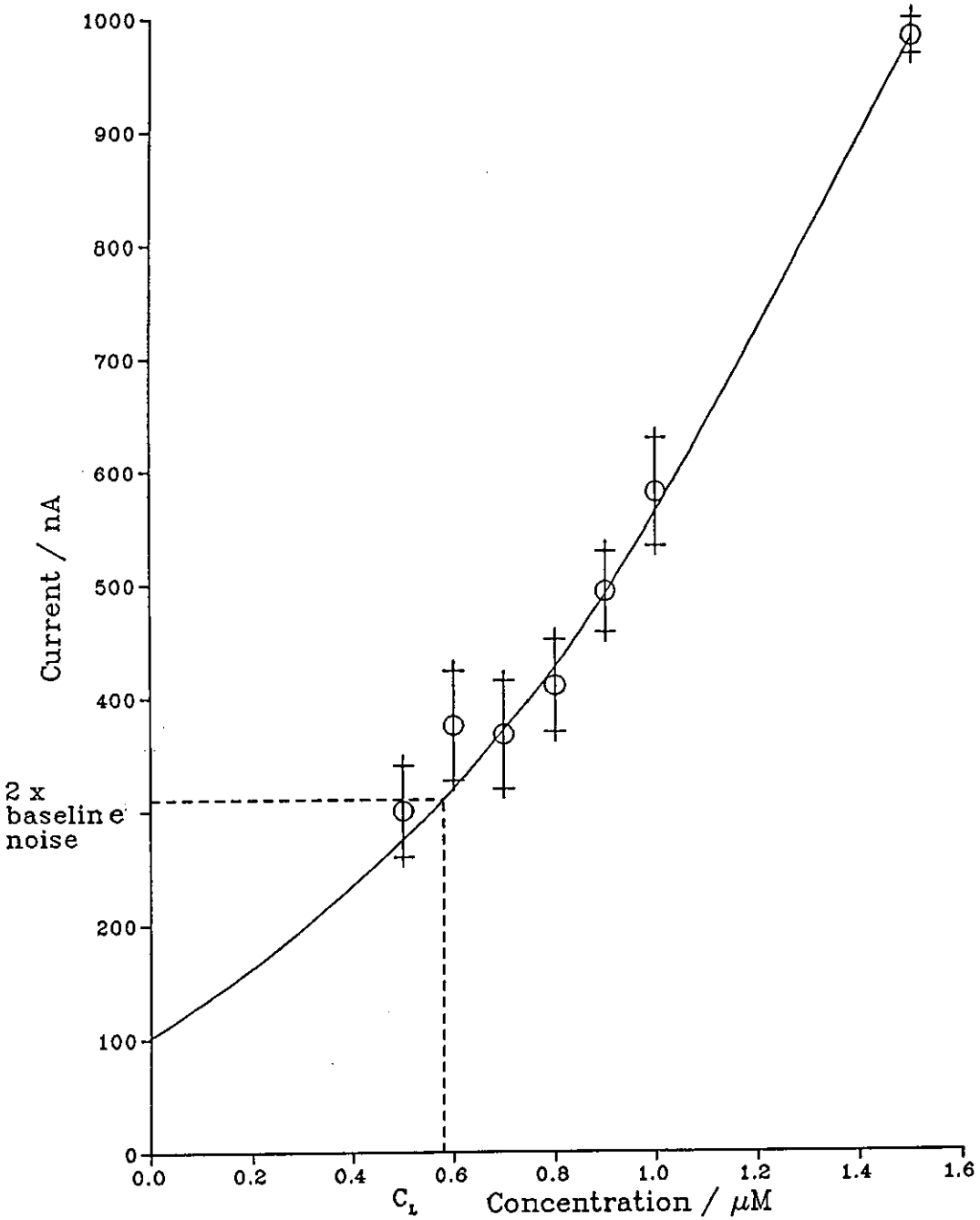

Fig. 33
Estimation of the DetectionLimit for Aniline using PAD (curve fitted by eye)

Conditions: E1 = 1.2V, Flow Rate = 3.0 cm^3 min^{-1}, C_L = Detection limit
Samples injected five times

4.5 Generation Collection and Detection of Aniline Vapour

4.5.1 Vapour System

Experimental

The apparatus for vapour generation was based on that used by Meddle and Smith[206] for the generation of amine vapours. The apparatus was rather simpler because the air was not humidified and there was no provision for dilution of the amine vapour. Also the diffusion tube was found to be too small to give a high enough concentration and so this was replaced with a B14 conical flask.

The vapour was collected in a dreshel bottle (gas washer). Impingers are more efficient because they can be used with higher gas flow rates and they have low dead volumes, but they were considered unsuitable for this application. This was because when sampling continuously from the impinger it was likely that air bubbles would be sucked into the sampling tube. This would cause problems with the PAD detector.It was decided to monitor the concentration of aniline in the trapping solution continuously. The dead volume of connecting tubing would be significant compared with the volume of trapping solution in an impinger, also it was not easy to sample from an impinger without collecting gas bubbles.

A schematic diagram of the gas generation apparatus is shown in fig. 34. It was decided to continuously sample from the bubbler by means of 0.5 mm i.d. PTFE tubing which needed to be placed at the bottom of the bubbler in order to avoid taking up gas bubbles. It was necessary to ensure that the layer of electrolyte close to the bottom

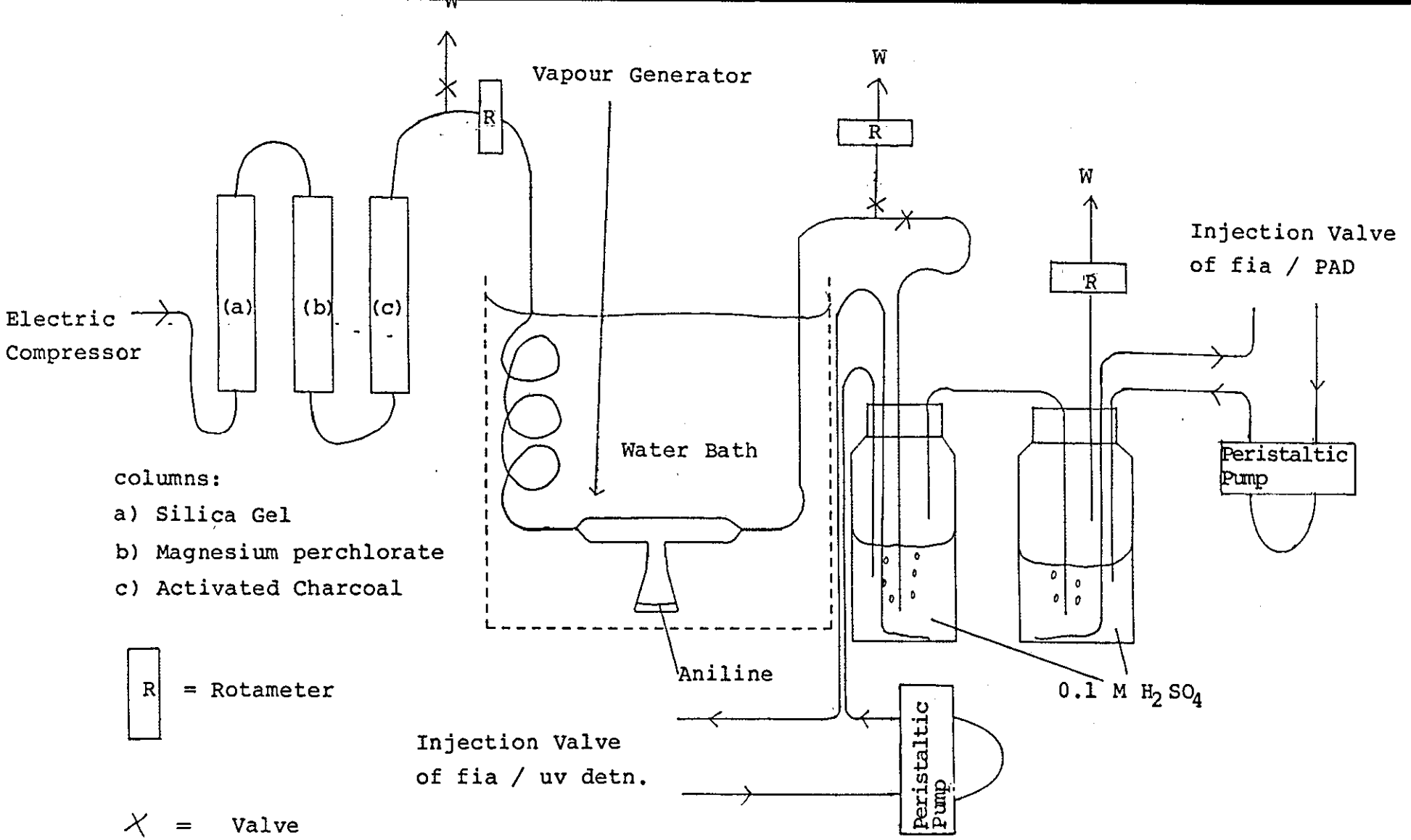

Fig. 34

Schematic diagram of apparatus for Generation and Collection of Aniline Vapour

of the bubbler was not stagnant. This was investigated by placing a crystal of potassium permanganate in a bubbler containing distilled water. Air was drawn through the bubbler at a steady rate (1 l min^{-1}) and the dissolution pattern of the permanganate crystal indicated a vortex created by the gas bubbles, but the sides near the bottom exhibited a dead zone, as might be expected. It was therefore necessary to place the pipes towards the centre of the bottom to minimise the response time of the detector.

By varying the temperature of the waterbath and the diameter and length of the diffusion tubes, concentrations in the desired range could be generated. Air was dryed and purified by pumping it through the towers in the apparatus. Dry air was used throughout as this simplified the apparatus but with a sacrifice in the evaporation of solvent from the bubbler. The apparatus was placed in a thermostated water bath, and the bubblers were placed alongside the waterbath to minimise condensation of the amine.

4.5.2 Optimisation of fia/uv Detection System

Experimental

An alternative method to PAD was required to measure the concentration of aniline trapped in the bubbler. It was decided to use fia with uv detection because it was straightforward to set up the method also it could be used to continuously monitor the aniline concentration. The method was required to give good accuracy and linearity in order to evaluate the vapour generation system and the trapping of aniline in the bubbler. Because of the expected inferior detection limit for the

fia/uv detection, for the lower aniline concentrations used with the fia/PAD the same vapour conditions must be assumed.

The uv absorbance spectrum was measured for aniline in 0.1M sulphuric acid and 0.1M sodium hydroxide (fig. 35) using a Pye Unicam PU 8600 uv/vis spectrophotometer controlled by a BBC microcomputer. The wavelength calibration was checked against a holmium filter, as was the LKB spectrophotometer as the latter was to be used for the fia experiments. These spectra were used to decide on what carrier to use for fia and the appropriate wavelength to set the detector.

A single line manifold was set up for the determination of aniline by injection of the acidified aniline sample into a carrier stream of 0.1 M sodium hydroxide. The detector was set at 307 nm. The flow cell was a Helma 8µl quartz. Refractive index 'peaks' were obtained which coincided with the peak for aniline.

A two line manifold was investigated in order to decrease the refractive index peak relative to the peak for aniline. The effect of flow rate on the relative size of the aniline / refractive index peaks was optimised for the two lines. Also the length and diameters of tubing in the manifold. The volume injected was kept to a minimum because this volume was to be removed from the bubbler on each injection. The concentration of sodium hydroxide down each line was also investigated.

Fig. 36 shows a schematic diagram of the fia manifold which was developed. A Gilson peristaltic pump was used to pump two flow lines of 0.1 M sodium hydroxide through a confluence point, then through a single bead string reactor to the detector. The acidified aniline sample was

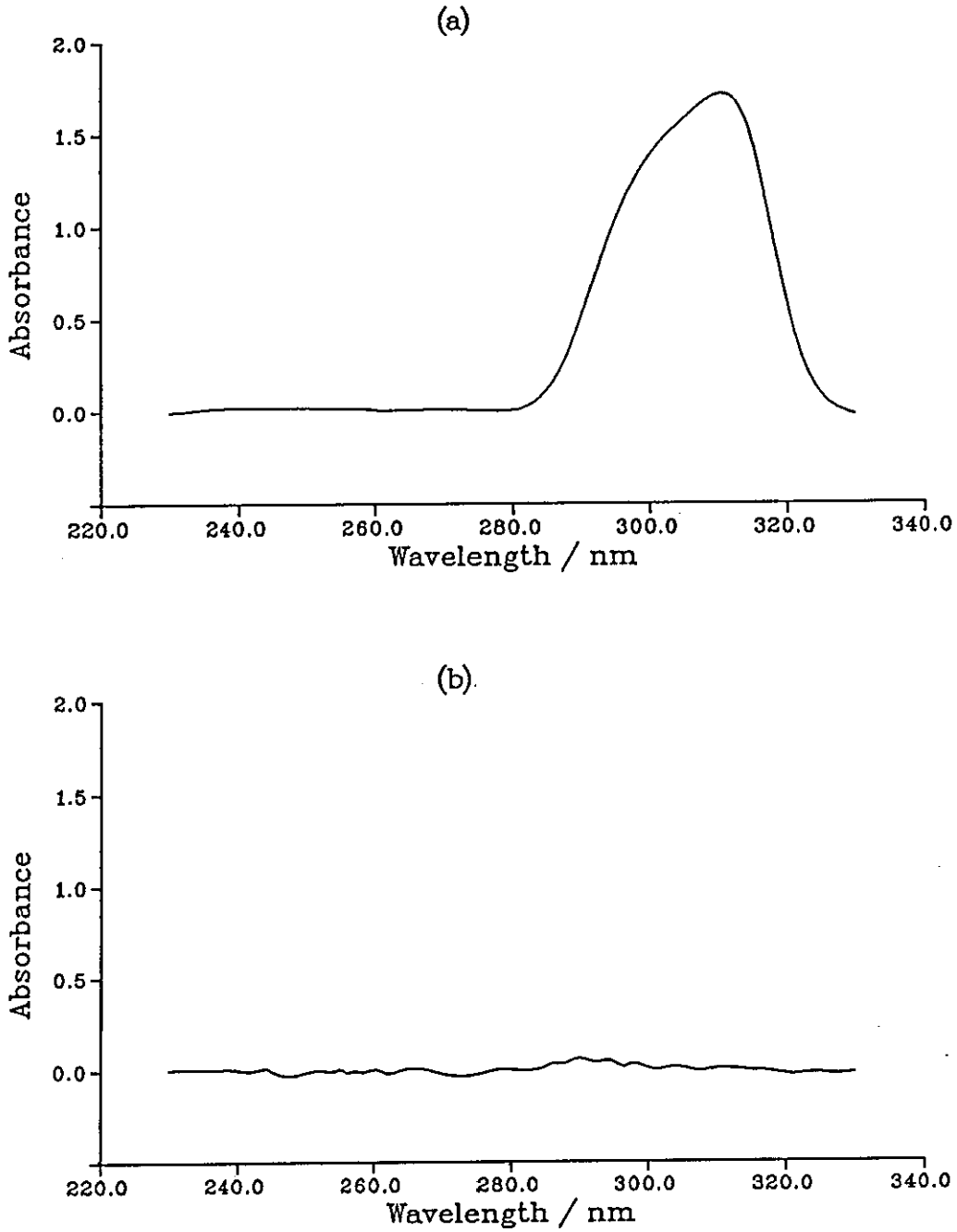

Fig. 35
UV Absorption Spectrum for Aniline (10 mM)

Conditions:
a) pH = 12
b) pH = 0.7

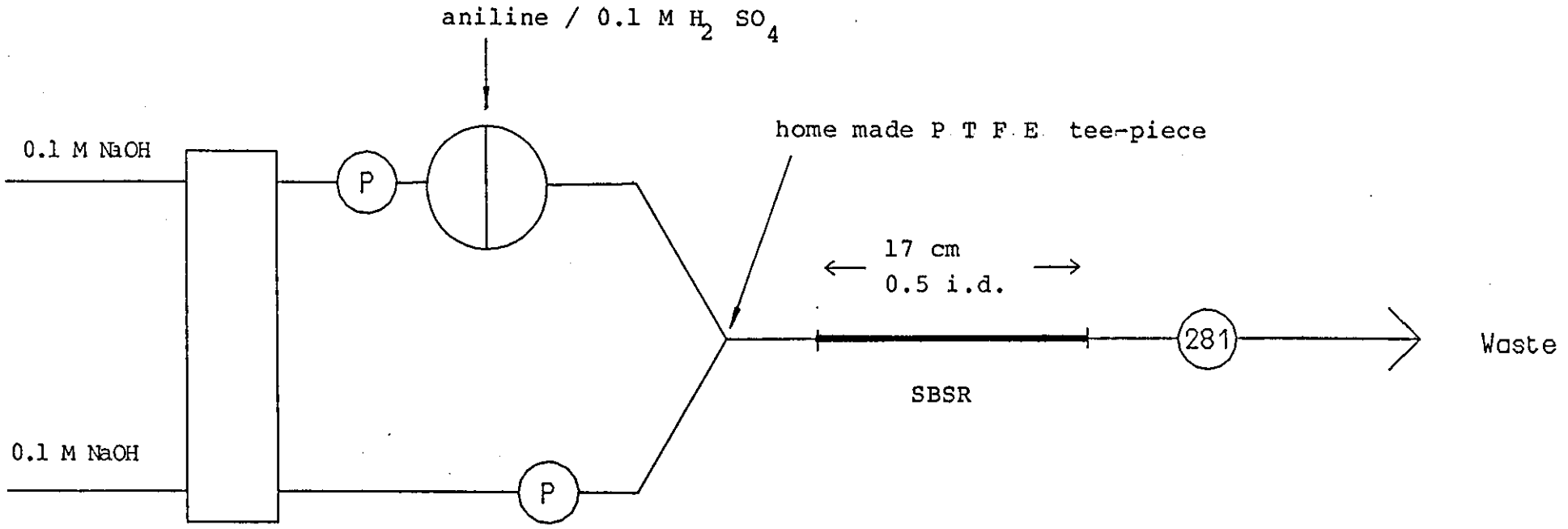

Fig. 3.6

Schematic diagram of Two Line Manifold for Detection of Trapped Aniline Vapour

Conditions: flow rate = 1.0 $cm^3 min^{-1}$, loop vol = ~30 µl

(P) = pulse damper SBSR = Single Bead String Reactor

injected into one of the lines by means of a Rheodyne rotary valve with a loop volume of about 30 µl. The flow lines were of 0.5 mm i.d. PTFE tubing apart from a 20 cm length of 0.8 mm i.d. PTFE tubing between the injection valve and the confluence point (a home made PTFE tee-piece). The flow rate down the injection line was 0.9 $cm^3 min^{-1}$ and down the other line 0.1 $cm^3 min^{-1}$. It was found necessary to degass the carrier to obtain the most stable baseline at the more sensitive detector settings. See section 2.2 for details of construction of the single bead string reactor (SBSR). The wavelength was optimised by changing it in increments of 5 nm (1 nm near the maxima) from 270 nm to 305 nm.

Results and Discussion

The refractive index 'peaks' for the single line peak were equivalent in height to about 100 µM aniline and made the detection limit too high. A two line manifold was investigated because it has been shown that the use of a confluence point followed by a SBSR can give good radial mixing with minimal dispersion.[244] It has the effect of breaking up the leading edge of the sample plug.

The refractive index effect is due to the different densities of the sample plug and the carrier solution. At either end of the sample plug the interface between carrier and sample plug tends to give some refraction of the light beam, this is registered at the photocell and changes the absorbance reading. The effect is well known in hplc using uv/visible detection. When the fia system was optimised for flow rate the wavelength was scanned manually to obtain the maximum signal (see fig. 37). The wavelength of maximum absorbance (λ_{max}) was found to be 281 nm and this setting was used in all subsequent

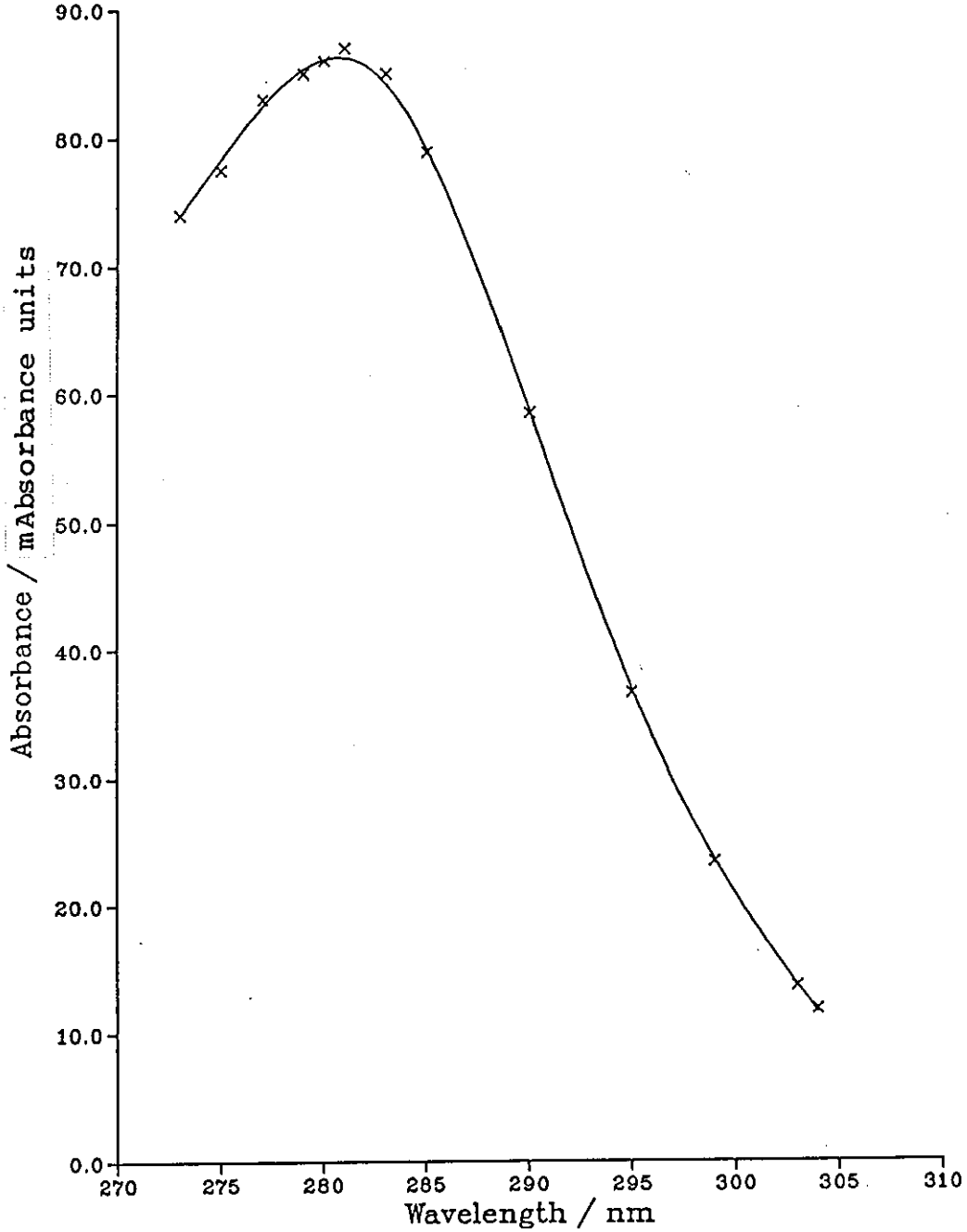

Fig. 37
Manual wavelength scan for fia/uv

experiments.

The detection limit was taken as the concentration twice the positive refractive index peak; giving a detection limit of 30μM. Table 9 shows least squares analysis for a typical set of calibration data. The rectilinearity becomes poorer at higher concentrations. This is usually observed in spectrophotometry at high absorbances and is due to stray light reaching the photocell.

The relative flow rates at the confluence point were optimised to give minimal aniline / refractive index peaks. An overall flow rate of 1.0 $cm^3 min^{-1}$ seemed to give the correct dispersion and mixing. The best carrier/sample stream composition was found to be 0.1M in both cases. The effect of the length and diameter of tubing was investigated. A combination of bore sizes with changing flow rates slightly affected the positive and negative refractive index peaks (width and height) and the width and height of the aniline peak.

The spectrum of aniline in 0.1M sulphuric acid did not show any strong absorbances (fig. 35). In alkali a strong absorbance (λ_{max} 307 nm) was recorded and so it was decided to inject the acidified aniline into an alkaline carrier and monitor at 307 nm. When the wavelength was scanned manually in the fia system, the λmax was found to be 281nm and so this wavelength was used. It appears that aniline exists in an anionic form at pH > 12 and the peak at 307nm was shifted from 208nm for the free base, due to the auxochromic contribution of the negative charge. The spectrum of the free base shows a more intense maxima at 230nm E=8,600,[245] which would have improved the detection limit by monitoring at this wavelength. The spectrum of the anilinium ion is almost the same as for benzene as there is no mesomeric

contribution from the nitrogen. The λ_{max} at 254nm is too weak to be useful and the λ_{max} at 203nm was too low.

Table 9 Least Squares analysis for results obtained using the fia/uv system.

Conc Range / mM	Corr. coeff	Stand. error of slope
0-2.0	0.99992	0.00704
0-4.0	0.99971	0.02577
0-10.0	0.99770	0.02849

4.5.3 Measurement of Aniline Vapour by fia/uv Detection

Experimental

The apparatus described earlier (4.5.1) was used at 50 ^{o}C and 80 ^{o}C to generate aniline vapours. The air was pumped at 1 lmin $^{-1}$. The aniline enriched air was passed through a bubbler which was sampled periodically by the fia / uv detector. The washed gas was then passed through a second bubbler, which was sampled by the fia / PAD detector. The bubblers were modified to take two PTFE tubes for sampling and returning the liquid. This second bubbler was to check for any carryover from the first bubbler. the bubblers contained 100 cm ^{3} of 0.1 M sulphuric acid to trap the aniline vapour. This experiment were designed to investigate the following:

a) Constant concentration of aniline in the vapour with time.

b) Efficient trapping of the aniline vapour.

c) The suitability of the sampling method with respect to

accuracy and no problems from trapped air in the detector cell.

Results and Discussion

Neither the uv nor the PAD system was adversely affected by the excess air dissolved in the sample. In the case of uv / fla, degassing of the carrier minimised any problems, also a backpressure coil after the flow cell made the baseline more stable. In the case of the PAD, it was found that if the eluent was degassed or saturated with nitrogen then a negative blank value was obtained. This was attributed to the response of the detector to dissolved oxygen. In both cases no carryover into the second bubbler was detected.

The concentration of aniline vapour was calculated from the gradient of the concentration/time profiles and from the loss in mass from the diffusion tube per unit time: given that the flow rate of air was 1 $lmin^{-1}$ and the volume of acid in the bubbler was 100 cm^3. The concentration time profiles for the two temperatures are shown in fig. 38. These profiles were calculated by dividing the gradient of the absorbance/time profile by the sensitivity of the calibration graph.The profile for 50 ^{o}C is rather noisy because the absorbance values are not large compared with the detection limit. The profile for 80 ^{o}C shows good linearity.

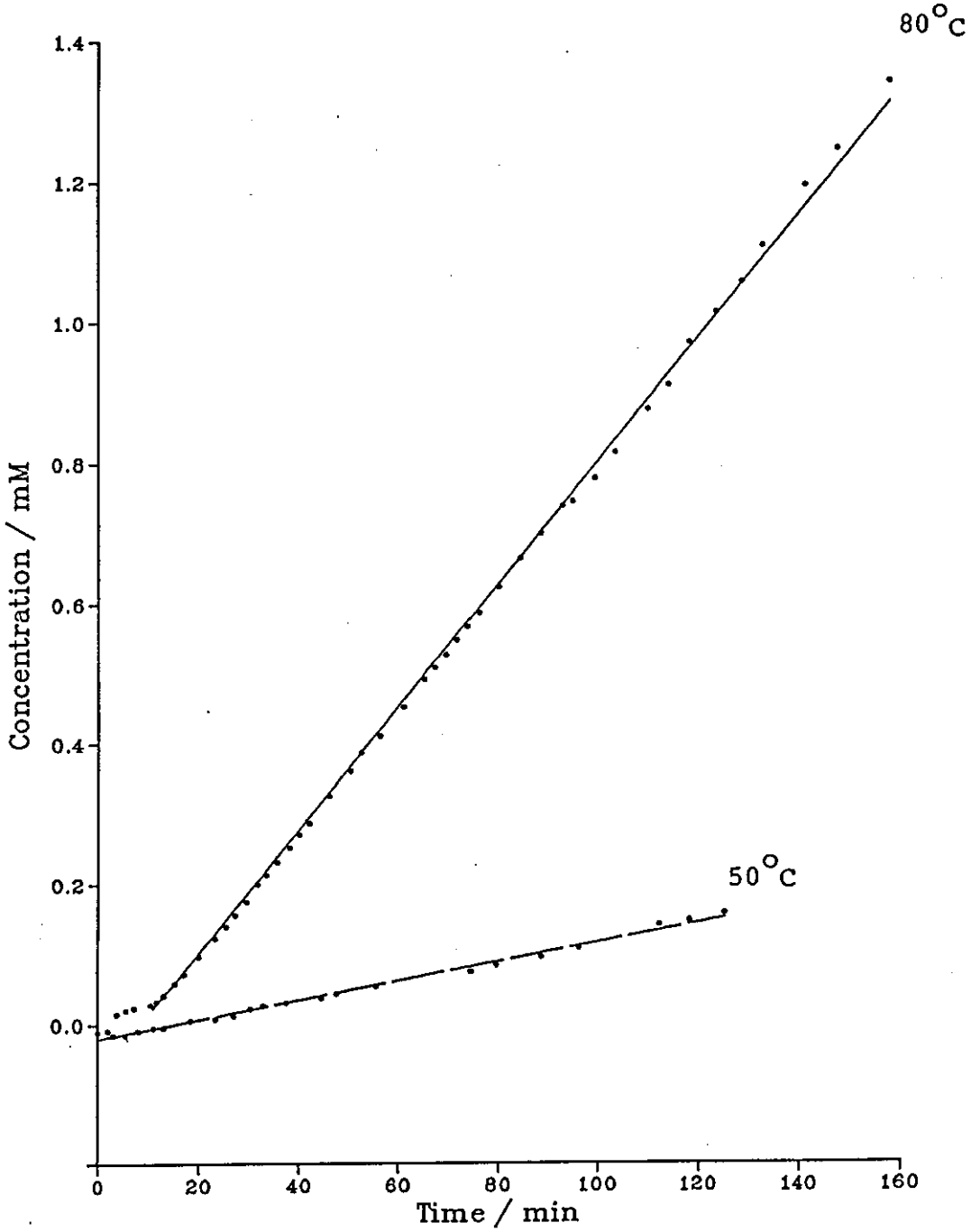

Fig. 38
Concentration / Time Profiles for Aniline Vapour determined by fia / uv detection

Conditions:
volume of absorption liquid (0.1 M H_2SO_4) = 100 cm^3
flow rate of vapour = 1 dm^3 min^{-1}

Table 10

Data from Conc / Time Profiles and Vapour Concentration

Temp /°C	Corr. Coeff.	Vapour Conc. calc. from Graph slope /mgm^{-3}	Vapour Conc calc. from Weight loss /mgm^{-3}	Weight loss /mg
50	0.9967	14.3	—	—
80	0.9991	88.1	98.8	158

Table 10 gives data for the concentration of aniline vapour. In the case of 50°C, there was a large error in the the mass loss, which made it of no value. For 80°C the linearity was good, the concentration calculated from the graph was 11% lower than the actual concentration from weight loss. There must be a constant error arrising from the lag of the detection system. There is also a combination of errors from the slope of the calibration graph and the concentration profile.

4.5.4 Measurement of Aniline Vapour for fia / PAD

Experimental

At 30°C, the concentration of aniline in the air was estimated by calculation to be such that it might be considered to constitute limit of detection for the fia/PAD sampling system.

The apparatus was the same as in (4.5.3). The contents of the first bubbler was sampled and the liquid passed through the injection valve of the fia/PAD, using the wall jet cell. The conditions for the PAD were the same as in section (4.4.2). The apparatus was allowed to equilibriate with the vapour going to waste. Blanks were taken from the bubbler then the vapour was switched in line and sampling of the bubbler began. The proceedure was repeated several times to obtain an average for the concentration time profile, using calibration data previously obtained for the PAD (see fig. 33). The apparatus was run for two days to try and give a measurable weight loss.

Results and Discussion

The concentration of aniline vapour was chosen to give a signal similar in size to the detection limit for aniline in the fia system after the vapour had been collected for a short period of time (a few minutes). This experiment was to give an estimate of the sort of low levels which might be detected by fia/PAD interfaced to a gas sampling system. Typical concentration / time profiles are shown in fig. 39 for aniline vapour in air generated at 30 ^{o}C. Fig. 40 shows a typical set of fia peaks for aniline sampled from the bubbler.

Because the profiles are curved the shallowest and steepest gradients were taken, giving the lowest and highest estimates relating to the vapour concentration. Estimates of the vapour concentrations calculated as before (4.5.3) are 1 to 2 mgm^{-3} of aniline in air. It was not possible to achieve a measurable weight loss from the diffusion flask containing aniline. Condensation of

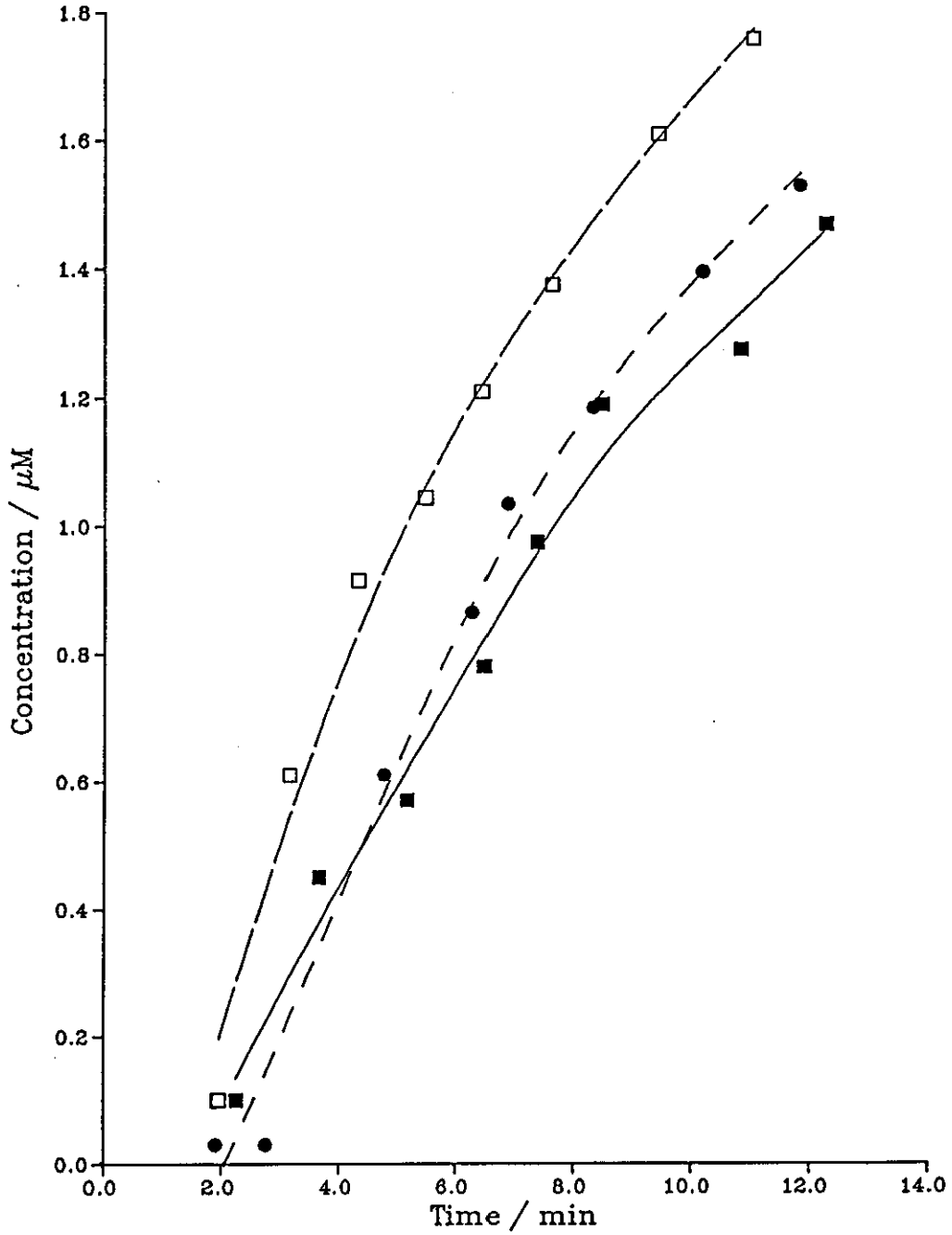

Fig. 39
Concentration / Time Profiles for Aniline Vapour determined by fia / PAD

Conditions: Temperature = 30°C
flow rate of vapour = 1.0 m^3 min^{-1}
volume of absorption liquid (0.1 M H_2SO_4) = 100 cm^3

■ □ ● } Separate determinations of aniline vapour under the same conditions

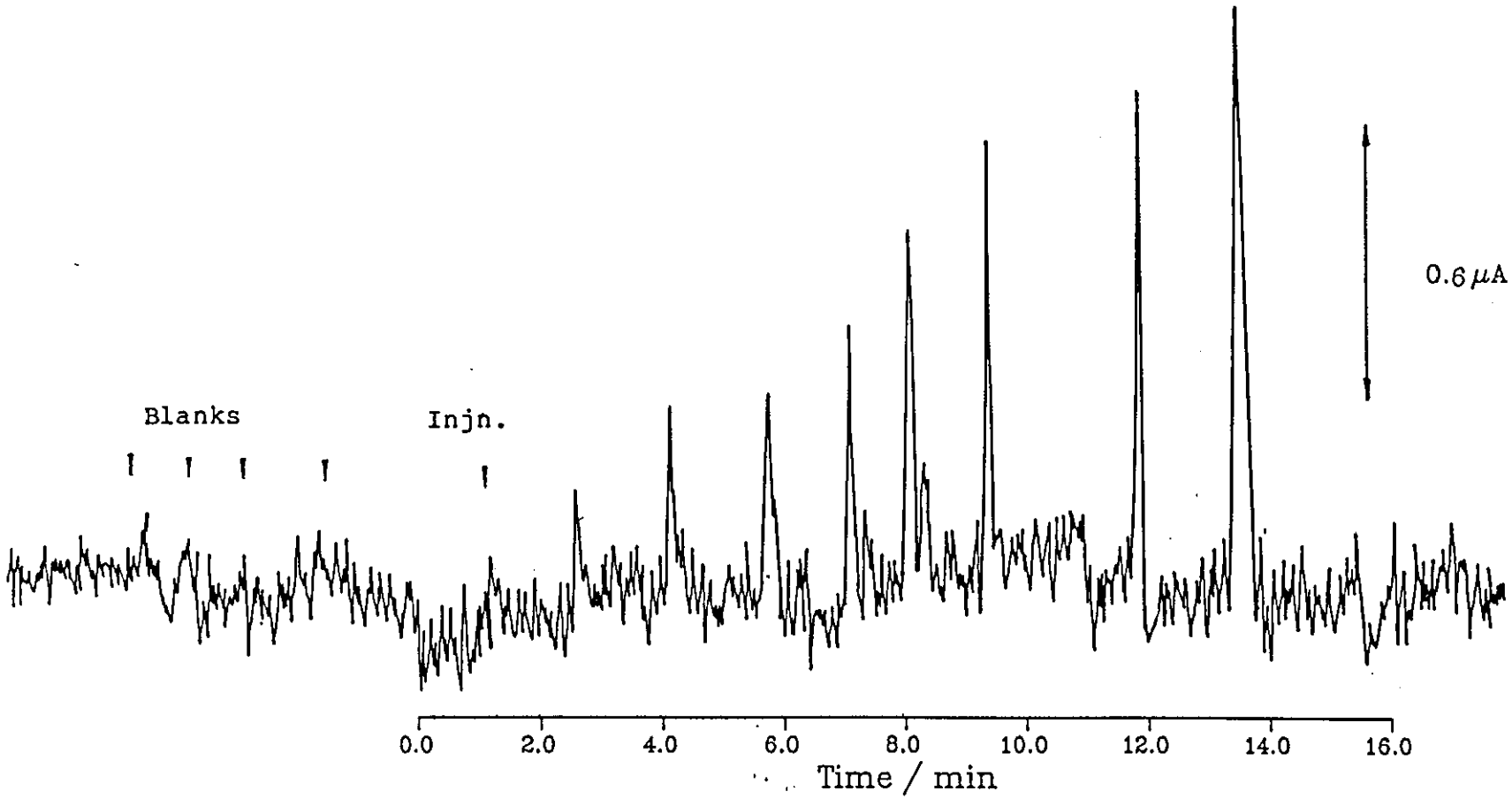

Fig. 40
Typical Peaks for fia with PAD of Aniline Vapour at 30°C

water vapour in the drying tubes became a problem after about 24 hours. The only means of estimating the concentration of aniline vapour at 30°C was by calculation using the concentration profiles for 50°C and 80°C. The following equation may be used to relate the rate of diffusion of a vapour to the temperature and the vapour pressure of the liquid.[246]

$$r = \frac{DPMA}{RTL} \ln(\pi)$$

where

r = diffusion rate
M = molecular weight of vapour
P = total pressure
A = cross-sectional area
L = length of tube
T = absolute temperature
R = gas constant
D = diffusion coefficient
p = vapour pressure of liquid
π = (P/P-p)

McKelvey and Hoelscher[247] used this equation to calibrate gas diffusion apparatus for organic compounds. They obtained a linear relationship for diffusion rates at different temperatures. In this instance by plotting the diffusion rate vs $\frac{1}{T} \ln(\pi)$ a linear relationship should be obtained which passes through the origin. The aniline vapour concentration at 30°C was calculated to be 5.2 mgm^{-3}. The results calculated from the fia/PAD do not compare very favorably with this value but, as they are of the same order of magnitude, they indicate that the concentration of aniline generated at 30°C is somewhat lower than the limit of detection of this system.

CHAPTER 5
SUPPORTING INVESTIGATIONS

5.1 Introduction

The performance of an analytical method is invariably characterised by the detection limit for a particular analyte. The detection limit of an analytical method is regarded as being the lowest concentration of the analyte that can be distinguished with reasonable confidence from a field blank, i.e. a hypothetical sample containing zero concentration of analyte. The detection limit has been defined by IUPAC[248] and it is clarified by a recommendation from the analytical methods committee.[243] For comparisons between similar detection systems it is convenient to quote the signal to noise ratio for a particular sample concentration, no calibration of the systems being required.

In fia amperometry the signal is due to the faradaic current generated by the sample undergoing redox processes at the electrode surface. The noise is normally defined as the peak to peak variation of the baseline. The noise is a summation of contributions from both physical and electrical sources. The fluctuations in flow caused by pump pulsations give rise to baseline noise which tends to be fairly regular in nature. Most of the other sources of noise tend to be random and include the following: charging currents (if a pulsed potential mode is used), residual currents due to breakdown of the solvent (if the measuring potential is large),[249] redox processes occuring at the electrode surface due to electroactive impurities in the eluent, electrical interference (either mains bourne or radio frequency), electronic noise generated by the the detector system.[250]

and static electricity (especially generated by the pumping system). Another source of noise is the injection valve. The valve tens to disturb the flow of carrier to the detector as it is switched from the load to inject position. This manifests itself in glitches in the baseline which may coincide with the leading edge of the peak, thus affecting the precision and thus the signal to noise ratio.

5.2 Assessment of the Wall Jet Cells and Injection Valves for fia Amperometry

5.2.1 Comparison of the Performance of Injection Valves

Experimental

The effect of two different injection valves on the flow of carrier to the detector was investigated. The valves were a Rheodyne 5020 and a Dionex slider valve. The valve slide is moved by pistons at either end, the pistons were actuated by compressed nitrogen. The pistons were actuated alternately by means of solenoid valves to switch the gas supply. The operation of the valves was characterised by using a flow rate device[218] (section 2.2), to monitor the effect of valve switching on the flow of eluent.

The fia system was the same as used previously (4.2.2). The flow rate device connected to the outlet from the flow cell. The flow rate of carrier (0.1M sulphuric acid) was 1.1 $cm^3 min^{-1}$. The injection loop volumes for the Rheodyne valve were about 50 µl and 200 µl. The residual volume of the connecting tubing attached to the valve being about 25 µl. Additional lengths of tubing were added to make the reqired volume. The Dionex valve was

equipped with a loop of about 50 µl. A sample of 1 µM aniline dissolved in carrier solution was injected, the detection waveform was WE. The output from the flow rate device was recorded on a separate recorder.

Results and Discussion

The output from the flow rate device is shown in fig 41. The device has a nearly linear response to flow rate. The pulsations due to the peristaltic pump are represented by fairly regular oscillations. The disturbance to the flow caused by the Rheodyne valve is larger and lasts much longer than that for the Dionex valve. The major advantage of the Dionex valve is the speed of switching between ports. The operating pressure for the valve was 100 psi, as recommended by the manufacturers, lower pressure gave a more sluggish response. The Rheodyne valve suffers from slowness and poor reproducibility of switching due to its manual operation, also the resistance of the injection loop is not counterbalanced when it is being loaded.

The Rheodyne valve is widely used in fia because of its reliability, cheapness and good injection precision but is less suitable for detectors which are flow sensitive and the performance of the Dionex valve was superior in this case. Hydrodynamic bypass loops have been used to smooth out the switching surges caused by the Rheodyne valve. This can be fairly successful but the precision of the fia peaks tends to suffer: this was established for earlier work on fia with DC amperometric detection. The precision of the slider valve for PAD of lower concentrations of aniline was of the order 1-3 % relative standard deviation over a long period of time. The Rheodyne valve was unusable for concentrations of aniline of 1 µM.

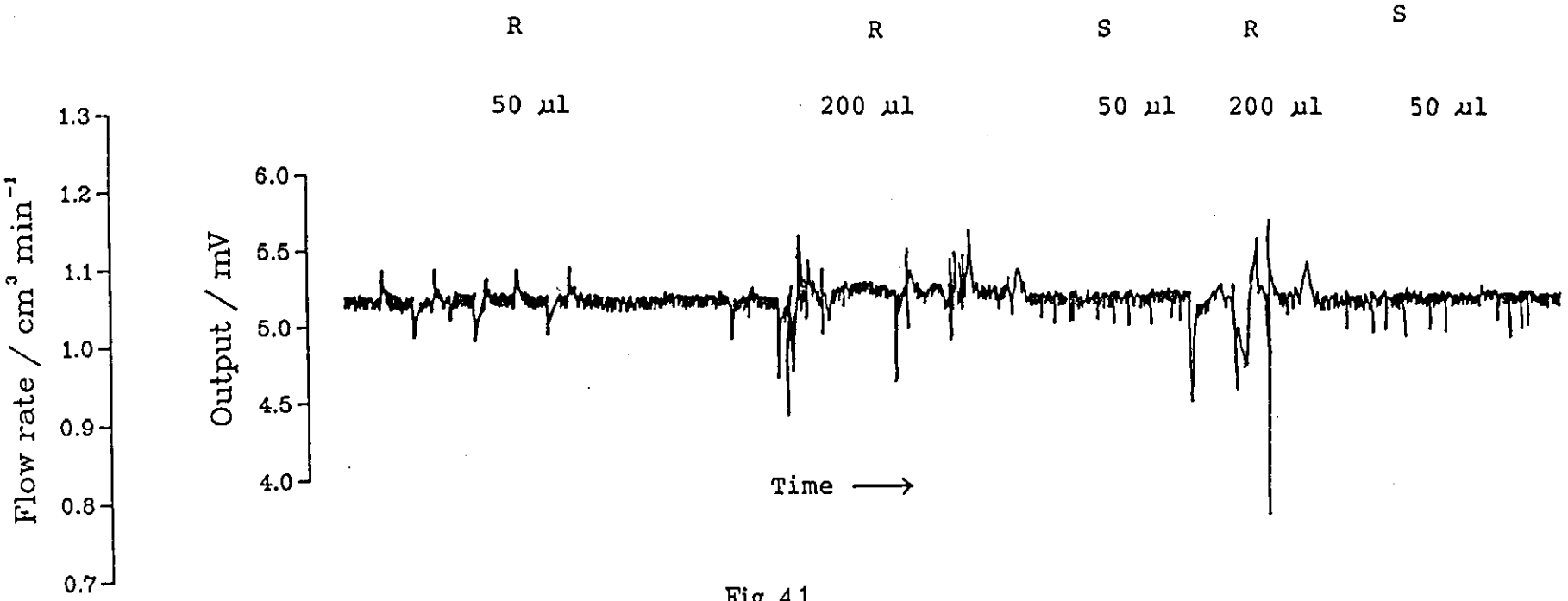

Fig. 41
Output from Flow Rate Device for two Injection Valves

R = Rheodyne rotary valve (5020)
S = Dionex slider valve

5.2.2 Comparison of Detector Cells

Experimental

An amperometric flow cell was required which could be employed as part of a portable monitor for atmospheric samples of aniline. The aniline samples were to be trapped in a liquid sorbent and so the samples introduced into the fia system would be saturated with dissolved air. This made one of the design features to be that the cell should not be susceptible to trapped air. Air lodged around the reference frit can be a problem, because the baseline becomes noisy and also the potential applied to the working electrode can be affected. This may well alter the response of the electrode. (See 1.3.1 for a discussion of flow cell design.)

The wall jets cells WJ1 and WJ3 were compared using fia with DC amperometric detection. A Gilson minipuls 2 peristaltic pump was connected to a Dionex slider valve equipped with a sample loop of about 70 µl, with the home made pulse damper and earthing connection in between. A 60cm length of 0.5mm i.d. PTFE tubing was used to connect the valve to the detectors. The wall jet cell WJ1 was held in a beaker containing background electrolyte; with the reference and auxiliary electrodes either side. The working electrode was glassy carbon (3.0 mm diameter).

A carrier of 0.1M sulphuric acid was used. A potential of + 0.7 V vs Ag/AgCl was applied by the Dionex detector. Injections of 0.1 µM o-dianisidine dissolved in carrier were made and the baseline noise was measured. The Dionex detector has three damping factors (response times of 0.3, 1.0 3.0 s), the response was recorded using each of these settings.

Results and Discussion

The results for the comparison of the two wall jet cells are shown in fig. 42, the WJ1 cell is visibly less noisy. The calculated signal to noise ratios for WJ1 and WJ3 were 10.2 and 5.6 respectively, with an uncertainty of about 10%, due to variation of the baseline noise. The effect of instrument damping is also illustrated in the same figure. By increasing the response time of the low pass filter, the signal to noise ratio was improved. The degree of electronic filtering needs to determined for each application, because it is depends on the rise time of the peaks and the frequency and type of noise. The apparent dead volume of the detector can be effected by this filtering.[251]

The WJ1 cell should be described as a restricted wall jet cell because the nozzle is close to the electrode (0.2mm) and the nozzle interferes with the hydrodynamic boundary layer. The nozzle body will cause a loss of momentum due to surface drag. The reduction of the cell volume to a value less than the boundary layer thickness results in increased linear flow rate, hence the cell has a significant percentage of thin layer character. The increased flow rate can partly compensate for the loss of momentum due to surface drag on the nozzle, but this trade-off is said not to be significant.[38] The author recommends that the nozzle be moved well back from the electrode, where the geometric cell volume does not affect the performance of the cell. The WJ3 cell was designed using this criterion, with a separation of 2.0mm between the nozzle and the electrode. The nozzle body was conical to minimise any interference to the boundary layer. The diameter of the nozzle was very similar to that of WJ1. The faradaic response of both cells was very

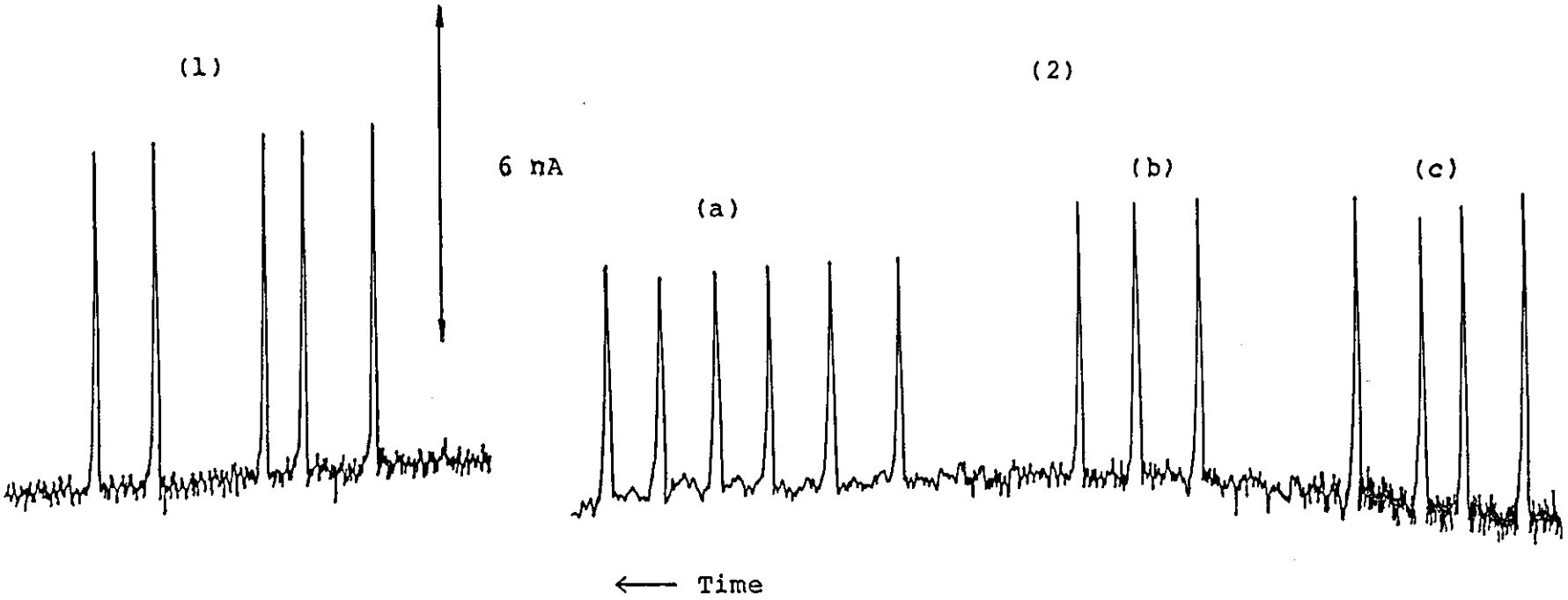

Fig. 42
Comparison of the Performance of two Wall Jet cells

Conditions: Analyte = o–dianisidine (0.1 μM), flow rate = 3.0 cm^3 min^{-1}
E = 0.7 V, electrode = glassy carbon (3.0 mm dia.), sample vol. = ~70 μl
1) cell = WJ1, t(resp) = 0.3 s
2) cell = WJ3, a) t(resp) = 3.0 s, b) t(resp) = 1.0 s, c) t(resp) = 0.3 s

similar but the baseline noise for WJ3 was about double that for WJ1.

Although much effort has been expended to understand mass transport in flow through cells, few optimisation schemes have been presented which make use of experimental data (especially noise levels). One scheme by Roe[252] includes signal, noise and band broadening.

5.3 Some Investigations of Electrodes

5.3.1 Micro-array Electrodes based on Reticulated Vitreous Carbon

Experimental

Electrodes were fabricated from reticulated vitreous carbon (RVC) 100 pores per inch according to reference (253). Cylinders were punched from a block of RVC using a small cork borer. The cylinders were cemented into glass capillary tubing (i.d. 2 mm, o.d. 7mm) using Araldite adhesive cured with 40% HF.[119] An electrical connection was made to the unexposed side of the RVC with a copper wire using graphite-epoxy cement cured with 40% HF. The surface was cut back with 600 grit wet and dry paper, a thin layer of epoxy was then applied to the surface to fill in cavities caused by gas bubbles. The surface was polished using 5 μm diamond paste followed by alumina (0.3 μm then 0.015 μm) until a constant low background was obtained for linear sweep voltammetry in 0.1M sulphuric acid.

Voltammetry was carried out using the Metrohm E 611 and E 612, detector and scanner. Cyclic voltammograms at the RVC electrodes were obtained for 0.5 mM o-dianisidine in

0.1 M sulphuric acid and at a glassy carbon electrode (3.0 mm diameter). Firstly the electrodes were conditioned by three cyclic scans in background electrolyte, then scans were recorded for the background and sample. The electrodes were then pretreated by applying a potential of +1.8 V for 3 minutes, then -0.2 V for 1 minute. (potentials vs Ag/AgCl). The background and sample scans were recorded as before.

A sample of 0.1 μM o-dianisidine in 0.1M sulphuric acid was prepared. An RVC electrode was mounted in the WJ1 cell and the response was recorded using the the same system and conditions as in (section 5.2.2). This was repeated for the glassy carbon electrode.

Results and Discussion

The voltammetric response of the RVC electrodes was investigated using the oxidation of o-dianisidine in 0.1M sulphuric acid. In reference (10) page 228, the oxidation at platinum and carbon paste electrodes is stated as an apparently reversible two-electron process with no evidence of chemical follow-up reactions. There is also no tendancy toward electrode filming.

Typical cyclic voltammograms are shown in fig. 43. The peak potentials for the RVC electrode after conditioning, were 611.5 mV and 527.5 mV, for the anodic and cathodic peaks respectively. For a reversible electrode reaction:

$$E_{pa} - E_{pc} \approx 0.058/n$$

For o-dianisidine n = 2, therefore ΔE_p should be 29 mV. In this case ΔE_p = 84 mV. For the case of pretreatment

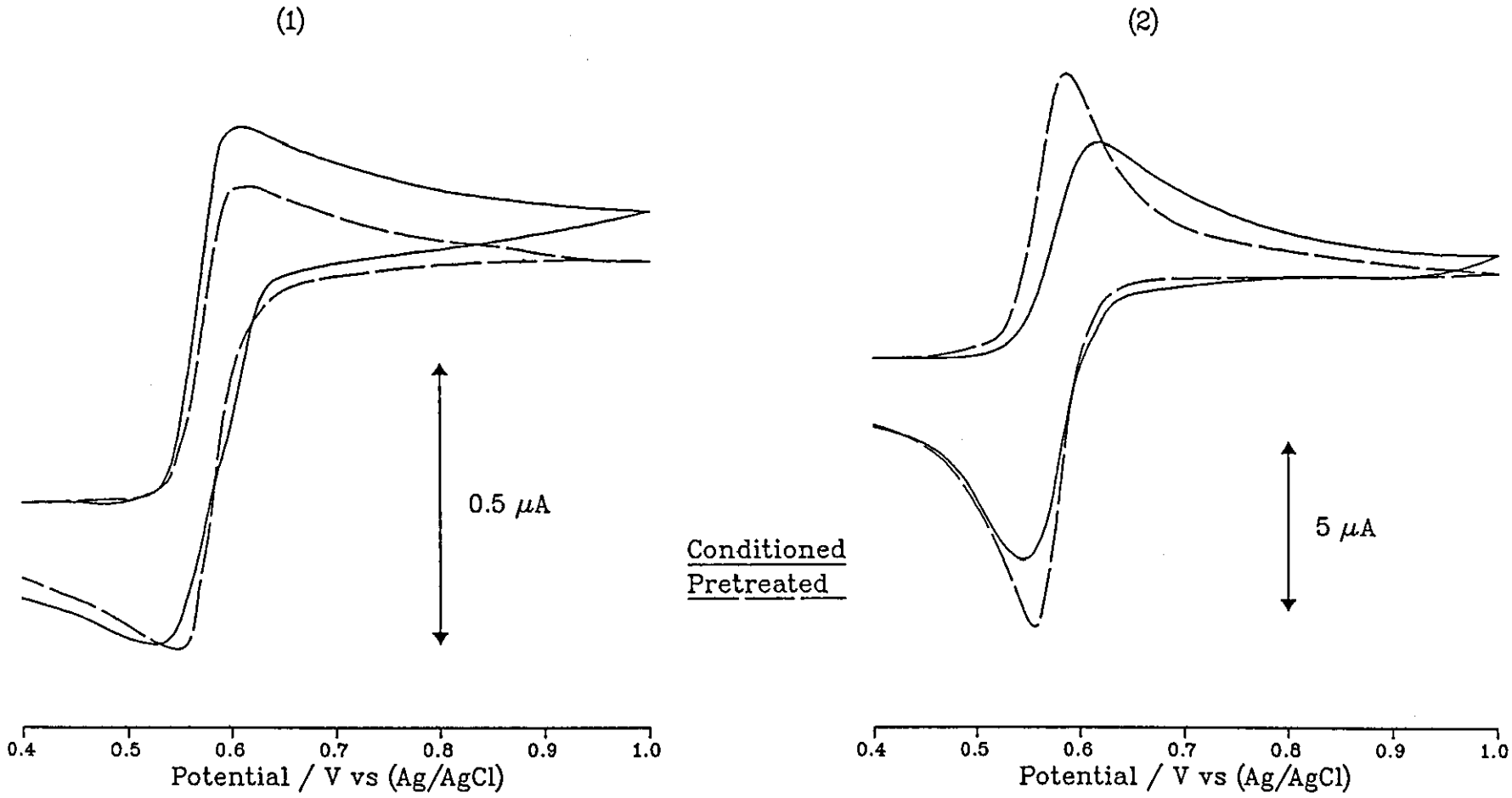

Fig. 43
Cyclic Voltammograms of o-dianisidine (0.5 mM)

Conditions: background = 0.1 M H_2SO_4, ν = 10 mVs^{-1}
1) RVC electrode (2 mm disc of 100 ppi)
2) Glassy carbon electrode (3.0 mm dia.)

E_{pa} and E_{pc} were 612 mV and 550 mV respectively, i.e. ΔE_p = 62 mV. At the conditioned glassy carbon electrode E_{pa} = 615.5 mV and E_{pc} = 547 mV, ΔE_p = 68.5 mV. For the pretreated electrode E_{pa} = 587 mV and E_{pc} = 557 mV, ΔE_p = 30 mV. The pretreated glassy carbon electrode gives an almost reversible electrode reaction for o-dianisidine, but this is not so when the electrode has been conditioned. The reversibility of the electrode reaction at the RVC electrode was poor even when it was pretreated. Slow charge transfer at micro-electrodes has been shown to occur when the steady-state diffusion layer thickness is comparable to the kinetic diffusion layer thickness.[253] This is a disadvantage because most organic compounds give irreversible electrode reactions, so the faradaic contribution to the signal to noise ratio will be decreased.

The RVC electrodes gave an S-shaped wave, rather than the normal peak shaped response (fig. 43). Under conditions of slow scan rates at micro-electrodes, the mass transport to the electrode surface becomes dominated by non-linear diffusion. The mass transport and hence the current is steady state. The surface of these electrodes consists of islands of carbon surrounded by insulating epoxy cement, and the electrode behaves almost like an array of micro-electrodes.

Samples of 0.1 μM o-dianisidine were determined by the fia system. The signal to noise ratio was calculated to be 9.3 for the RVC electrode and was 10.2 for the glassy carbon electrode using the same conditions (i.e. no pretreatment). The uncertainty due to variations in the baseline noise was 11%. The peak current for the RVC electrode was 0.36 nA compared with 6 nA for the glassy carbon electrode. The predicted benefit from flow rate independence does not seem to be borne out experimentally

for the RVC epoxy electrode. Although the noise encountered for this electrode may depend on sources other than the flow rate.

Noise levels become undesirably high when sub-nanoamp currents are measured with conventional instruments. Simple two electrode systems have been shown to be advantageous for the determination of sub-micromolar analyte concentrations with micro-electrodes[254] and other workers have modified the potentiostat to reduce electronic noise.[162]

5.3.2 Selectivity of a Glassy Carbon Electrode coated with a Poly(N,N-dimethyl-p-toluidine) Film

Experimental

An experiment was devised to ascertain whether the response of a poisoned electrode could be monitored by an electroactive compound which does not affect the electrode. A fia system including an injection valve and a stream switching valve was assembled. A Minipuls 2 peristaltic pump was used to propel the carrier (0.1 M sulphuric acid) through a Rheodyne 5020 valve used as a stream switching valve, through another equipped with an injection loop of about 70 µl, then to the WJ1 detector cell, immersed in a beaker of electrolyte. A platinum counter electrode and a Ag/AgCl reference electrode were placed alongside the cell in the beaker. A 1 m length of 0.5 mm i.d. PTFE tubing connected the valve to the detector cell. A seperate flow line was connected to the switching valve, containing a solution of 0.2 mM potassium hexacyanoferrate(II) in 0.1M sulphuric acid. The waste from the switching valve was of the same dimensions as the flow manifold to keep the backpressures on the two flow lines the same, hence the flow rates

should be vey similar. The flow rates in each line were adjusted to 6.0 $cm^3 min^{-1}$. The potentiostat was a Metrohm E 611 detector, with a potential of 0.9V applied to the working electrode.

The switching valve was positioned to allow the acid carrier to the cell and the electrode (3.0 mm diameter glassy carbon) was allowed to stabilise. The other valve was used to inject three samples of 20 µM o-dianisidine in 0.1M sulphuric acid. The switching valve was turned to allow the $K_4Fe(CN)_6$ to pass to the cell. This was continued until a steady reading was obtained for the oxidation of this compound at the electrode. The valve was then switched back to acid carrier and when the baseline had stabilised, five injections were made of 1mM N,N-dimethyl-p-toluidine, in order to form a film on the electrode surface. The o-dianisidine was injected as before and also the $K_4Fe(CN)_6$ was switched through the cell. $K_4Fe(CN)_6$ does not affect the electrode, and so it was possible to pass the solution through the cell directly, thus eliminating any contribution from the injection process. Four sets of injections of N,N-dimethyl-p-toluidine were made.

Results and Discussion

The average drop in response due to 20 µM N,N-dimethyl-p-toluidine after 20 injections of 1 mM concentration of the same was about 30%. The response to o-dianisidine fell by an average of about 10%, and the response to potassium hexacyanoferrate(II) was hardly changed within experimental error. The film does not affect the redox reaction of the $K_4Fe(CN)_6$, and so it is likely that electron transfer occurs at the surface of the polymer film because the rate of diffusion of the ion

in the film is likely to be slow compared with its mass transport to the bare electrode. The large size and charge of this complex ion would tend to hinder its mobility in the film.

Oyama et al[255] prepared polymer films of aniline and other substituted anilines by electrolysis of the amines in pH 1.0 buffer at carbon and platinum electrodes. They found that the films were electroactive in acidic solution and selective towards redox reactions with redox potentials within the potential limits of the films electroactivity. The oxidation of $[Fe(CN)_6]^{3-}$, and I^- ions occured at both bare and polymer coated electrodes at almost the same redox potential and the same limiting current value. They suggest that the electron transfer is possible via reduced or oxidised forms of the polymer. Ions with redox potentials outside the limits of electroactivity of the film i.e. $[Ru(CN)_6]^{4-}$ and others were hardly active at the polymer covered electrodes, because the oxidation was not catalysed by the film and the rate of diffusion of the ions in the film was low.

The decreased response of the o-dianisidine and N,N-dimethyl-p-toluidine at the electrode covered with a film of the latter, seems to be due to poor catalysis of their oxidation by the redox site on the polymer surface. The polymer films appear to be impenetrable by most species apart from hydrogen ions which are small. Ohnuki et al[256] demonstrated that platinum electrodes coated with films prepared from the electropolymerisation of phenol and substituted anilines can be used as pH sensors. The polymer film exhibited selectivity towards the electroactive species according to their redox potential and the use of a different compound to measure the response of an electrode which is being poisoned is not feasible in this case.

CHAPTER 6
FINAL DISCUSSIONS

6.1 Conclusions

The work on anodic voltammetry of anilines showed that least poisoning of the electrode occurs in organic solvents and that it is almost impossible to prevent the build up of polymer film on the electrode surface. This is because follow up chemical reactions of the oxidised species are very rapid and the presence of a large excess of reagent or solvent only serves to minimise the number of these reactions occuring. Organic solvents were not used for analysis because of the high background currents and other problems.[250] The most suitable aqueous conditions for limiting the electrode poisoning were at either high pH or low pH. The analysis of low levels of aniline by fia with amperometric detection (fia/ec) was not feasible due to the drop off in response after each injection.

The most suitable alternative to aniline with respect to volatility (its atmospheric detection was required) and freedom from electrode fouling was found to be N,N-dimethyl-p-toluidine. The analysis of this compound by fia/ec was useful for a reasonable number of samples of concentration below 10 μM, before the decrease in response became unacceptable. The use of this compound was not pursued any further however because the requirement was to be able to monitor the release of an organic vapour into the atmosphere and the peak in concentration would be sufficient to poison the electrode.

The use of double pulse amperometric detection prolonged

the electrode stability, but decreased the detection limit to an unacceptable level due to the introduction of irreproducible background currents. As for fia/ec it was not possible to prevent polymerisation of aniline and subsequent adsorption onto the electrode surface. Poisoning with other substituted anilines was less severe. Little advantage is gained due to desorption of electrode reaction products because most of the organic redox reactions are irreversible and the reaction products tend to undergo rapid follow up chemical reactions leading to strongly adsorbed material.

Johnson and co-workers have studied the detection of organic compounds by catalytic oxidation of adsorbed analyte at metal electrodes using PAD waveforms. In the research reported here, the anodic oxidation mechanism for aniline seemed to be either surface catalysed or to take place by direct electron transfer depending upon the applied potential. This is suggested from the hydrodynamic voltammograms (see section 4.3.6). There were two distinct regions of potential where electroactivity was observed. The region where direct electron transfer was predominant was preferred because the signal to background noise levels were greatest and there appeared to be more selectivity.

The detection limits for PAD were not as low as by DC amperometry, but were acceptable being sub micromolar for the wall jet cell and lower levels (c.a. one order of magnitude) were achievable with the Dionex thin layer cell, but this was not suitable for monitoring samples from the gas bubbler. As with most fia systems with amperometric detection one of the main drawbacks is the propulsion system. The peristaltic pump produced flow pulsations, which, because of the flow dependence of the detector, was the major sources of noise. The drift in

flow rate due to pump tube wear was also a nuisance. Better pumps are available e.g. dual piston pumps for hplc, but the increased cost is often not justified, owing to the limited application of amperometric detectors to real samples.

The response of the PAD to aniline was non-linear and required the development a curve fitting program which gave satisfactory fits of the data. The curve fitting algorithm was based on the Langmuir isotherm. The lower potentials fitted well (0.4 - 0.6 V vs Ag/AgCl), but the higher potentials (>0.7 V vs Ag/AgCl) needed an additional term which is proposed to allow for the mass transport of aniline due to direct electrochemical oxidation. Johnson and co-worker initially recommended linearisation of the calibration data by plotting reciprocal concentration against reciprocal current but this is now not recommended.[239] In this work it was found that the result of using this type of plot was merely to transfer the fitting error of the straight line from the distant part of the calibration line to the part close to the origin.

The limit of detection for aniline in air was higher than 5 mg m^{-3} as this concentration was detected with an error between -250% and -500%. The apparatus used to generate and collect the vapour was somewhat crude, but effective enough to demonstrate that reasonably low levels of vapour could be detected. The most difficult part is to interface the gas with the absorption liquid in order to continuously monitor the vapour concentration and also achieve an adequate level of analyte enrichment.

For carbon electrodes, electrochemical pretreatment was found to be useful where the redox reaction is rather irreversible, for example, the secondary anilines. The

advantage of using micro-array electrodes in amperometric detectors is lost to some extent by the electronic noise introduced when measuring the small faradaic currents and by the poorer reversibility of redox reactions.

6.2 Further Work

One of the encouraging aspects of this work was the analysis of aniline using PAD. The self cleaning of the electrode by the applied waveform is a great advantage where the analyte causes electrode fouling using conventional amperometric techniques. The noise generated by the potential pulses limits the detection limit, but could well be superior to other alternative techniques. One major disadvantage of the technique is the difficulty in optimising waveforms for new conditions e.g. changing the pH or optimising for a diffusion limited current rather than a catalytic current.

There are numerous organic analytes which give a diffusion limited current for oxidation at solid electrodes, but present problems due to electrode fouling. This is one of biggest problems with solid electrodes, and where the DME has the most significant advantage of a renewable surface. Smyth compared uv and amperometric detection for hplc of phenols in beer.[257] Electrode fouling with a reasonable number of sample injections was a problem and the use of PAD was suggested for improved electrode stability.

The PAD waveform might be applied in the same manner as for aniline so that the current is mainly due to diffusion limited mass transport with direct electron transfer, rather than a surface catalysed current. The detection is then tunable in the same way as DC

amperometric detection by varying the measuring potential and thereby achieving a degree of selectivity. In order to achieve this the integration time needs to be increased. By doing this the noise will be increased as the delay is shortened. A possible answer to the increased noise would be to employ a micro-array of platinum electrodes. There would be advantages due to faster decay of charging current and less noise due to flow pulsations. The larger faradaic currents generated by the potential pulse methods (PAD), should not be a problem to measure using conventional potentiostats.

Calibration of the PAD response is a problem because of its non linear nature. Johnson and co-workers have shown that for analytes which give currents due solely to surface confined catalytic oxidation then the response follows the Langmuir isotherm. In many cases the fit is not satisfactory due to additional mass transport and the linearisation of the response by employing pulsed coulometric detection is now being investigated. The use of non linear regression analysis seems the only reasonable alternative apart from curve fitting by eye. The development of an expression for the current is more satisfactory than employing a general polynomial equation and ought to give better fits to the calibration data. The computer program, running on a BBC microcomputer demonstrated that a readily available least squares polynomial curve fitting program, might be modified to fit a particular function to the PAD calibration, with satisfactory results.

From the results of this work it seems quite reasonable to suggest that a portable device might be developed to monitor the release of aniline into the atmosphere according to the original requirements of the sponsor. (see section 1.8). As has been mentioned earlier the main

difficulty is in interfacing the vapour with the trapping liquid. Miniaturisation of the electronics should not be a problem for example it is a feasible proposition to have a potentiostat made on a single custom built chip. The pumping system poses problems in being able to deliver a smooth flow from a small portable unit, and this probably determines the detection limit. The sensor has obviously limited selectivity, but it is probably sufficient for the application for which it is intended.

There are two approaches which might be used to solve the problem of interfacing the vapour with the trapping liquid in a portable vapour monitor (see section 1.7.2) and they may be summarised as follows:

1) Vapour / Membrane / liquid

This approach is most widely used because the structure may be made simple and compact. A degree of selectivity is conferred by the choice of membrane, but the sensitivity is decreased and a lag in response is introduced. There tend to be losses of solvent due to leakage and evaporation. Provided that the membrane is sufficiently permeable to aniline then this seems to be the best approach.

2) Gas / liquid

Both scrubbers and impinger are used for sampling vapour because they are simple robust and effective. They are infrequently incorporated into portable detectors because they are difficult to miniaturise, they introduce an integrating effect and their use is orientation dependent.

REFERENCES

1 Meites L., Nurnburg H.W. and Zuman P., Pure Appl. Chem., 45, (1976), 83

2 Kolthoff I.M. and Lingane J.J., Polarography, Wiley (Interscience), New York, 2nd edition, (1952)

3 Flato J.D., Anal. Chem., 44, (1972), No 11, 75A

4 Borman S.A., Anal. Chem., 54, (1982), 698A

5 Florence T.M., Analyst, 111, (1986), 489

6 Wang J., Stripping Analysis, Principles, Instrumentation and Applications, VCH Publishers Inc., Florida, (1985)

7 Macdonald D.D., Transient Techniques in Electrochemistry, Plenum, New York, (1977)

8 Galus Z., Fundementals of Electrochemical Analysis, Ellis Horwood, Chichester, (1976)

9 Bard A.J. and Faulkner L.R., Electrochemical Methods, Wiley, New York, (1980)

10 Adams R.N., Electrochemistry at Solid Electrodes, Marcel Dekker, New York, (1969)

11 Bond A.M., Modern Polarographic Methods, Marcel Dekker, New York, (1980)

12 Randles J.E.B., Trans. Faraday Soc., 44, (1948), 327

13 Sevcik A., Coll. Czech. Chem. Communs., 13, (1948), 349

14 Matsuda H. and Ayabe Y., Z. Elektrochem., 59, (1955), 494

15 Eggins B.R., Farad. Disuss. Chem. Soc., 56, (1973), 276

16 Nelson S.F., Kessel C.R., Brien D.J. and Weinbold F., J. Org. Chem. 45, (1980), 2116

17 Evans D.F., Acc. Chem. Res., 10, (1977), 313

18 Nicholson R.S. and Shane J., Anal. Chem., 36, (1964), 706

19 Kissinger P.T. and Heineman W.R., J. Chem. Ed., 60, (1983), 702

20 Mabbott G.A., J. Chem. Ed., 60, (1983), 697
21 Bond A.M. and Jones R.D., Anal. Chim. Acta., 121, (1980), 1
22 Dieker J.W., van der Linden W.E. and Poppe H.E., Talanta, 25, (1978), 151
23 Chey W.M.,Adams R.N. and Yllo M.S, J. Electroanal. Chem., 75, (1977), 731
24 Smith D.E, CRC, Crit. Rev. Anal. Chem., 2, (1971), 247
25 Osteryoung J. and O'Dea J.J., Electroanalytical Chemistry, ed. Bard A.J., Marcel Dekker, New York, 14, (1986), 209
26 Anderson J.E., Bond A.M., Anal. Chem., 53, (1981), 1394
27 Ivaska A.U., Smith D.E., Anal. Chem., 57, (185), 1910
28 Zachowski E.J., Wojciechowski M., Osteryoung J. Anal. Chim. Acta, 183, (1986), 47,
29 Levich V.G., Physicochemical Hydrodynamics, Prentice- Hall, Englewood Cliffs, New Jersey, (1962)
30 Newman J., Electroanalytical Chemistry, ed. Bard A.J., Marcel Dekker, New York, 6, (1973), 187
31 Pungor E., Feher Z. and Varadi M., CRC, Crit. Rev. Anal. Chem., 9, (1980), 97
32 Bruckstein S. and Miller B., Acc. Chem. Res., 10, (1977), 54
33 Albery W.J. and Hitchman M.L., Ring Disc Electrodes, Oxford University Press, London (1971)
34 Matsuda H., J. Electroanal. Chem., 15, (1967), 325
35 Yamada J. and Matsuda H., J. Electroanal. Chem., 44, (1973), 189
36 Elbiki J.M., Morgan D.M. and Weber S.G., Anal. Chem., 56, (1984), 978
37 Gunasingham H., Tay B.T., Ang K.P., Anal. Chem. 56, (1984), 2422
38 Gunasingham H., Anal. Chim. Acta, 159, (1984), 139

39 Levich V.G., Discuss. Faraday Soc., 1, (1947), 37
40 Weber S.G., J. Electroanal. Chem., 145, (1983), 1
41 Vohra S.K. and Harrington G.W., J. Chromatogr. Sci, 18, (1980), 379
42 Hackman M.R., Brooks M.A., J. Chromatogr., 222, (1981), 179
43 Dieker J.W., van der Linden W.E. and Poppe H., Talanta, 26, (1979), 551
44 Stulik K. and Pacakova V., J. Chromatogr., 192, (1980), 135
45 Stulik K. and Pacakova V., 208, (1981), 269
46 Kissinger P.T., Anal. Chem., 49, (1977), 447A
47 Bratin K. and Kissinger P.T., J. Liq. Chromatogr., 4, (1981), 321
48 Stulik W. and Pacakova V., J. Electroanal. Chem., 129, (1981), 1
49 Swartzfager D.W., Anal. Chem., 48, (1976), 2189
50 Mayer W.J. and Greenberg M.S., J. Chromatogr. Sci. 17, (1974), 614
51 Beauchamp R. Boinay P., Fombon J.J., Tacussel J., Breant M., Georges J., Porthault M. and Vittori O., J. Chromatogr., 204, (1981), 123
52 Lund W. Hannisdal M. and Greibrokk T., J. Chromatogr., 173, (1979), 249
53 MacCrehan W.A., Anal. Chem., 53, (1981), 74
54 Fleet B. and Little C.J., J. Chromatogr. Sci., 12, (1974), 747
55 Stulik K. and Hora V., J. Electroanal. Chem., 70, (1976), 253
56 Austin D.S., Polta J.A., Polta T.Z., Tang A.P.-C., Cabelka T.D. and Johnson D.C., J. Electroanal. Chem., 168, (1984), 227
57 Baizer M.M. and Lund H., Organic Electrochemistry, 2nd edit., Marcel Dekker, New York, (1983)
58 Ross S.D., Finkelstein M. and Rudd E.J., Anodic Oxidation, Academic Press, New York, (1975)

59 Bard A.J. and Lund H., Encyclopedia of Electrochemistry of the Elements, XI-XIV, (Organic Section), Marcel Dekker, New York, (1978-80)

60 Johnson D.C. Polta J.A., Polta T.Z. Neuberger G.G., Johnson J., Tang A.P.-C., Yeo I.-H. and Baur J., J. Chem. Soc. Faraday Trans. 1, 82, (1986), 1081

61 Hughes S. and Johnson D.C., Anal. Chim. Acta, 149, (1983), 1

62 Polta J.A. and Johnson D.C., J. Liq. Chromatog., 6, (1983), 1727

63 Polta J.A., Johnson D.C. and Merkel K.E., J. Chromatogr., 324, (1985), 407

64 Ruzicka J. and Hansen E.H., Anal. Chim. Acta, 78, (1975), 145

65 Proceedings of the International Conference on Flow Analysis III, Great Britain, 5th Sept. 1985, Anal. Chim. Acta, 179, (1986), 7

66 Valcarcel M., Luque De Castro M.D., Flow Injection Analysis, Ellis Horwood, Chichester, (1987)
Ruzicka J. and Hansen E.H., Flow Injection Analysis, Wiley-Interscience, New York, (1981)

67 Ruzicka J. and Hansen E.H., Flow Injection Analysis, Wiley-Interscience, New York, (1981)

68 Mottola H.A., Anal. Chem., 53, 1312A

69 Ruzicka J. and Hansen E.H., Anal. Chim. Acta, 114, (1980), 19

70 Ranger C.B., Anal. Chem., 53, (1981), 20A

71 Stewart K.K., Anal. Chem., 55, (1983), 931A

72 Appelqvist R., Beecher G.R., Bergamin H., den Boef F.G., Emneus J., Fang Zhaolun, Gorton L., Hansen E.H., Hare P.E., Harris J.M., Harrow J.J., Ishibashi N., Janata J., Johansson G., Karlberg B., Krug F.G., van der Linden W.E., Luque de Castro M.D., Markovarga G., Miller J.N., Mottola H.A., Muller H., Pacey G.E., Riley C., Ruzicka J., Schothorst R.C., Stewart K.K., Townshend A., Tyson J.F., Ueno K., Valcarcel

M., Vanderslice J., Worsfold P.J., Yoza N., and Zagatto E.A., Anal. Chim. Acta, 180, (1976), 1

73 Ruzicka J. Hansen E.H. and Zagatto E.A., Anal. Chim. Acta, 88, (1977), 1

74 Matson W.R., Langlais P., Volicer L., Gamache P.H., Bird E., Mark K.A., Clin. Chem., 30, (1984), 1477

75 Roe D.K. and Ho I.P., Paper number 532, Pittsburg Conference, (1984)

76 MacCrehan N.A. and Durst R.A., Anal. Chem., 53, (1981), 1700

77 Roston D.A. and Kissinger P.T., Anal. Chem., 54, (1984), 429

78 Johnson D.C., Weber S.G., Bond A.M., Wightman R.M., Shroup R.E. and Krull I.S., Anal. Chim. Acta, 180, (1986), 214

79 Hubbard A.T. and Anson F.C., Electroanalytical Chemistry, (ed. Bard A.J.), 4, Marcel Dekker, New York, (1970), 129-214

80 Brunt K. and Bruins C.H.P., J. Chromatogr., 52, (1980), 1304

81 Hanekamp H.B., van Nieuwkerk H.J., Anal. Chim. Acta, 121, (1980), 13

82 Hanekamp H.B. and de Jong H.G., Anal. Chim. Acta, 135, (1982), 351

83 Patthy M., Genynge R. and Salat J., J. Chromatogr., 241, (1982), 131

84 Stulik K. and Pacakova V., Ann. Chim. (Rome), 76, (1986), 315

85 Kissinger P.T. and Heinman W.R., Laboratory Techniques in Electroanalytical Chemistry, Marcel Dekker, New York, (1984)

86 Compton R.G. and Unwin P.R., J. Electroanal. Chem., 205, (1986), 1

87 van der Linden W.E. and Dieker J.W., Anal. Chim. Acta, 119, (1980), 1

88 Fogg A.G. and Summan A.M., Analyst, 109, (1984),

1029

89 Gunasingham H. and Fleet B., Anal. Chem., 55, (1983), 1409

90 Albery W.J. and Brett C.M.A., J. Electroanal. Chem., 148, (1983), 201

91 Gunasingham H., Ang K.P., Ngo C.C. and Thiak P.C., J. Electroanal. Chem., 186, (1985), 51

92 Peterson W.M., Am. Lab., 11, (1979), 69

93 Fleet B. and Little C.J., J. Chromatogr. Sci., 12, (1974), 747

94 Neeb R., Z. Anal. Chem., 171, (1959), 321

95 Florence T.M., J. Electroanal. Chem., 27, (1970), 273

96 Bratin K., Kissinger P.T., Briner R.C. and Brundlett C.S., Anal. Chim. Acta, 130, (1981), 295

97 Bratin K. and Kissinger P.T., Talanta, 29, (1982), 365

98 Gross J. and Jordan J., Pure Appl. Chem., 56, (1984), 1095

99 Gaylor V.F., Elving P.J. and Conrad A.L., Anal. Chem., 29, (1957), 224

100 Elving P.J. and Smith D.E., Anal. Chem., 32, (1960), 1849

101 Adams R.N., Anal. Chem., 30, (1958), 1576

102 Olson C.L. and Adams R.N., Anal. Chim. Acta, 29, (1963), 358

103 Olson C.L. and Adams R.N., Anal. Chim. Acta, (1960), 582

104 Pungor E. and Szepesvary E., Anal. Chim. Acta, 43, (1968), 289

105 Kissinger P.T., Refshauge C., Dreiling R. and Adams R.N., Anal. Lett., 6, (1973), 465

106 Caliguri E.J. and Mefford C.N., Brain Res., 296, (1984), 156

107 Marcoux L.S., Prater B.G. and Adams R.N., Anal. Chem., 37, (1965), 1446

108 Atuma S.S. and Lindquist J., Analyst, 98, (1973), 886
109 Rice M.E., Galus Z. and Adams R.N., J. Electroanal. Chem., 143, (1983), 89
110 Albahadily F.N. and Mottola H.A., Anal. Chem., 59, (1987), 958
111 Chambers C.A. and Lee J.K., J. Electroanal. Chem., 14, (1967), 309
112 Meier E.P. and Chambers J.Q., Anal. Chem., 41, (1969), 914
113 Chesney D.J., Anderson J.L., Weisshaar D.E. and Tallman D.E., Anal. Chim. Acta, 124, (1981), 321
114 Stulik K. and Pacakova V., J. Chromatogr., 203, (1981), 269
115 Stulik K., Pacakova V. and Starkova B., J. Chromatog., 213, (1981), 41
116 Fenn R.J. Siggia S. and Curran D.J., Anal. Chem., 50, (1979), 1067
117 Prete M.P., Kauffmann J.M. and Vire J.C., Anal. Lett., 17, (1984), 1391
118 Wang J., Anal. Chem., 53, (1981), 2280
119 Henriques H.P. and Fogg A.G., Analyst, 109, (1984), 1195
120 Armentrout D.N., McLean J.D. and Long M.W., Anal. Chem., 51, (1979), 1039
121 Walker Jnr. P.L., Am. Sci., 50, (1962), 259
122 Panzer R.E. and Elving P.J., J Electrochem. Soc., 119, (1972), 864
123 Heplar B.R., Weber S.G. and Purdy W.C., Anal. Chim. Acta, 102, (1978), 41
124 Wightman R.M., Paik E.C., Borman S. and Dayton M.A., Anal. Chem., 50, (1978), 1410
125 International committee for the Characterization and Terminology of Carbon, Carbon, 20, (1982), 445
126 Yamada S. and Sato H., Nature, 193, (1962), 261
127 Jenkins G.M. and Kawamura K., Nature, 231, (1971),

195
128 Randin J.P. and Yieger E., J. Electroanal. Chem., 58, (1975), 313
129 Laser D. and Ariel M., J. Electroanal. Chem., 52, (1974), 291
130 Panzer R.E. and Elving P.J., Electrochim. Acta, 20, (1975), 635
131 Blurton K.F., Electrochim. Acta, 18, (1973), 869
132 Vasil'ev Yu.B., Kanevskii L.S., Lushikov V.I. and Skundin A.M., Sov. Electrochem., 19, (1977), 377
133 Gunasingham H. and Fleet B., Analyst, 107, 896
134 Monien H., Specker H. and Zinke., Z. Anal. Chem., 37, (19659, 200
135 Hu I.F., Karweik D.H. and Kuwana T., J. Electroanal. Chem., 188, (1985), 59
136 Amatore C., Saveant J.M. and Tesslar D., J. Electroanal. Chem., 146, (1983), 37
137 Kumau G.N., Willis W.S. and Rusling J.F., Anal. Chem., 57, (1985), 545
138 Engstrom R.C., Anal. Chem., 54, (1982), 2310
139 Gonon F.G., Fombarlet C.M., Buda M.J. and Pujol J.F., Anal. Chem., 53, (1981), 1386
140 Wang J. and Hutchins L.D., Anal. Chim. Acta, 167, (1985), 325
141 Taylor R.J. and Humffray A.A., J. Electroanal. Chem., 42, (1973), 347
142 Evans J. and Kuwanta T., Anal. Chem., 51, (1979), 358
143 Zak J. and Kuwanta T., J. Amer. Chem. Soc., 104, (1982), 5514
144 Hershenhart E., McCreedy R.L. and Knight R.D., Anal. Chem., 56, (1984), 2256
145 Poon M. and McCreedy R.L., Anal. Chem., 58, (1986), 2745
146 Wang J. and Tuzhi P., Anal. Chem., 58, (1986), 1787
147 Hoogvliet J.C., Van den Beld C.M.B., Van der Poel

C.J. and Van Bennekom W.P., J. Electroanal. Chem., 201, (1986), 11

148 Poon M. and McCreedy R.L., Anal. Chem., 59 (1987), 1615

149 Van Rooijen H.W. and Poppe H., Anal. Chim. Acta, 130, (1981), 9

150 James D.S., J. Electrochem. Soc., 114, (1967), 1113

151 Fetham A.M. and Spiro M., Chem. Reviews, 71, (1971), 177

152 Goldstein E.L. and Van de Mark M.R., Electrochim. Acta, 27, (1982), 1079

153 Gaur J.N. and Schmid G.M., J. Electroanal. Chem., 24, (1976), 279

154 Sawer D.T. and Roberts Jnr., Experimental Electrochemistry for Chemists, Wiley, New York, (1974)

155 Fleischmann K., Korinek K. and Pletcher D.J., Electroanal. Chem., 31, (1971), 39

156 Filardo G., Di Quarto S., Gamino S. and Silvestri G., J. Appl. Electrochem., 12, (1982), 127

157 Shih H.W. and Huber C.O., Anal. Chim. Acta, 178, (1985), 313

158 Fourdeaux A., Perret R. and Ruland W., Carbon fibres, Their Composites and Applications, Proc. Inter. Conference of the Plastics Institute, London, (1971)

159 Anderson C.W. and Cushman M.R., J. Neurosci. Methods, 4, (1981), 435

160 Wightman R.M., Anal. Chem., 53, (1981), 1125A

161 Howell J.O. and Wightman R.M., Anal. Chem., 56, (1984), 524

162 Caudill W.L., Howell J.O. and Wightman R.M., Anal. Chem., 54, (1982), 2532

163 Anderson J.L., Whiten K.K., Brewster J.D., Ou T.Y. and Nonidez W.K., Anal. Chem., 57, (1985), 1366

164 Anderson J.E., Tallman D.E., Chesney D.J. and

Anderson J.L., Anal. Chem., 50, (1978), 1051
165 Edmonds T.E., Anal. Chim. Acta, 175, (1985), 1
166 Murray R.W., Electroanalytical Chemistry, 13, (Ed. Bard A.J.), Marcel Dekker, New York, (1984)
167 Murray R.W., Ewing A.G. and Durst R.A., Anal. Chem., 59, (1987), 379A
168 IARC Monographs on the Evaluation of the Carcinogenic Risk of Chemicals to Humans. Supplement 1. Chemicals and Ind. Processes Associated with Cancer in Humans , Inter. Agency for Research on Cancer, Lyon, (1979)
169 Radomski J.L., Ann. Rev. Pharmacol. Toxicol., 19, (1979), 129
170 Rappaport S.M. and Morales R., Anal. Chem., 51, (1979), 19
171 Yasuda S.K., J. Chromatogr., 104, (1975), 283
172 Bosset J.O., Knecht I. and Knecht P., Mitt. Geb. Lebensmitt. Hyg., 72, (1981), 123
173 Hrabeczy-Pall A., Toth K., Pungor E. and Vallo F., Anal. Chim. Acta, 77, (1975), 278
174 Stepanenko V.E. and Krichmar S.I., Zavod. Lab., 38, (1972), 1200
175 Krichmar S.I., Zh. Anal. Khim., 35, (1980), 965
176 Ramasamy S.M. and Mottola H.A., Anal. Chem., 54, (1982), 283
177 Ferm F., Atmos. Environ., 13, (1979), 1385
178 De Santis F. and Perrino C., Ann. Chim., 76, (1986), 355
179 Dasgupta P.K., McDowell W.L. and Rhee J.S., Analyst, 111, (1986), 87
180 Vecera Z. and Janak J., Anal. Chem., 59, (1987), 1494
181 Kato M., Yamada M. and Suzuki S., Anal. Chem., 56, (1984), 2529
182 Meddle D.W. and Smith A.F., Analyst, 106, (1981), 1088

183 Qureshi M. and Khan I.A., Anal. Chim. Acta, 86, (1976), 309

184 Albi M.A. and Vioque A., Grasas Aceites (Seville), 34, (1983), 24

185 Kupfer D. and Bruggeman L.L., Analyt. Biochem., 17, (1966), 502

186 Bratton A.C. and Marshall E.K., J. Biol. Chem., 128, (1939), 537

187 Chrastil J. and Wilson J.T., Bichem. Med., 13, (1975), 89

188 Norwitz G. and Keliher P.N., Talanta, 29, (1982), 407

189 Rowat J.P. and Singh J.P., Anal. Chem., 47, (1975), 758

190 El-Dib M.A., J. Assoc. Off. Anal. Chem., 54, (1971), 1383

191 Zavorovskaya N.A. and Nekhorosheva E.V., Zh. Anal. Khim., 36, (1981), 1808

192 Tomkins B.A., Ostrum V.H. and Ho C.H., Anal. Lett., Part A, 13, (1980), 589

193 Dombrowski L.J. and Pratt E.L., Anal. Chem., 43, (1971), 1042

194 Olabiran M.O., M.Sc. Dissertation, Loughborough University of Technology, (1983)

195 Taylor M.G. and Edmonds T.E., Anal. Proc. 23, (1986), 28

196 Fogg A.G., Bsebsu N.K. and Abdalla M.A., Analyst, 107, (1982), 1462

197 Fogg A.G., Ali M.A., Abdalla M.A., Analyst, 108, 840

198 Guadalupe A.R., Jhaveri S.S., Liu K.E. and Abruna H.D., Anal. Chem., 59, (1987), 2436

199 Ghoroghchian J., Sarfarazi F., Dibble T., Cassidy J., Smith J.J., Russell A., Dunmore G., Fleishmann M. and Pons S., Anal. Chem., 58, (1986), 2278

200 Blurton K.F. and Stettor J.R., J. Chromatogr., 155, (1978), 35

201 Stetter J.R., Tellefsen R.A. and Saunders R.A, Talanta, 26,(1979), 799

202 Luckas B. and Lorenzen W., Dtsch. Lebensm. Rundsch, 78, (1982), 119

203 Cooper S.W., Jayanty R.K., Knoll M. and Midgett M.R., J. Chromatogr. Sci., 24, (1986), 204

204 Riggin R.M., Cole T.F. and Billets S., Anal. Chem., 55, (1983), 1862

205 Coutts R.T., Hargesheimer E.E., Pasutta F.M. and Baker G.B., J. Chromatogr. Sci., 19, (1981), 151

206 Meddle D.W. and Smith A.F., Analyst, 106, (1981), 1082

207 Varney M.S. and Preston M.R., J. Chromatogr., 348, (1985), 265

208 Lores E.M., Bristol D.W. and Moseman R.F., J. Chromatogr. Sci., 16, (1978), 358

209 Concialini V., Chiavari G. and Vitali P., J. Chromatogr., 258, (1983), 244

210 Barek J., Pacakova V., Stulik K. and Zima J., Talanta, 32, (1985), 279

211 Radzic D.M. and Kissinger P.T., Anal. Biochem., 140, (1984), 74

212 Purnell C.J. and Warwick C.J., Analyst, 105, (1980), 861

213 Rice J.R. and Kissinger P.T., Environ. Sci. Technol., 16, (1980), 263

214 Hunniker H.R. and Miserez A., Mitt. Geb. Lebensmittelunters Hyg., 72, (1981), 216

215 Stahl E., Zimmer C., Juell S.Z., Lebensm. -Unters. -Forsch., 175, (1982), 88

216 Baumann U. and Marke B., Mitt. Geb. Lebensmittelunters Hyg. 71, (1980), 468

217 Letheby H., J. Chem. Soc., 15, (1862), 161

218 Bysouth S.R., Ph.D. Dissertation, Loughborough University, (1988)

219 Lord S.S. and Rogers L.B., Anal. Chem., 26, (1954),

284

220 Mohliner D.M., Adams R.N. and Argersinger W.J., J. Amer. Chem. Soc., 84, (1962), 3618

221 Desideri P.G., Lepri L. and Heimler D., J. Electroanal. Chem., 32, (1971), 225

222 Breitenbach M. and Heckner K.-H., J. Electroanal. Chem., 43, (1973), 267

223 Sharma L.R., Manchanda A.K., Singh G. and Verma R.S., Electrochim. Acta, 27, (1982), 223

224 Galus Z. and Adams R.N., J. Phys. Chem., 67, (1963), 862

225 Galus Z. and Adams R.N., J. Amer. Chem. Soc., 86, (1964), 1666

226 Melicharek M. and Nelson R.F., J. Electroanal. Chem., 26, (1970), 201

227 Paul E.W. Ricco A.J. and Wrighton M.S., J. Phys. Chem, 89, (1985), 1441

228 Sasaki K., Kaya M., Yano J, Kitani A. and Kunai A., J. Electroanal. Chem., 215, (1986), 401

229 Desideri P.G., Lepri L. Heimler D., J. Electroanal. Chem., 52, (1974), 105

230 Polta J.A., Yeo I. -H. and Johnson D.C., Anal. Chem., 57, (1985), 563

231 Norman P. and Ebdon L., Simplex Optimisation Program for Atomic Absorption Instruments, for Apple II Microcomputers, (1984)

232 Yarbro L.A. and Denning S.N., Anal. Chim. Acta, 73, (1974), 391

233 Miller J.C. and Miller J.N., Statistics for Analytical Chemists, Ellis Horwood, Chichester, (1984)

234 Smith S.B., Sainz M.A. and Schleicher R.G., Spectrochim. Acta, Part B, 42B, (1987), 323

235 Polta T.Z., Johnson D.C. and Luecke G.R., J. Electroanal. Chem., 209, (1986), 171

236 Taylor M.G. and Bysouth S.R., Unpublished Work

237 Miller A.R., Basic Programs for Scientists and Engineers, Sybex, Berkeley, (1981)

238 Polta T.Z. and Johnson D.C., J. Electroanal. Chem., 209, (1986), 159

239 Neuberger G.G. and Johnson D.C., Anal. Chim. acta, 192, (1987), 205

240 Blomgren E. and Bockris J.'O'M., J. Phys. Chem. 63, (1959), 1475

241 Frumkin A., Z. Physik, 35, (1926), 792

242 Hansen R.S., Mintunn R.E. and Hickson D.A., J. Phys. Chem., 61, (1957), 953

243 Analytical Methods Committee, Analyst, 112, (1987), 199

244 Patton C.J. and Crouch S.R., Anal. Chim. Acta, 179, (1986), 189

245 Timmons C.J. and Gillam A.E., Introduction to Electronic Absorption Spectroscopy in Organic Chemistry, Edward Arnold, London (1970)

246 Sherwood T.R. and Pigford R.L., Absorption and Extraction, p6, McGraw-Hill, New York, (1952)

247 McKelvey J.M. and Hoelscher H.E., Anal. Chem., 29, (1957), 123

248 Nomenclature, Symbols, Units and Their Usage in Spectrochemical Analysis-II, Spectrochim. Acta, Part B, 33, (1978), 242

249 Charlet G., Badoz-Lambling J. and Tremillon B., Electrochemical Reactions, Elsevier, Amsterdam, (1962)

250 Van Rooijen H.W. and Poppe H., J. Liq. Chromatogr., 6, (1983), 231

251 Kissinger P.T., Felice L.J., Miner D.J., Preddy C.R. and Shoup R.E., in Hercules D.M., Hieftje G.M., Snyder L.R. and Evenson M.A. (Eds.), Contempory Topics in Analytical and Clinical Chemistry, 2, Plenum, New York, (1978)

252 Roe D.K., Anal. Lett., 16, (1983), 613

253 Sleszynski N., Osteryoung J. and Carter M., Anal. Chem., 56, (1984), 130

254 Bixler J.W., Bond A.M., Lay P.A., Thormann W., Van Den Bosch P., Fleischmann M. and Pons B.S., Anal. Chim. Acta, 187, (1986), 67

255 Oyama N., Ohnuki Y., Chiba K. and Ohsaka T., Chem. Lett. (Japan), (1983), 1759

256 Ohnuki Y., Matsuda H., Ohsaka T. and Oyama N., J. Electroanal. Chem., 158, (1985), 55

257 Hayes P.J., Smyth M.R. and McMurrough I., Analyst, 112, (1987), 1205

APPENDICES

APPENDIX (i)

Derivation of the Curve Fitting Equations

It might reasonably be assumed that the current (I) arrising from oxidative desorption of adsorbed electroactive species is proportional to the surface coverage (θ) of the electrode by that species.

i.e. $I \propto \theta$

Using a constant (κ) to form an equality

$$I = \kappa\theta$$

It has been proposed by Johnson and co-workers that the adsorption of analyte on the electrode surface follows the Langmuir isotherm.[56] The current may then be equated to the concentration of the analyte sample injected as follows:

$$I = \frac{\kappa . KC}{1 + KC}$$

combining constants, i.e. $\kappa . K = K_1$ renaming $K = K_2$

$$I = \frac{K_1 C}{1 + K_2 C}$$

The above rational equation must be rearranged into a linear form in order to use it in the polynomial fitting equation.

$$I + IK_2C = K_1C$$

$$I = K_1C - K_2IC$$

If an additional term is introduced to allow for the current due to electroactive species arriving at the electrode surface due to convective diffusional mass transport during the current measuring period at the end of T . Then the modified equation is as follows:

$$I = \frac{K_1 C}{1 + K_2 C} + K_3 C$$

The above equation needs to be converted into a linear form as before.

$$I = (K_1 + K_3)C - IK_2C + K_2K_3C^2$$

In order to use this equation in the program the equation is simplified by combining constants as follows:

$$I = k_1 C - I\, k_2 C + k_3 C^2$$

$$K_1 = k_1 - k_3 / k_2$$

$$K_2 = k_2$$

$$K_3 = k_3 / k_2$$

For the case of a non-zero intercept the constant (A) must be introduced into the equation.

$$I = A + \frac{K_1 C}{1 + K_2 C} + K_3 C$$

This equation is linearised as follows:

$$I = A + C(AK_2 + K_1 + K_3) - CIK_2 + K_2K_3C^2$$

and is used in the program in the following simplified form:

$$I = k_1C + k_2C - k_3IC + k_4 C^2$$

APPENDIX (ii)

Curve Fitting Program

This program written to run on a BBC micro computer, fits a polynomial function to PAD calibration data. The program forces the curve through the origin (0,0). A modified version of the program has an additional term to allow a non-zero intercept.

```
 90*TV0,1
100IF PAGE>&E00 THEN MODE 4 ELSE MODE 0:CLS
110*FX6
120TM=3:N2=0:N4=0:M1=35
130DIMZ(TM),A(TM,TM),C1(5),Y(20),U(20,TM),ZP(5,5)
140DIMW(TM,1),B(TM,TM),I2(TM,3),X(20),Y1(20)
150DIMY2(35),E2(TM),R3(35)
160PRINT"ELECTROCHEM CURVE  FITTING R=K1C/(1+K2C) +
   K3C"
170INPUT"NUMBER OF STANDARDS=";N1
180INPUT"HIGHEST CONCN. OF STANDARDS =";ZM
190INPUT"LARGEST CURRENT =";ZI
200@%=&2040C
210PRINT""
220IFN2=0THENGOSUB340
230IFN2=TMTHENGOTO1960
240N2=N2+1
250L3=(N1-1)*2+1
260IFN4=1THEN390
280GOSUB410
290GOSUB940
300GOSUB1090
310GOSUB480
320GOTO210
340PRINT"INPUT CONCN. & RESP. VALUES"
```

```
350PRINT""
360FORI=1TON1
370INPUT;Y1(I),X(I)
380NEXT
390RETURN
410FORI=1TON1
420U(I,1)=Y1(I)
430U(I,2)=-Y1(I)*X(I)
440U(I,3)=(Y1(I))^2
450Y(I)=X(I)
460NEXTI
470RETURN
480 REM
490S7=0
500S8=0
510T6=0
520FORI=1TON1
530Y2=0
540FORJ=1TON2
550Y2=Y2+C1(J)*U(I,J)
560NEXTJ
570R3(I)=Y2-Y(I)
580Y2(I)=Y2
590T6=T6+R3(I)*R3(I)
600S7=S7+Y(I)
610S8=S8+Y(I)*Y(I)
620NEXTI
630IFN2>0THENC3=SQR(1-T6/(S8-S7*S7/N1))
640IFN1=N2THENE5=SQR(T6)
650IFN1<N2THENE5=SQR(T6/(N2-N1))
660IFN1>N2THENE5=SQR(T6/(N1-N2))
670FORJ=1TON2
680E2(J)=E5*SQR(ABS(B(J,J)))
690NEXTJ
700IFC1(2)=0THENZP(N2,1)=C1(1)ELSEZP(N2,1)=
   C1(1)-C1(3)/C1(2)
```

```
710ZP(N2,2)=Cl(2)
720IFCl(2)=0THENZP(N2,3)=0ELSEZP(N2,3)=Cl(3)/Cl(2)
730kl=ZP(N2,1):k2=ZP(N2,2):k3=ZP(N2,3)
740PROCpoints:IFN2>0THENPROCplot(ZP(N2,1),ZP(N2,2),
   ZP(N2,3))
750PRINTTAB(0,0)"DO YOU WANT RESULTS SENT TO PRINTER?
   Y/N":BB$=GET$
760IFBB$="Y"THENVDU2
770CLS:PRINT"":PRINT""
780PRINT"   CURRENT      CONC    CURRENT    RESID"
785PRINT"                        (calc)"
790PRINT""
800FORI=1TON1:@%=&2040A
810PRINTX(I),Y1(I),Y2(I),R3(I)
820NEXT
830PRINT"":PRINT"":@%=&2050A
840PRINT"Coefficients            Errors"
850PRINT""
860FORI=1TON2:PRINT;ZP(N2,I),SPC(8),E2(I):NEXT
870PRINT""
880PRINT"CORRELATION COEFFICIENT =   "C3
890VDU3
900ZP(N2,0)=C3
910PRINTTAB(0,0)"PRESS ANY KEY TO
   CONTINUE          ":CC$=GET$
920IFCC$=""THEN@%=&0040C
930RETURN
940 REM
950FORK=1TON2
960FORL=1TOK
970A(K,L)=0
980FORI=1TON1
990A(K,L)=A(K,L)+U(I,L)*U(I,K)
1000IFK<>LTHENA(L,K)=A(K,L)
1010NEXTI
1020NEXTL
```

```
1030Z(K)=0
1040FORI=1TON1
1050Z(K)=Z(K)+Y(I)*U(I,K)
1060NEXTI
1070NEXTK
1080RETURN
1090 REM
1100E1=0
1110I5=1
1120N3=1
1130FORI=1TON2
1140FORJ=1TON2
1150B(I,J)=A(I,J)
1160NEXTJ
1170W(I,1)=Z(I)
1180I2(I,3)=0
1190NEXTI
1200D3=1
1210FORI=1TON2
1220B1=0
1230FORJ=1TON2
1240IFI2(J,3)=1THEN1330
1250FORK=1TON2
1260IFI2(K,3)>1THEN1930
1270IFI2(K,3)=1THEN1320
1280IFB1>=ABS(B(J,K))THEN1320
1290I3=J
1300I4=K
1310B1=ABS(B(J,K))
1320NEXTK
1330NEXTJ
1340I2(I4,3)=I2(I4,3)+1
1350I2(I,1)=I3
1360I2(I,2)=I4
1370IFI3=I4THEN1500
1380D3=-D3
```

```
1390FORL=1TON2
1400H1=B(I3,L)
1410B(I3,L)=B(I4,L)
1420B(I4,L)=H1
1430NEXTL
1440IFN3<1THEN1500
1450FORL=1TON3
1460H1=W(I3,L)
1470W(I3,L)=W(I4,L)
1480W(I4,L)=H1
1490NEXTL
1500P1=B(I4,I4)
1510D3=D3*P1
1520B(I4,I4)=1
1530FORL=1TON2
1540B(I4,L)=B(I4,L)/P1
1550NEXTL
1560IFN3<1THEN1600
1570FORL=1TON3
1580W(I4,L)=W(I4,L)/P1
1590NEXTL
1600FORL1=1TON2
1610IFL1=I4THEN1710
1620T=B(L1,I4)
1630B(L1,I4)=0
1640FORL=1TON2
1650B(L1,L)=B(L1,L)-B(I4,L)*T
1660NEXTL
1670IFN3<1THEN1710
1680FORL=1TON3
1690W(L1,L)=W(L1,L)-W(I4,L)*T
1700NEXTL
1710NEXTL1
1720NEXTI
1730FORI=1TON2
1740L=N2-I+1
```

```
1750IFI2(L,1)=I2(L,2)THEN1830
1760I3=I2(L,1)
1770I4=I2(L,2)
1780FORK=1TON2
1790H1=B(K,I3)
1800B(K,I3)=B(K,I4)
1810B(K,I4)=H1
1820NEXTK
1830NEXTI
1840FORK=1TON2
1850IFI2(K,3)<>1THEN1930
1860NEXTK
1870E1=0
1880FORI=1TON2
1890C1(I)=W(I,1)
1900NEXTI
1910IFI5=1THEN1950
1920PRINT""
1930E1=1
1940CLS:PRINT"ERROR~MATRIX SINGULAR":STOP
1950RETURN
1960CLS:PRINT"PARAMETERS, INCLUDING
   CONSTANT":PRINT"":PRINT""
1970PRINT"          K1          K2       K3          COCOE"
1980FORI=1TON2
1990PRINT"":@%=&2050B
2000PRINTZP(I,1),ZP(I,2),ZP(I,3),ZP(I,0):NEXTI:
    @%=&2000A:PRINT"":PRINT""
2010VDU3
2020PRINTTAB(15)"WHICH FUNCTION DO YOU REQUIRE?
    1-";N2:INPUTK%
2030PRINT"TO ESCAPE THE TRAP TYPE ANY LETTER"
2040CLS:PRINT"       EQUATION      ";K%
2050PRINT"DO YOU WANT TO SAVE DATA Y/N"
2060M$=GET$:IFM$="Y"THENPROCsavdata(ZP(K%,1),ZP(K%,2),
    ZP(K%,3))
```

```
2070PRINT" INPUT CURRENT AND I'LL RETURN CONCENTRATION"
2080ONERRORGOTO2010
2090INPUT"RESP.=";ZS
2100T1=.000001:X=-3
2110GOSUB2130
2120GOTO2210
2130X1=X
2140GOSUB2180
2150D6=F/F1:X=X1-D6
2160IF(ABS(D6)>=ABS(T1*X))THEN2130
2170RETURN
2180F=(ZP(K%,1)*X/(1+ZP(K%,2)*X)+ZP(K%,3)*X)-ZS
2190F1=ZP(K%,1)/((1+ZP(K%,2)*X)^2)+ZP(K%,3)
2200RETURN
2210@%=&2030C:PRINT"CONC=";X:GOTO2090
2220END
2240DEFPROCplot(a,b,c)
2250MOVE150,100:I%=0:REPEAT
2260IFb=0THENF3=a*ZM*I%//200
2270F3=a*(ZM*I%/200)/(1+b*ZM*I%/200)+c*(ZM*I%/200)
2280DRAW(I%*1055/200+150),(F3*800/ZI+100)
2290I%=I%+1
2300UNTILI%>200
2310ENDPROC
2320DEFPROCpoints
2330CLS:MOVE150,900:DRAW150,100:DRAW1200,100:@%=&02010A
2340A%=0:REPEATMOVE150,(100+A%*800/4):PLOT1,-22,0
2350PLOT0,-180,14:VDU5:PRINT(ZI*A%/4):VDU4
2360MOVE(150+A%*1055/4),100:PLOT1,0,-22
2370C$=STR$(A%*1055/4)
2380PLOT0,(-LEN(C$)-150)*.82,-20:VDU5:
    PRINT(ZM*A%/4):VDU4
2390A%=A%+1:UNTILA%>4
2400FORI=1TON1
2410MOVE(150+1050*Y1(I)/ZM),(100+800*X(I)/ZI)
2420PLOT0,11,11:PLOT1,-22,-22:PLOT0,0,22:
```

```
    PLOT1,22,-22:NEXT
2430ENDPROC
2440DEFPROCsavdata(a,b,c)
2450REPEAT:INPUT"WHICH DRIVE";Q%:UNTILQ%=0ORQ%=4
2460IFQ%=0THENGOTO2470:ELSE2490
2470*DRIVE0
2480GOTO2510
2490*DRIVE4
2500*DRIVE4
2510INPUT"DATAFILENAME    ";FM$
2520PRINT""
    :PRINT"             PLEASE WAIT WHILST DATA IS SAVED"
2530CLOSE#0
2540R%=OPENOUTFM$
2550AX$="                ":AY$="                "
2560X$="                ":Y$="                "
2570XX$="                ":YY$="                "
2580BX$="                ":BY$="                "
2590I=1:REPEAT:X2=Y1(I):Y4=X(I)
2600AX$=STR$(X2)
2610I%=1:REPEAT:BX$=LEFT$(AX$,I%):
    BPUT#R%,ASC(RIGHT$(BX$,1)):I%=I%+1
2620UNTILI%>LEN(AX$)
2630AY$=STR$(Y4):BPUT#R%,&20
2640I%=1:REPEAT:BY$=LEFT$(AY$,I%):
    BPUT#R%,ASC(RIGHT$(BY$,1)):I%=I%+1
2650UNTILI%>LEN(AY$):BPUT#R%,&D:BPUT#R%,&A
2660I=I+1:UNTILI>N1
2670BPUT#R%,&D:BPUT#R%,&A:BPUT#R%,&D:BPUT#R%,&A
2680I%=0:REPEAT:F3=a*(I%*X2/200)/(1+b*I%*X2/200)
    +c*I%*X2/200
2690X=I%*X2/200:Y=F3
2700X$=STR$(X)
2710Y$=STR$(Y)
2720B%=1:REPEAT:XX$=LEFT$(X$,B%):BPUT#R%,
    ASC(RIGHT$(XX$,1)):B%=B%+1
```

```
2730UNTILB%>LEN(X$):BPUT#R%,&20
2740B%=1:REPEAT:YY$=LEFT$(Y$,B%):BPUT#R%,
    ASC(RIGHT$(YY$,1)):B%=B%+1
2750UNTILB%>LEN(Y$):BPUT#R%,&D:BPUT#R%,&A
2760I%=I%+1:UNTILX>X2
2770CLOSE#R%:CLS
2780ENDPROC
```